

**Synthesis, Characterization and Optical Properties of  
a Bay- Functionalized Perylene Dye: N,N'-Didodecyl-  
1,7-di(3-methylphenoxy)- perylene-3,4:9,10-  
tetracarboxylic Acid Bisimide**

**Basma Basil Ismael Al-Khateeb**

Submitted to the  
Institute of Graduate Studies and Research  
in partial fulfillment of the requirements for the Degree of

Master of Science  
in  
Chemistry

Eastern Mediterranean University  
January 2014  
Gazimağusa, North Cyprus

Approval of the Institute of Graduate Studies and Research

---

Prof. Dr. Elvan Yılmaz  
Director

I certify that this thesis satisfies the requirements as a thesis for the degree of Master of Science in Chemistry

---

Prof. Dr. Mustafa Halilsoy  
Chair, Department of Chemistry

We certify that we have read this thesis and that in our opinion it is fully in scope and quality as a thesis for the degree of Master of Science in Chemistry.

---

Prof. Dr. Huriye İcil  
Supervisor

---

Examining Committee

1. Prof. Dr. Huriye İcil

2. Asst. Prof. Dr. Nur P. Aydınlik

3. Asst. Prof. Dr. Hatice N. Hasipoglu

## ABSTRACT

Perylene chromophore has an excellent aromatic conjugation and offers numerous advantages in many fields of application. One of their greatest advantages is the capability to functionalize the chromophore at its core/bay and imide positions with various substituents according to the desired application.

In the present research on perylene dyes, we have synthesized a new core substituted perylene diimide in three consecutive steps focusing the application toward solar cells. Firstly, the starting raw material perylene dianhydride was brominated at 1,7-positions of the perylene chromophore to yield brominated dianhydride (Br-PDA). The product was imidized in the second step with a long dodecyl alkyl chain to yield brominated perylene diimide (Br-PDI). Finally, the targeted core substituted perylene diimide (PDI-m-Cresol) was synthesized upon bay substitution of perylene chromophore with m-cresol. The final compound is highly pure and characterized by FTIR, UV-vis and Emission measurements. For comparison, photophysics of the intermediate products were carried out in parallel.

The absorption spectra of three perylene derivatives in nonpolar aprotic solvents and polar protic solvents show characteristic aromatic  $\pi-\pi^*$  transition absorption peaks. In contrary, absorption in dipolar aprotic solvents shows irregular additional absorption bands (Br-PDA in NMP; Br-PDI in DMF; and PDI-m-Cresol in DMF and NMP) at higher wavelengths which were remained after microfiltering the solution.

Interestingly, the emission spectra of the three perylene derivatives have shown traditional three characteristic emission peaks and were not influenced by additional weak absorption bands.

**Keywords:** Perylene dyes, perylene derivatives, Bay-substitution, characterization of perylene derivatives.

## ÖZ

Mükemmel bir aromatik konjugasyon yapısına sahip olan perilen boyar maddeleri pekçok uygulama alanında kullanılabilecek üstün özellikler sunmaktadırlar. En önemli üstünlüklerden biri gerek çekirdek/körfez gerekse imid pozisyonlarında çeşitli süstituentlerle perilen boyalarının fonksiyonelleştirilebilmesidir. Bu çalışmada, güneş hücreleri uygulamalarında kullanılmak amacıyla üç ardışık basamaklı reaksiyonlar ile körfez pozisyonunda fonksiyonleştirilen yeni bir perilen diimid sentezlenmiştir. İlk basamakta perilen anhidrit 1,7-pozisyonlarında bromlanmıştır (Br-PDA). İkinci basamakta dodesil süstitientli ve bromlanmış diimid sentezlenmiştir (Br-PDI). En son basamakta ise perilen diimid körfez pozisyonunda m-kresol ile süstitüe edilmiştir (PDI-m-Cresol). Saflandırılan ürünler FTIR, UV-Vis ve emisyon ölçümleri ile karakterize edilmiştir. Karşılaştırma için, ara ürünlerin fotofiziksel özellikleri de paralel biçimde incelenmiştir. Üç ayrı perilen türevinin apolar aprotik ve polar protik çözümlerde ölçülen absorpsiyon spektrumlarında karakteristik  $\pi-\pi^*$  geçiş absorpsiyon bandları gözlenmiştir. Buna karşın, dipolar aprotik çözümlerde ölçülen absorpsiyon spektrumlarında mikro süzgeçten geçirildiğinde dahi yok olmayan düzensiz ve yeni bandlar gözlenmiştir (NMP'de Br-PDA; DMF'te Br-PDI; ve DMF ile NMP'de PDI-m-kresol). İlginç biçimde, üç ayrı perilen türevlerinin emisyon spektrumlarında düzensiz ve yeni absorpsiyon bandlarından etkilenmeyen karakteristik üç ayrı emisyon bandları yer almaktadır.

**Keywords:** perylene diimid, körfez süstitüe, fotonik, solar hücre.

## **ACKNOWLEDGMENTS**

I would like to express my appreciation to the jury members. Special thanks to Prof. Dr. Huriye Icil for her knowledge, time, patience, and understanding. It has been an honor to work with her. This research would have not been possible without her help.

I would like to sincerely thank my colleagues for their help and support, my mother, father and sisters I can't thank you enough.

# TABLE OF CONTENTS

ABSTRACT.....	iii
ÖZ.....	v
ACKNOWLEDGMENTS .....	vi
LIST OF TABLES .....	x
LIST OF FIGURES .....	xix
LIST OF ILLUSTRATIONS .....	xviii
LIST OF SYMBOLS/ABBREVIATIONS .....	xix
1 INTRODUCTION .....	1
2 THEORETICAL .....	9
2.1 Properties of Perylene Diimide Dyes.....	9
2.1.1 Optical Characteristics of Perylene Diimide Dyes .....	10
2.1.2 Perylene Diimide Dyes; Bay-Substituted Derivatives .....	10
2.1.3 Electron Acceptor Properties of Perylene Diimide Dyes for Photovoltaic Applications .....	11
2.1.4 Perylene Diimide Dyes; Conversion Efficiency of Solar Energy into Electrical Energy.....	12
2.2 The Future and Commercialization of Dye Sensitized Solar Cells.....	13
3 EXPERIMENTAL .....	14
3.1 Materials.....	15
3.2 Instruments.....	16

3.3 Methods of Synthesis.....	17
3.4 Synthesis of Brominated Perylene Bisanhydride (PABr).....	18
3.5 Synthesis of N, N'-Didodecyl-1, 7-dibromoperylene-3, 4, 9, 10-tetracarboxylic Acid Bisimide (DBPDI).....	19
3.6 Synthesis of N, N'-Didodecyl-1, 7-diphenoxy- perylene-3, 4:9, 10-tetracarboxylic acid bisimide (BPPDI).....	20
3.7 General Reaction Mechanism of Perylene Dyes.....	20
4 DATA AND CONCLUSION.....	21
4.1 Calculations of Maximum Extinction Co-efficient ( $\epsilon_{max}$ ).....	22
4.2 calculations of Half-width of the selected Absorption ( $\Delta\nu_{1/2}$ ).....	23
4.3 Calculations of Theoretical Radiative Lifetimes ( $\tau_0$ ).....	24
4.4 Calculations of Fluorescence Rate Constant ( $k_f$ ).....	29
4.5 Calculations of oscillator strength ( $f$ ).....	31
4.6 Calculations of Singlet Energy.....	33
4.6 Calculations of Optical Band Gap Energies.....	35
4.7 Calculations of Optical Band Gap Energies.....	37
5 RESULTS AND DISCUSSION.....	93
5.1 Synthesis of the Compounds.....	93
5.2 Solubility of the synthesized perylene derivatives.....	95
5.3 Analysis of FTIR spectra.....	97
5.4 Analysis of the UV-vis Absorption Spectra.....	97
5.5 Analysis of the Emission Spectra.....	101

6 CONCLUSION .....	104
REFERENCES.....	105

## LIST OF TABLES

Table 4-1: Molar Absorptivity Data of Br-PDA, Br-PDI and PDI-M-Cresol in CHL ....	23
Table 4-2: Molar Absorptivity Data of Br-PDA, Br-PDI and PDI-m-Cresol in DMF ....	23
Table 4-3: Molar Absorptivity Data of Br-PDA, Br-PDI and PDI-m-Cresol in NMP ....	23
Table 4-4: Molar Absorptivity Data of Br-PDA, Br-PDI and PDI-m-Cresol in EtOH ...	24
Table 4-5: Molar Absorptivity Data of Br-PDA, Br-PDI and PDI-m-Cresol in Acetone .....	24
Table 4-6: Half Width of the Selected Absorptions of PDI-M-Cresol and Measured in Different Solvents .....	26
Table 4-7: Half Width of the Selected Absorptions of Br-PDI and Measured in Different Solvents .....	26
Table 4-8: Half width of the Selected Absorptions of Br-PDA and Measured in Different Solvents .....	26
Table 4-9: Theoretical Radiative Lifetimes of PDI-M-Cresol Measured in Different Solvents.....	28
Table 4-10: Theoretical Radiative Lifetimes of Br-PDI Measured in Different Solvents.....	28
Table 4-11: Theoretical Radiative Lifetimes of Br-PDA Measured in Different Solvents.....	28
Table 4-12: Fluorescence Rate Constants Data of PDI-M-Cresol in Different Solvents.....	29
Table 4-13: Fluorescence Rate Constants Data of Br-PDI in Different Solvents.....	29
Table 4-14: Fluorescence Rate Constants Data of Br-PDA in Different Solvents .....	29

Table 4-15: Oscillator Strength Data of PDI-M-Cresol Measured in Different Solvents .....	30
Table 4-16: Oscillator Strength Data of Br-PDI Measured in Different Solvents .....	31
Table 4-17: Oscillator Strength Data of Br-PDA Measured in Different Solvents .....	31
Table 4-18: Singlet Energies Data of PDI-m-Cresol in Different Solvents .....	32
Table 4-19: Singlet Energies Data of Br-PDI in Different Solvents .....	32
Table 4-20: Singlet Energies Data of Br-PDA in Different Solvents .....	32
Table 4-21: Band Gap Energies of PDI-M-Cresol Were Calculated in Different Solvents .....	33
Table 4-22: Band Gap Energies of Br-PDI Were Calculated in Different Solvents .....	34
Table 4-23: Band Gap Energies of Br-PDA Were Calculated in Different Solvents .....	34

## LIST OF FIGURES

Figure 1-1: Chemical structure of Dibromo Perylene Diimide.....	1
Figure 1-2: The structures of dibromo perylene tetracarboxylic anhydride .....	5
Figure 1-3: The structures of Disubstituted perylene diimide .....	6
Figure 1-4: The structures of BPPDI .....	12
Figure 2-1: The structure of DSSC based on Donor- $\pi$ -acceptor dye.....	12
Figure 4-1: Absorption spectrum of PDI-M-Cresol in chloroform at $1 \times 10^{-5} M$ .....	22
Figure 4-2: Absorption spectrum of PDI-M-Cresol in chloroform and half-width representation .....	24
Figure 4-3: Absorption spectrum of PDI-M-Cresol and the cut-off wavelength.....	35
Figure 4-4: FTIR spectrum of Br-PDA.....	
Figure 4.5 FTIR spectrum of Br-PDI.....	38
Figure 4.6 FTIR spectrum of PDI-m-Cresol .....	39
Figure 4.7: Absorption spectrum of Br-PDA in DMF.....	40
Figure 4.8: Absorption spectrum of Br-PDA in DMF after micro filtration .....	41
Figure 4.9: Absorption spectrum of Br-PDA in NMP .....	42
Figure 4.10: Absorption spectrum of Br-PDA in NMP after micro filtration.....	43

Figure 4.11: Absorption spectrum of Br-PDA in DMF and DMF after microfiltration

.....  
44

Figure 4.12: Absorption spectrum of Br-PDA in NMP and in NMP after microfiltration

.....  
..45

Figure 4.13: Absorption spectrum of Br-PDA in DMF and NMP (after microfiltration).....

46

Figure 4.14: Absorption spectrum of Br-PDI in DMF

.....47

Figure 4.15: Absorption spectrum of Br-PDI in DMF after micro filtration

.....48

Figure 4.16: Absorption spectrum of Br-PDI in NMP

..... 49

Figure 4.17: Absorption spectrum of Br-PDI in

CHL.....50

Figure 4.18: Absorption spectrum of Br-PDI in DMF and DMF after micro filtration.....

51

Figure 4.19: Absorption spectrum of Br-PDI in DMF,NMP and CHL

.....52

Figure 4.20: Absorption spectrum of PDI-m-Cresol in DMF.....	53
Figure 4.21: Absorption spectrum of PDI-m-Cresol in NMP.....	54
Figure 4.22: Absorption spectrum of PDI-m-Cresol in NMP after micro filtration .....	.55
Figure 4.23: Absorption spectrum of PDI-m-Cresol in NMP and NMP micro filtration.....	.56
Figure 4.24: Absorption spectrum of PDI-m-Cresol in CHL.....	57
Figure 4.25: Absorption spectrum of PDI-m-Cresol in Acetone.....	58
Figure 4.26: Absorption spectrum of PDI-m-Cresol in EtOH .....	59
Figure 4.27: Absorption spectrum of PDI-m-Cresol in DMF,NMP,CHL,Acetone and EtOH.....	.60
Figure 4.28: Absorption spectrum of PDI-m-Cresol,Br-PDI and Br-PDA in DMF .....	...61
Figure 4.29: Absorption spectrum of PDI-m-Cresol,Br-PDI and Br-PDA in NMP .....	...62

Figure 4.30: Absorption spectrum of PDI-m-Cresol and Br-PDI in CHL	63
Figure 4.31 Emission spectrum ( $\lambda_{exc}=485nm$ ) of Br-PDA in DMF	64
Figure 4.32: Emission spectrum ( $\lambda_{exc}=485nm$ ) of Br-PDA in DMF after micro filtration	65
Figure 4.33 Emission spectrum ( $\lambda_{exc}=485nm$ ) of Br-PDA in DMF and in DMF after micro filtration	66
Figure 4.34: Emission spectrum ( $\lambda_{exc}=485nm$ ) of Br-PDA in NMP	67
Figure 4.35: Emission spectrum ( $\lambda_{exc}=485nm$ ) of Br-PDA in NMP after micro filtration	68
Figure 4.36 Emission spectrum ( $\lambda_{exc}=485nm$ ) of Br-PDA in NMP and NMP after micro filtration	69
Figure 4.37 Emission spectrum ( $\lambda_{exc}=485nm$ ) of Br-PDA in NMP and DMF	70
Figure 4.38 Emission spectrum ( $\lambda_{exc}=485nm$ ) of Br-PDI in DMF	71

Figure 4.39 Emission spectrum ( $\lambda_{exc}=485nm$ ) of Br-PDI in DMF after micro filtration	.....
	..72
Figure 4.40 Emission spectrum ( $\lambda_{exc}=485nm$ ) of Br-PDI in DMF and DMF aftermicro filtration	.....
	73
Figure 4.41 Emission spectrum ( $\lambda_{exc}=485nm$ ) of Br-PDI in NMP.....	74
Figure 4.42 Emission spectrum ( $\lambda_{exc}=485nm$ ) of Br-PDI in CHL	.....
	75
Figure 4.43 Emission spectrum ( $\lambda_{exc}=485nm$ ) of Br-PDI in DMF ,NMP and CHL.....	
	.76
Figure 4.44 Emission spectrum ( $\lambda_{exc}=485nm$ ) of PDI-m-Cresol in DMF	.....
	77
Figure 4.45 Emission spectrum ( $\lambda_{exc}=485nm$ ) of PDI-m-Cresol in NMP	.....
	78
Figure 4.46 Emission spectrum ( $\lambda_{exc}=485nm$ ) of PDI-m-Cresol in NMP after micro filtration.....	
	..79
Figure 4.47 Emission spectrum ( $\lambda_{exc}=485nm$ ) of PDI-m-Cresol in NMP and in NMP after micro filtration.....	80

Figure 4.48 Emission spectrum ( $\lambda_{exc}=485nm$ ) of PDI-m-Cresol in CHL	
.....	81
Figure 4.49 Emission spectrum ( $\lambda_{exc}=485nm$ ) of PDI-m-Cresol in EtOH	
.....	82
Figure 4.50 Emission spectrum ( $\lambda_{exc}=485nm$ ) of PDI-m-Cresol in Acetone	
.....	83
Figure 4.51 Emission spectrum ( $\lambda_{exc}=485nm$ ) of PDI-m-Cresol in DMF, NMP,	
CHL, EtOH and	
Acetone.....	84
Figure 4.52 Emission spectrum ( $\lambda_{exc}=485nm$ ) of PDI-m-Cresol,Br-PDI and Br-PDA	
in DMF	
.....	85
Figure 4.53 Emission spectrum ( $\lambda_{exc}=485nm$ ) of PDI-m-Cresol,Br-PDI and Br-PDA	
in NMP	
.....	86
Figure 4.54 Emission spectrum ( $\lambda_{exc}=485nm$ ) of PDI-m-Cresol and Br-PDI in CHL	
.....	87

## LIST OF ILLUSTRATIONS

Scheme 3.1 Synthesis of Brominated Perylene Bisanhydride.....	34
Scheme 3.2 Synthesis of N, N'-Didodecyl-1, 7-dibromoperylene-3, 4, 9, 10-tetracarboxylic Acid Bisimide.....	35
Scheme 3.3 Synthesis of N, N'-Didodecyl-1, 7-diphenoxy- perylene-3, 4:9, 10-tetracarboxylic acid Bisimide .....	36

## LIST OF SYMBOLS/ABBREVIATION

$\text{\AA}$	Armstrong
Cm	Centimeter
$^{\circ}\text{C}$	Degrees celcius
$\Delta V_{1/2}$	Half-width of the selected absorption
$\epsilon_{\text{max}}$	Maximum extinction coefficient
$E_s$	Singlet energy
F	Oscillator strength
$\lambda_{\text{exc}}$	Excitation wavelength
$\lambda_{\text{max}}$	Absorption wavelength maximum
$\Delta$	Chemical shift (ppm)
$\tau_0$	Theoretical radiative lifetime
$\tau_f$	Fluorescence lifetime
$\Phi_f$	Fluorescence quantum yield
Nm	Nanometer
A.nitrile	Acetonitrile

CDCl <sub>3</sub>	Deutero-Chloroform
CF <sub>3</sub> COOD	Deutero-Trifloroaceticacid
CH <sub>2</sub> Cl <sub>2</sub>	Dichloromethane
CHCl <sub>3</sub>	Chloroform
CHL	Chloroform
CH <sub>3</sub> CN	Acetonitrile
CV	Cyclic Voltammetry
DMF	N, N'-dimethylformamide
DMSO	N, N'-dimethyl sulfoxide
DNA	Deoxyribonucleic acid
DSC	Differential Scanning Calorimetry
Et.Acetate	Ethylacetate
EtOH	Ethanol
FT-IR	Fourier Transform Infrared Spectroscopy
HCl	Hydrochloric acid
KBr	Potassium bromide

$K_d$	Rate constant of Radiationless deactivation
$K_f$	Theoretical fluorescence rate constant
KOH	Potassium hydroxide
M	molar concentration
MeOH	Methanol
NaOH	Sodium hydroxide
NMR	Nuclear Magnetic Resonance Spectroscopy
RNA	Ribonucleic acid
TGA	Thermogravimetric Analysis
UV-vis	Ultraviolet visible absorption spectroscopy

# Chapter 1

## INTRODUCTION

Perylene-3,4,9,10-tetra carboxylic acid Diimide derivatives are exceptional compounds, which magnetize a great attention owing to their optical and electronic features, they have been considered as industrial dyes due to their low cost, high color strength and their emission color can be altered by suitable substituent from green to red [1-5].

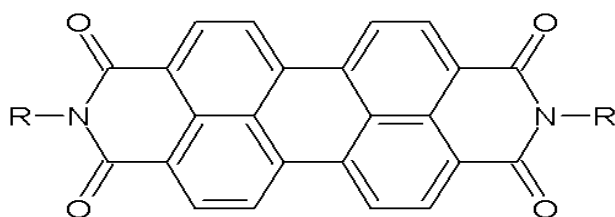


Figure 1-1: Chemical structure of Perylene Diimide

Perylene Diimides are a type of n-type semiconductors showing high electron affinity through large band gap compounds, and they are photo active and electro active materials [2].

Perylene Diimide and its derivatives (PDIs) constitute an important part of strongly fluorescent, high performance dyes that have superior chemical, photo, thermal and environmental stability. PDI derivatives are widely used as effective components in modern systems for example organic thin film transistors, fluorescent light collectors, organic solar cells and optical power limiters, due to their set of attractive

properties such as a very high fluorescence quantum efficiency , a vigorous electron-acceptor nature and two -photon absorption features[6-8].

The fundamental source of energy on the earth's surface is the sun; Sunlight can be transformed to electricity by utilizing solar systems, Solar power is renewable, superabundant, environmentally safe, and cost-effective way to take advantage of that power for homes and businesses, decreasing our reliance on fossil fuels, producing considerable economic, public health and environmental benefits ; people have made use of solar energy during history, conspicuously as fountainhead of light and heat.

The most efficient uses of solar power as an alternative energy can be divided into Solar Thermal, which has been applied to heat water in more sophisticated cities, and solar cells; which provide minimum cost production and sufficient capacity to catch the solar energy and transform it to electrical energy. So far, many of the solar energy devices are remarkably overpriced compared with the classical choices such as engines, gas heaters and grid electricity. Therefore, in order to rival with the conventional alternatives, the price, efficiency and accessibility of these devices should be improved. Photovoltaic cells which represent the first descent of solar technology demand a relatively thick layer of silicon in order to obtain a high capacity of photoncapture, and silicon is an overpriced material. Last decade there have been many attempts to decrease this cost, significantly the thin-film which is the second generation of solar cells approached the target, however, to date limited applications have seen because of several practical problems. The trend of nanotechnology has lately reached to the field of Photovoltaic energy diversion; new photovoltaic materials and devices that would result in realization

of low-cost solar cells in the future have produced. These materials comprise various types of synthetic organic compounds and inorganic nanoparticles. The solar cells based on these materials known as organic photovoltaic cells or inorganic photovoltaic cells. OPVs and DSSCs represent the 3rd descent of photovoltaic cells. OPVs and DSSCs work on various physical techniques. Organic photovoltaic cells utilize organic compounds as semiconductors to transform the solar energy to electrical energy, whereas dye sensitized solar cells work just like the photosynthesis processes by which dyes produce the photo excited electrons. The dye synthesized solar cell, which is the most well-known and studied photovoltaic device, has been around for a long time. It inclines to offer good solutions in term of Ease of production; low-priced manufacturing in addition to accessibility of compounds required [9-18].

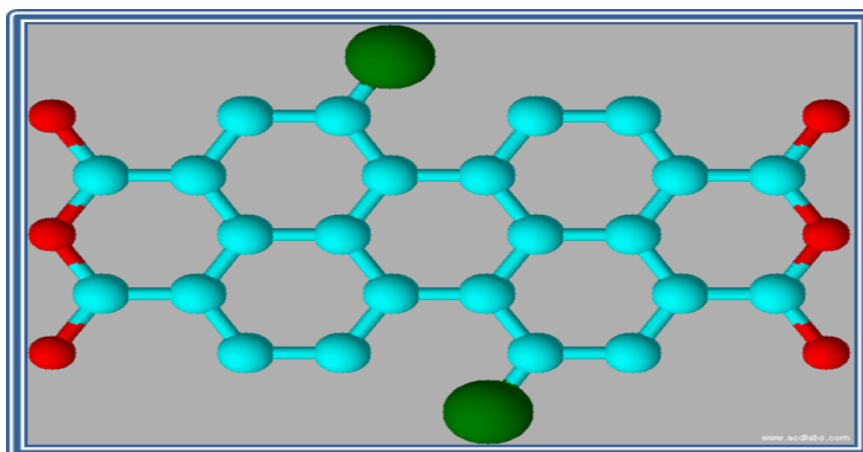
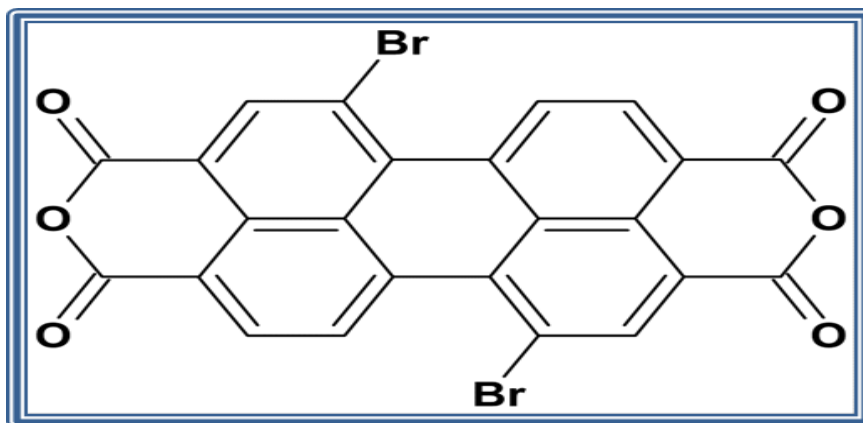
DSSCs based on PDI derivatives are appealing because of improved light absorption owing to their high molar extinction coefficient and perfect electron transport features, in addition to these properties; high electron mobility over  $\pi$ - $\pi$  stacking prefers intermolecular charge transfer and increasing the charge separation, due to their Novel Donor- $\pi$ -acceptor structures [19].

The dye sensitized solar cell, developed by Prof. Michael Grätzel, is an important way for acquiring Energy from the Sun. DSSC based on using dye compounds to catch the solar irradiation, recent dye sensitized solar cells contain various layers of materials arranged in a series, comprising a substrate which is made of glass, diaphanous conducting layer, Titanium dioxide, dye compounds, electrolyte, and counter electrode coated by sealing layer [20].

A superior property of the PDI core is that structural alterations at bay sites or/and the imide sites can be easily achieved, the bay substitution causes a twisting of the  $\pi$ -conjugated system which offers conformational flexibility and gives rise to keep producing various new materials. In general, bay-substitution of Perylene chromophore is an efficient strategy to tune both the optical and electrochemical properties. Especially, the band gap tunability can be achieved which is very advantageous concerning the applications of field effect transistors and photovoltaic systems. Additionally, the bay-substituted compounds give rise to interesting fluorescence properties near to the fluorescence quantum yields of unity. In many cases, the low solubility of perylene diimide is also improved by inserting polar side chains on perylene bay-area which could be an additional benefit for easy processing of the compounds [21-23].

The aim of this thesis is to synthesize a novel bay-functionalized perylene diimide namely N,N'-Didodecyl-1,7-diphenoxy- perylene-3,4:9,10-tetracarboxylic acid bisimide (PDI-m-Cresol). The synthesis of the product was carried out from Perylene-3,4,9,10-tetracarboxylic dianhydride (PDA) in three different steps according to the route shown in Scheme 3.1 In the first reaction step, dibromo perylene tetracarboxylic anhydride was prepared by the bromination of PDA. The second step was imidization, in the course of which N,N'-Didodecyl-1,7-dibromoperylene-3,4,9,10-tetracarboxylic Acid bisimide (Br-PDI) was formed. Finally, N,N'-Didodecyl-1,7-dibromoperylene-3,4,9,10-tetracarboxylic Acid bisimide was reacted with m-cresol to produce N,N'-Didodecyl-1,7-di(3-methylphenoxy)- perylene-3,4:9,10-tetracarboxylic acid bisimide (PDI-m-Cresol) by the nucleophilic substitution of two bromine atoms as shown

in Scheme 3.3 The products were purified and characterized by spectroscopic techniques. The photophysical and photochemical properties of the products were investigated and discussed in detail.



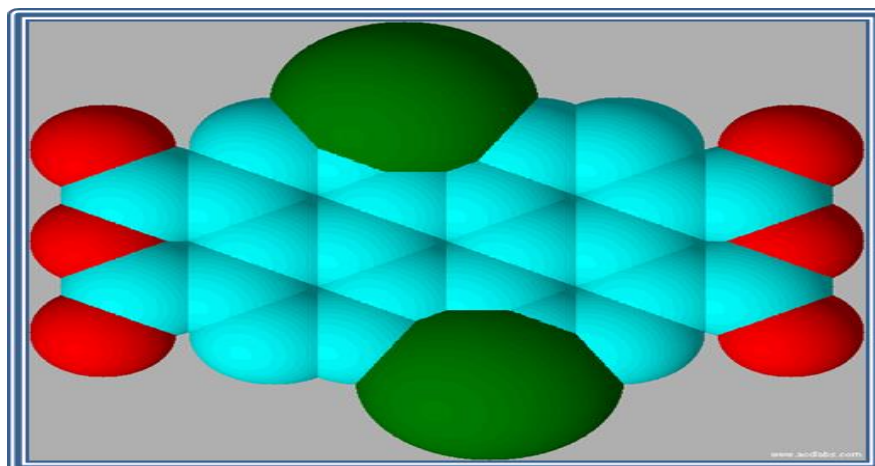
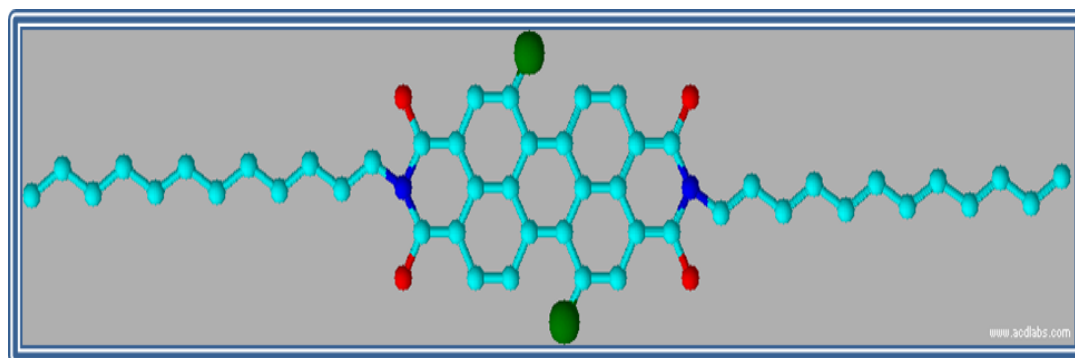
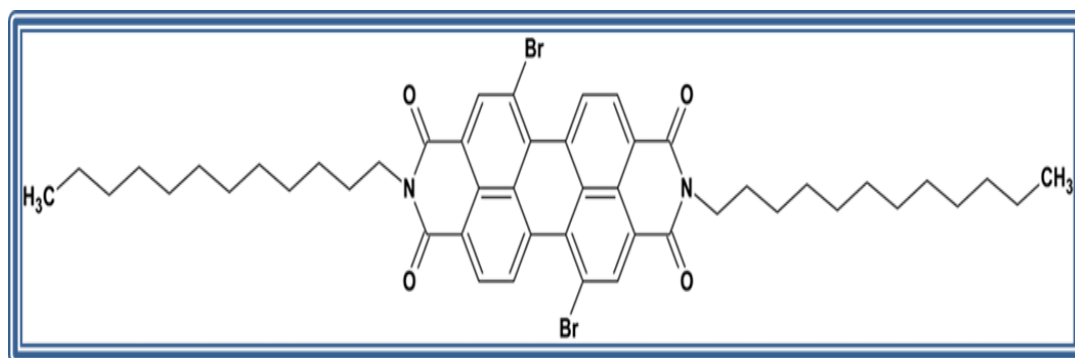


Figure 1-2: The structures of dibromo perylene tetracarboxylic anhydride



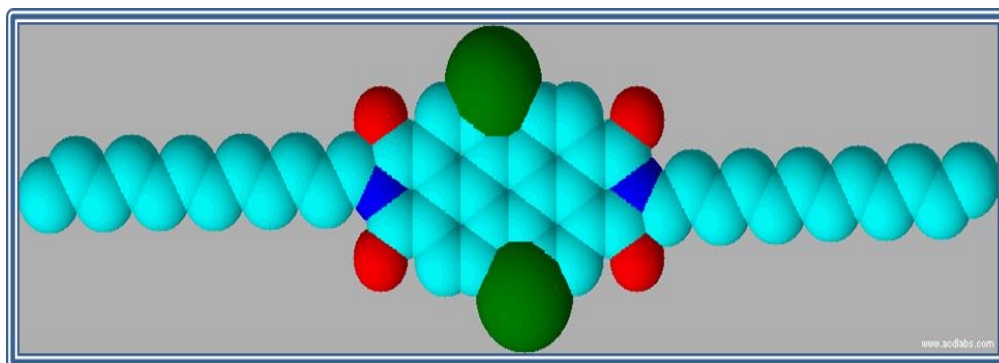
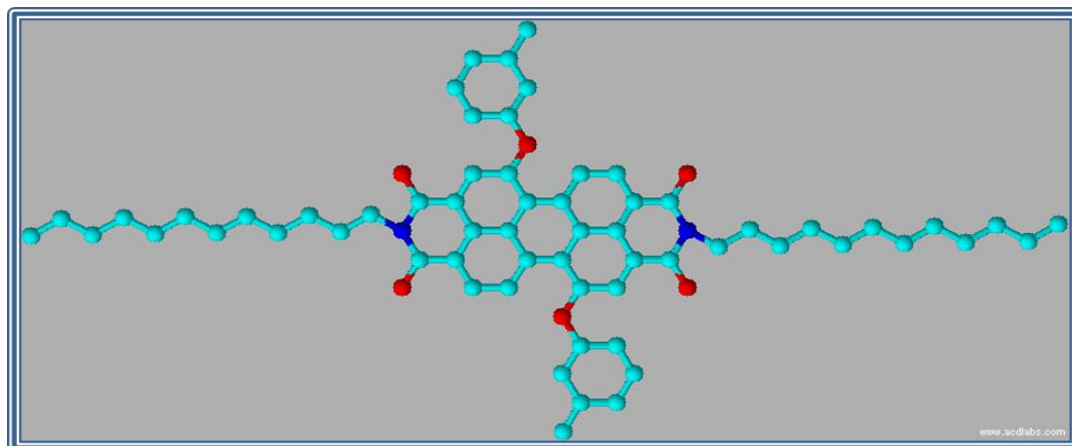
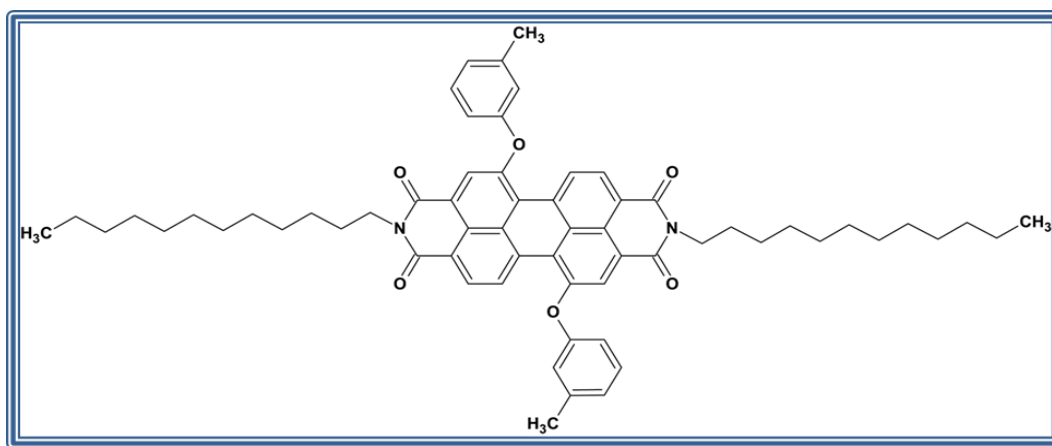


Figure 1-3: The structures of Brominated Perylene Diimide



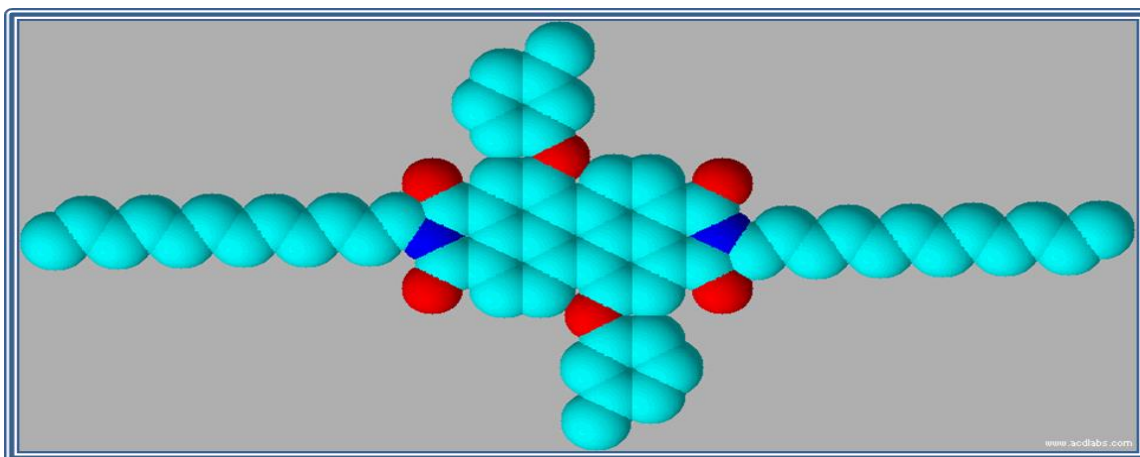


Figure 1-4: The structures of Br-PDI

## Chapter 2

### THEORETICAL

#### 2.1 Properties of Perylene Diimide Dyes

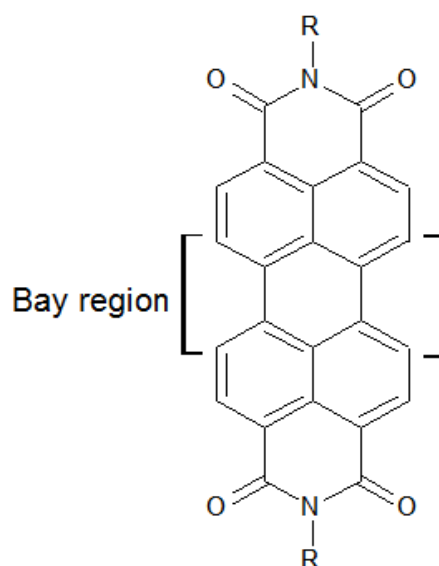
Perylene Diimide derivatives which represent a class of organic dyes have drawn significant attention due to their exceptional properties such as high melting points, high photo chemical, weather and thermal stability, excellent visible light absorption, strong electron acceptor feature, and high fluorescence quantum yield, in addition to their special optical, electro chemical and structural properties. These properties make Perylene diimide dyes successful competitor for use in various fields like solar cells, fluorescent light collectors and organic thin film transistors [24-30].

##### 2.1.1 Optical Characteristics of Perylene Diimide Dyes

Perylene Diimide dyes are generally red compounds and their color can be changed through substitution from green to red. Perylene Diimides present excellent optical properties because of their superior chemical and thermal stability; they are extremely stable upon solar irradiation and surrounding conditions. PDIs are described by their vibronic structure, strong absorption in the visible region around (400 – 550 nm) as well as strong fluorescence like mirror image of the absorption in various organic solvents and high fluorescence quantum yield [31-33]. Optical characteristics of perylene diimide dyes rely on the concentration, polarity of the solvent and the temperature; for example high concentration solutions give rise to bathochromic shift with broad absorption peak extend to near infrared region [34].

### 2.1.2 Perylene Diimide Dyes; Bay-Substituted Derivatives

Perylene diimide derivatives are mostly synthesized through functionalizing the perylene moiety in the bay region, the substitution in bay positions (1, 6, 7, and 12) produce spectacular modification in the electronic and optical properties [1, 34]



Bay substitutions of PDIs with strong electron withdrawing or electron donating groups have been used to modify the HOMO, LUMO levels by stabilizing the LUMO energy level and decreasing the band gap due to intra molecular charge transfer, affect the redox potentials which facilitates the reduction process and increase the oxidation potentials in addition to significant alteration of absorption and emission to longer wavelength (visible-near infrared region) because of the strong electronic connection between the  $\pi$  orbitals of perylene diimides and the substituents on bay area consequently improved the absorption of solar irradiation. Moreover, the solubility of perylene diimides strongly relies on the substitution in the bay positions, for example water solubility can be enhanced by introducing polar substituents on the perylene bay positions [35-42].

### **2.1.3 Electron Acceptor Properties of Perylene Diimide Dyes for Photovoltaic Applications**

Perylene diimides present elevated charge mobility, high electron affinity and perform as excellent n-type substances. Intramolecular charge transfer has been improved through the substitution in the bay positions of perylene diimides which act as acceptors with various donor materials. Perylene diimides derivatives with their donor- $\pi$ -acceptor have drawn a great attention owing to their photo induced charge transfer processes, and they have been widely used in solar applications. The reason behind designing these compounds is to dominate the energy of  $\pi$  system which affects the HOMO and LUMO levels as well as the band gap [45].

Organic photovoltaic cells based on donor- $\pi$ -acceptor types of organic dyes such as perylene diimide derivatives produce the hetero junction which prefers the division of exciton to two carriers. Subsequently these two carriers which are the electrons and the positive holes transferred to the electrodes through materials that generate exciton, these materials should have special properties such as good light capturing and superior carriers transferring features [46].

### **2.1.4 Perylene Diimide Dyes; Conversion Efficiency of Solar Energy into Electrical Energy**

The principle of dye sensitized solar cells is to convert the sun light into electrical energy, and the most significant functions of these devices are to alter the photons that absorbed by dye to carriers in addition to transfer these generated carriers through the cells [43-44].

Dyes are the key component in dye sensitized solar cell which generate the photo excited electrons ,the performance of solar cells affected by several features like the

morphology and structure ,the particle size and the porous size of the titanium dioxide layer which is acting as a photo electrode in DSSC ,the molar absorptivity, absorption range of the dyes, type and quality of the electrolytes , electron transformation and reincorporation rates taking place inside the cell [46].

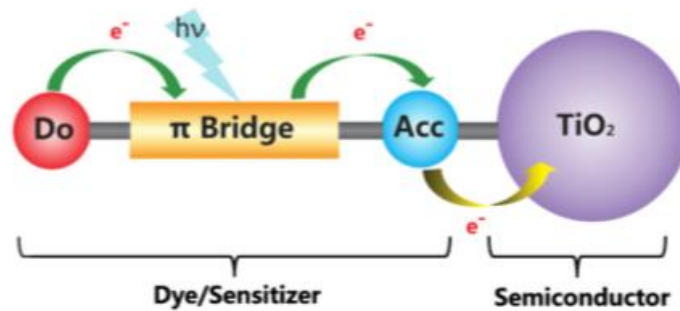


Figure 2-1: The structure of DSSC based on Donor- $\pi$ -acceptor dye

## 2.2 The Future and Commercialization of Dye Sensitized Solar Cells

Dye sensitized solar cells are economical devices that show comparatively high energy conversion efficiency, high and long term stability, easy manufacturing in addition to their high sensitivity toward visible light that make them labor better than silicon photo voltaic cells in more tenebrous conditions these special features should improve to keep the quick commercialization of dye sensitized solar cells.

Presently, dye sensitized solar cells are still in the evolution stage, many laboratory researches taking place to improve their energy conversion efficiencies for various implementations, these developments include synthesis of more sophisticated dyes with superior optical ,electro chemical and structural properties.

In addition to improve the performance and the efficiency of dye sensitized solar cells, inexpensive materials should be used in order to compete with the traditional photovoltaic devices [47, 48].

## Chapter 3

### EXPERIMENTAL

#### 3.1 Materials

PDA, isoquinoline, dodecyl amine, 2-decyl-1-tetradecanol, acetic acid, iodine, bromine and m-cresol were obtained from Sigma Aldrich and used without further purification, potassium carbonate obtained from MERCK, dimethyl formamide supplied by fluka, solvents like methanol, acetone and chloroform which obtained from Aldrich purified by distillation, m-cresol and isoquinoline stored over 4Å molecular sieves.

Molecular sieves of size 4Å (4-8 mesh) which supplied by sigma Aldrich were activated at 500°C and used for drying liquid reagents.

For spectroscopic analysis, pure spectroscopic grade solvents were used without further purification.

All the reactions were controlled by Thin Layer Chromatography (TLC aluminum sheets 5×10 cm silica gel 60 F<sub>254</sub>) which visualize by UV light and/or placing the plate in acidic vanillin solution.

## **3.2 Instruments**

Infrared spectra were recorded with potassium bromide pellets using JASCO FT/IR-6200 (Fourier transform infrared spectrometer).

Ultraviolet Absorption spectra (UV) were measured with Cary-100 UV-Visible Spectrophotometer.

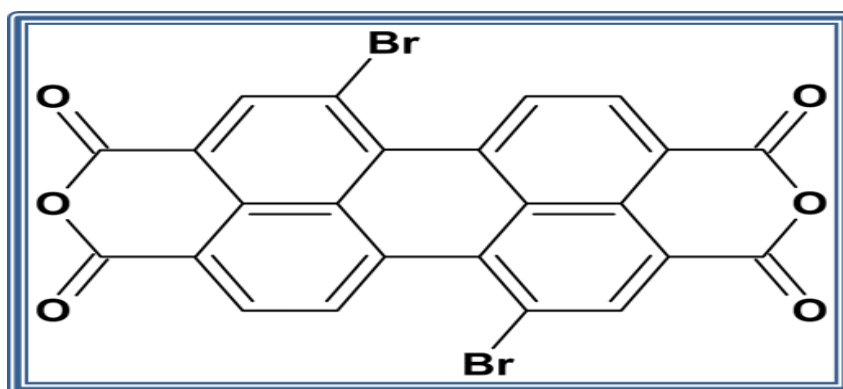
Emission spectra and Fluorescence Quantum yield were measured by Varian Cary Eclipse Fluorescence Spectrophotometer.

## **3.3 Methods of synthesis**

The aim of this thesis is to synthesize a bay substituted perylene diimide which is N, N'-Didodecyl-1, 7-diphenoxy- perylene-3, 4:9, 10-tetracarboxylic acid bisimide; this synthesis was achieved by three steps.

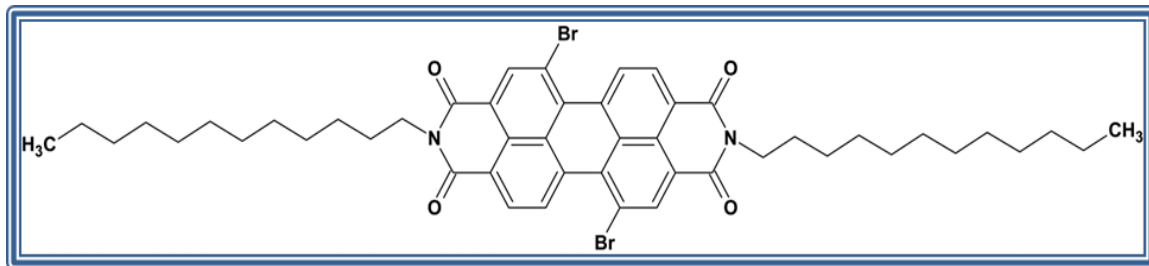
These three steps were explained in this section, step one represent the synthesis of dibromo perylene tetracarboxylic anhydride, step two illustrate the Synthesis of N,N'-Didodecyl-1,7-dibromoperylene-3,4,9,10-tetracarboxylic Acid bisimide and the final step perform the synthesis of Dodecyl-PDI-m-cresol.

### 3.4 Synthesis of Brominated Perylene Bisanhydride (Br-PDA)



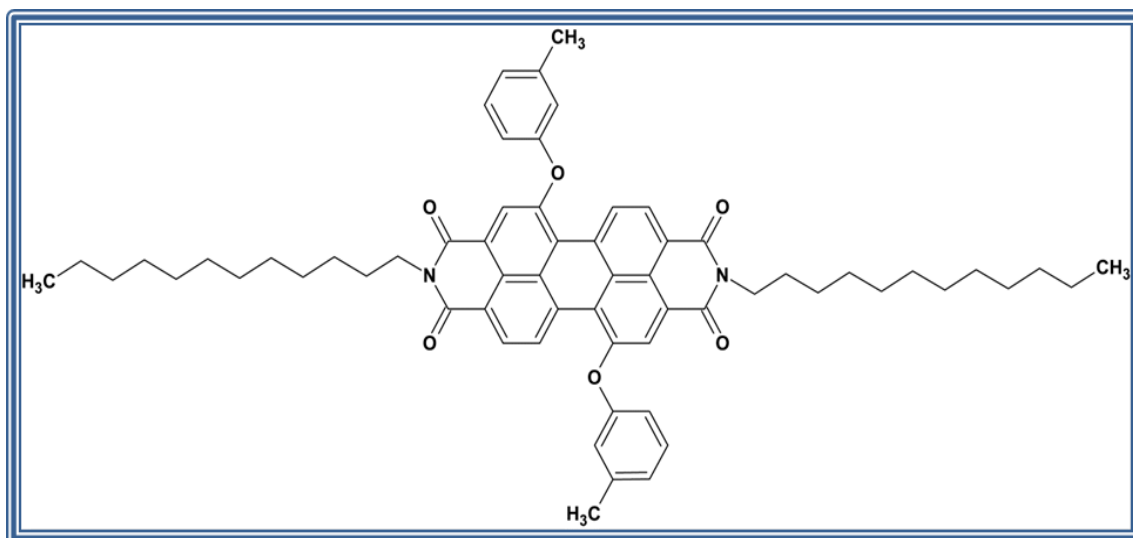
A mixture of 7.8503g (20.00 mmol ) of perylene-3, 4:9, 10-tetra carboxylic acid di anhydride and 64 ml of 95-97 wt% sulfuric acid ( density =1.84 g/cm<sup>3</sup>).then subsequently iodine (I<sub>2</sub>) 0.1925 g 0.75mmol was added. The reaction mixture was heated to 35°C for 1 hour, 45°C for 1 hour then 55°Cfor 16 hours. 2.26 ml (44mmol, density 3.119 g/ml) of bromine was added drop wise over a time period of 2 hour at room temperature. The reaction mixture was stirred 48h at room temperature then heated to 40 °C for 24h and 85°C for 6h, then cooled to room temperature. The excess of bromine was removed by passing a gentle stream of argon gas. The reaction mixture was added into a beaker contain 500 ml of water (ratio 1:5) and kept overnight in the fridge. The mixture was filtered by a suction filtration. The precipitate was washed with a mixture of ( 500 ml water and 75 ml 86% Sulfuric Acid ) and kept overnight in a fridge. For purification, the precipitate was purified by a water soxhlet for 24 h. Then the sample has been dried by using vacuum oven [49].

### 3.5 Synthesis of N, N'-Didodecyl-1, 7-dibromoperylene-3, 4, 9, 10-tetracarboxylic Acid Bisimide (Br-PDI)



A mixture of 1,7-Dibromoperylene-3,4,9,10-tetracarboxylic dianhydride ( 2 g ,3.6mmol) and dodecyl amine ( 1.5g, 8.1mmol ) and isoquinoline (40 mL) mixed under argon gas . Heat up the mixture to 60°C for 2h, 80 °C 2h, 100°C for 4h and 160°C for 6h. The temperature was raised to 180°C around 8h then the reaction completed with continuous stirring at 200°C for more than 10h. 400 mL of methanol was refrigerated for 30 minutes then the reaction mixture was poured into it, covered with foil paper, refrigerated for 1 day for complete precipitation. The resulting precipitate was filtered by suction filtration, and then the precipitate was purified by methanol soxhlet around 24h. Then it was dried by a vacuum oven.

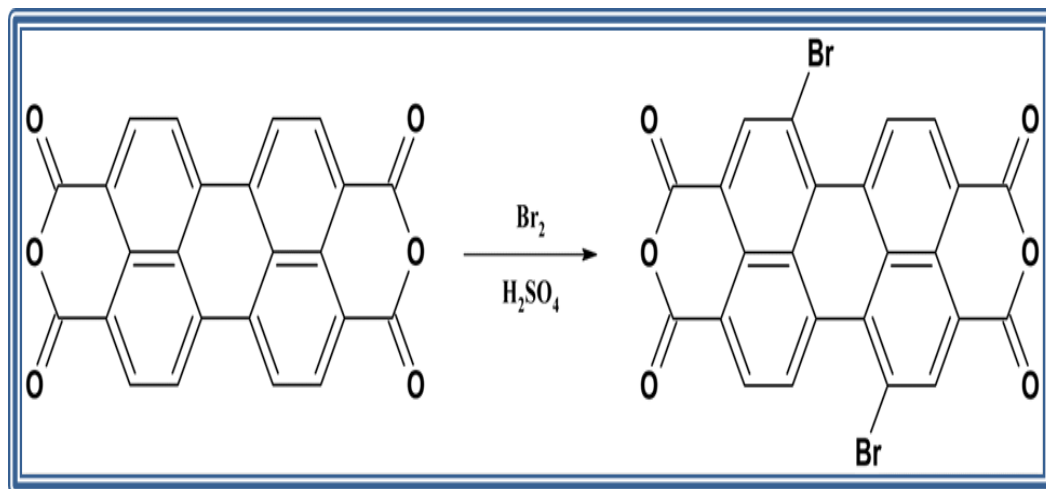
### 3.6 Synthesis of N, N'-Didodecyl-1, 7-diphenoxy- perylene-3, 4:9, 10-tetracarboxylic acid bisimide (BPPDI)



A solution of PDI-Br (0.5 g, 0.56 mmol), 0.146ml (0.15139g, 1.4mmol) m-cresol and  $K_2CO_3$  (0.1972 g, 1.427mmol) are mixed in 100 mL DMF were brought to reflux for 30 h under argon gas with stirring. The reaction mixture was then poured into a mixture of 20 mL cold acetic acid and 50 mL cold water and kept in the fridge overnight. The mixture was filtered by using vacuum filtration; then the precipitate was purified by a water soxhlet for 24 h, and then dried with vacuum oven [49].3.7

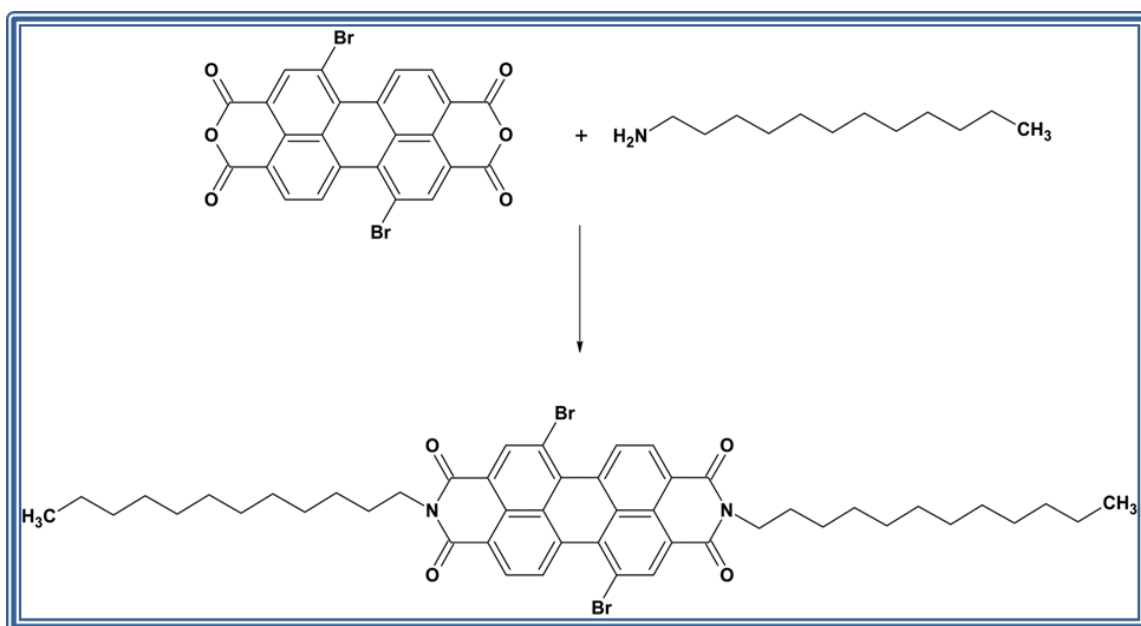
General Reaction Mechanism of Perylene Dyes:

### Step 1: Synthesis of PDA-Br



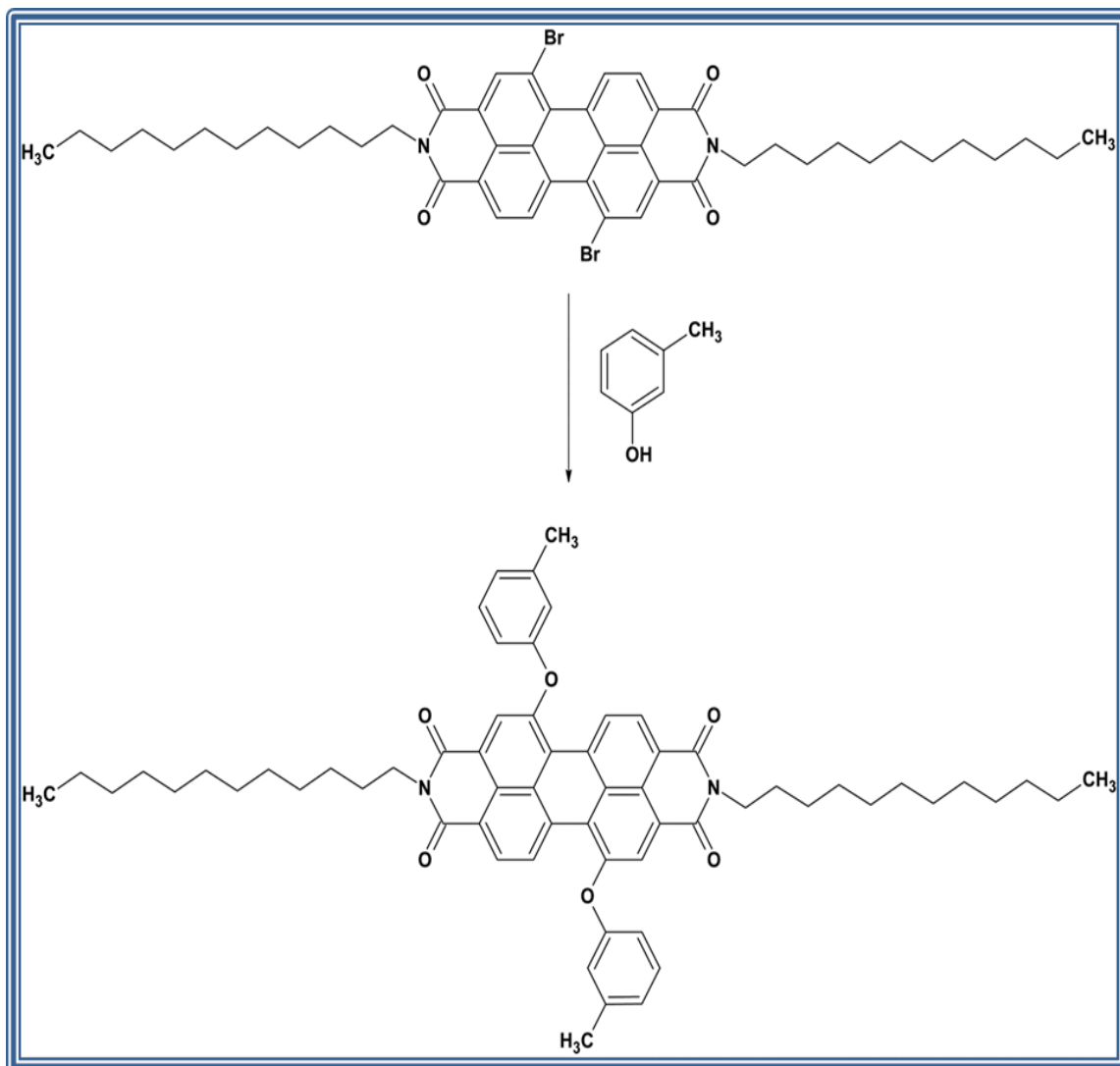
Scheme 3.1: Synthesis of Br-PDA

### Step 2: Synthesis of Br-PDI



Scheme3.2: Synthesis of Br-PDI

### Step 3: Synthesis of Dodecyl-PDI-m-cresol



Scheme3.3: Synthesis of Dodecyl-PDI-m-cresol

## Chapter 4

### DATA AND CONCLUSION

#### 4.1 Calculations of Maximum Extinction Co-efficient ( $\epsilon_{\max}$ )

According to beer-lambert law extinction coefficient can be calculated by

$$\epsilon_{\max} = A/cl$$

A: Absorption

C: concentration

l: length of the cell

$\epsilon_{\max}$  Calculation of PDI-M-Cresol

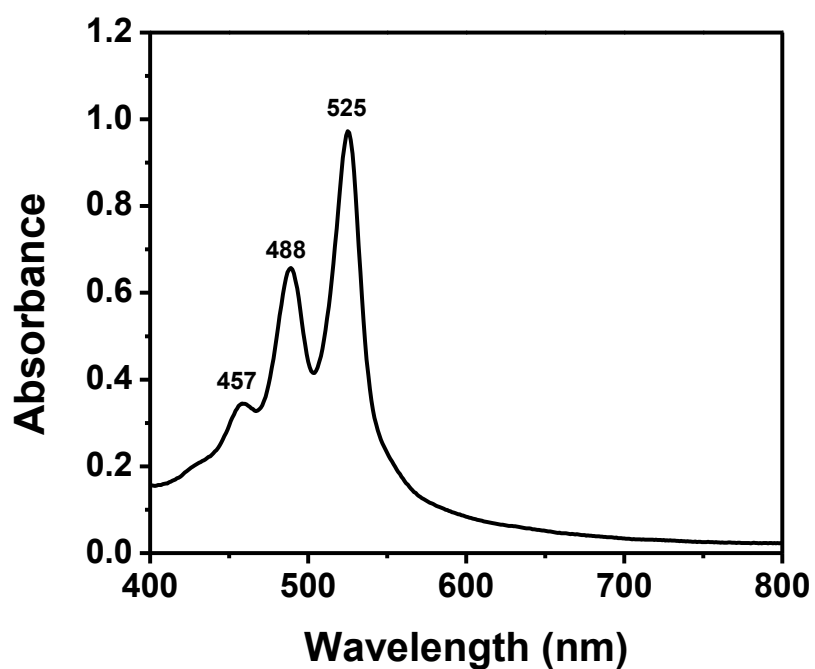


Figure 4.1: Absorption spectrum of PDI-m-Cresol in chloroform at  $1 \times 10^{-5} \text{ M}$

Concentration according to the absorption spectrum of PDI-M-Cresol (figure 4.1) the absorption is 0.97 for the concentration of  $1 \times 10^{-5} \text{ M}$  at the wavelength,  $\lambda_{\text{max}} = 525 \text{ nm}$ .

$$\epsilon_{\text{max}} = \frac{0.97}{1 \times 10^{-5}}$$

$\epsilon_{\text{max}}$  of PDI-M-Cresol =  $97000 \text{ L.mole}^{-1}.\text{cm}^{-1}$

The molar absorptivities of the synthesized compounds were calculated in the similar method and listed below (Table 4.1).

Table 4-1: Molar Absorptivity Data of Br-PDA, Br-PDI and PDI-M-Cresol in CHL

Compound	Concentration (M)	Absorbance	$\lambda_{\max}$	$\epsilon_{\max}(\text{L M}^{-1} \text{cm}^{-1})$
PDA	-----	-----	-----	-----
PDI	$1 \times 10^{-5}$	1.2	526	120000
PDI-m-Cresol	$1 \times 10^{-5}$	0.97	525	97000

Table 4-2: Molar Absorptivity Data of Br-PDA, Br-PDI and PDI-m-Cresol in DMF

Compound	Concentration	Absorbance	$\lambda_{\max}$ (nm)	$\epsilon_{\max}(\text{L.M-1 cm-1})$
Br-PDA	$1 \times 10^{-5}$ M	0.8	518	80000
Br-PDI	$1 \times 10^{-5}$ M	0.9	523	90000
PDI-m-Cresol	$1 \times 10^{-5}$ M	1.1	525	110000

Table 4-3: Molar Absorptivity Data of Br-PDA, Br-PDI and PDI-m-Cresol in NMP

Compound	Concentration	Absorbance	$\lambda_{\max}$ (nm)	$\epsilon_{\max}(\text{L.M}^{-1} \text{cm}^{-1})$
Br-PDA	$1 \times 10^{-5}$ M	0.3	515	30000
Br-PDI	$1 \times 10^{-5}$ M	0.2	523	20000
PDI-m-Cresol	$1 \times 10^{-5}$ M	1.06	525	106000

Table 4-4: Molar Absorptivity Data of Br-PDA, Br-PDI and PDI-m-Cresol in EtOH

Compound	Concentration	Absorbance	$\lambda_{\max}$ (nm)	$\epsilon_{\max}$ (L.M <sup>-1</sup> cm <sup>-1</sup> )
Br-PDA	-----	-----	-----	-----
Br-PDI	-----	-----	-----	-----
PDI-m-Cresol	1×10 <sup>-5</sup> M	0.3	520	30000

Table 4-5: Molar Absorptivity Data of Br-PDA, Br-PDI and PDI-m-Cresol in Acetone

Compound	Concentration (M)	Absorbance	$\lambda_{\max}$ (nm)	$\epsilon_{\max}$ (L.M <sup>-1</sup> cm <sup>-1</sup> )
Br-PDA	-----	-----	-----	-----
Br-PDI	-----	-----	-----	-----
PDI-m-Cresol	1×10 <sup>-5</sup>	0.4	515	40000

## 4.2 Calculations of Half-width of the selected Absorption ( $\Delta\nu_{1/2}$ )

The half-width of the selected maximum absorption is the full width at half maximum and can be calculated from the following equation.

$$\Delta\nu_{1/2} = \nu_{\text{I}} - \nu_{\text{II}}$$

Where,  $\nu_{\text{I}}$ ,  $\nu_{\text{II}}$ : The frequencies from the absorption spectrum in cm<sup>-1</sup>

$\Delta\nu_{1/2}$ : Half-width of the selected maximum absorption in cm<sup>-1</sup>

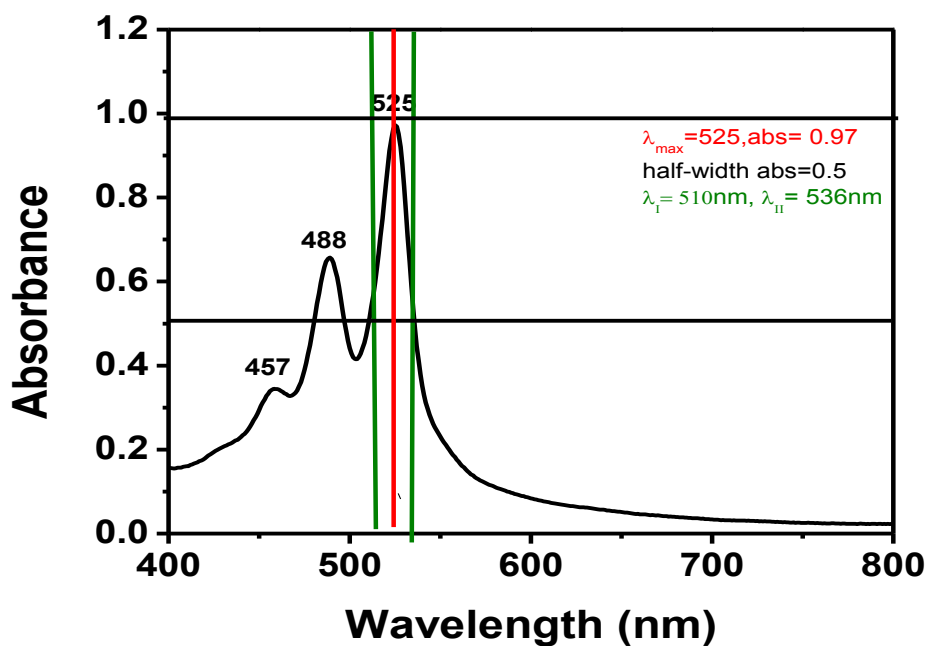


Figure 4-2: Absorption spectrum of PDI-M-Cresol in chloroform and half-width representation

From the Figure 4.2:

$$\lambda_{\text{I}} = 510 \text{ nm}$$

$$\lambda_{\text{I}} = 510 \times \frac{10^{-9} \text{ m}}{1 \text{ nm}} \times \frac{1 \text{ cm}}{10^{-2} \text{ m}} = 5.10 \times 10^{-5} \text{ cm}$$

$$\nu_{\text{I}} = \frac{1}{5.10 \times 10^{-5} \text{ cm}} = 19607.8 \text{ cm}^{-1}$$

$$\lambda_{\text{II}} = 536 \text{ nm}$$

$$\lambda_{\text{II}} = 536 \text{ nm} \times \frac{10^{-9} \text{ m}}{1 \text{ nm}} \times \frac{1 \text{ cm}}{10^{-2} \text{ m}} = 5.36 \times 10^{-5} \text{ cm}$$

$$\nu_{\text{II}} = \frac{1}{5.36 \times 10^{-5} \text{ cm}} = 186507 \text{ cm}^{-1}$$

$$\Delta\nu_{1/2} = \nu_I - \nu_{II} = 19607.8 \text{ cm}^{-1} - 18656.7 \text{ cm}^{-1} = 951.1 \text{ cm}^{-1}$$

It is required to estimate the half-width of the compounds in order to calculate the theoretical radiative lifetimes of the compounds. In the similar manner shown above, the half-width were calculated and presented below in table 4-6

Table 4-6: Half Width of the Selected Absorptions of PDI-M-Cresol and Measured in Different Solvents

Solvent	$\lambda_I(\text{nm})$	$\lambda_{II}(\text{nm})$	$(\text{cm}^{-1})\Delta\nu_{1/2}$
DMF	504	547	59.7
NMP	505	541	1317.7
NMP/M.f	505	542	1351.8
Acetone	597	543	1516.3
Ethanol	500	539	1447.2

Table 4-7: Half Width of the Selected Absorptions of Br-PDI and Measured in Different Solvents

Solvent	$\lambda_I(\text{nm})$	$\lambda_{II}(\text{nm})$	$(\text{cm}^{-1})\Delta\nu_{1/2}$
DMF	503	537	1258.73
DMF/M.F	503	537	1258.73
NMP	500	534	1273.41
CHL	502	531	1087.91

Table 4-8: Half width of the Selected Absorptions of Br-PDA and Measured in Different Solvents

Solvent	$\lambda_I(\text{nm})$	$\lambda_{II}(\text{nm})$	$\Delta\nu_{1/2}(\text{cm}^{-1})$
DMF	495	533	1440.32
DMF/M.F	498	529	1176.7
NMP	498	527	1104.96
NMP/M.F	498	532	1283.1

### 4.3 Calculations of Theoretical Radiative Lifetimes ( $\tau_0$ )

The theoretical radiative lifetime of a molecule refers to the lifetime of an excited molecule theoretically measured in the absence of non-radiative transitions.

$$\tau_0 = \frac{3.5 \times 10^8}{\nu_{\max}^2 \times \epsilon_{\max} \times \Delta\nu_{1/2}}$$

Where,  $\tau_0$ : Theoretical radiative lifetime in ns

$\nu_{\max}$ : Mean frequency of the maximum absorption band in  $\text{cm}^{-1}$

$\epsilon_{\max}$ : The maximum extinction coefficient in  $\text{L. mol}^{-1} \cdot \text{cm}^{-1}$  at the maximum absorption wavelength,  $\lambda_{\max}$

$\Delta\nu_{1/2}$  = Half-width of the selected absorption in units of  $\text{cm}^{-1}$ .

### **Theoretical radiative lifetime of PDI-m-Cresol in chloroform**

With the help of calculated molar absorptivity and half-width of selected absorptions of PDI-M-Cresol:

From the Figure 4.1 and 4.2,  $\lambda_{\max} = 525\text{nm}$

$$\lambda_{\max} = 525\text{nm} \times \frac{10^{-9}\text{m}}{1\text{nm}} \times \frac{1\text{cm}}{10^{-2}\text{m}} = 5.25 \times 10^{-5}\text{cm}$$

$$\nu_{\max} = \frac{1}{5.25 \times 10^{-5}} = 19047.6 \text{ cm}^{-1}$$

$$\nu_{\max}^2 = 3.63 \times 10^8 (\text{cm}^{-1})^2$$

$$\tau_0 = \frac{3.5 \times 10^8}{3.63 \times 10^8 \times 97000 \times 951.1} = 1.05 \times 10^{-8} \text{ s} = 10.5 \text{ ns}$$

With similar method of calculation, theoretical radiative lifetimes were calculated for the other synthesized compounds in chloroform and the data was presented below.

Table 4-9: Theoretical Radiative Lifetimes of PDI-M-Cresol Measured in Different Solvents

Solvent	$\lambda_{\max}$ (nm)	$E_{\max}(\text{L.M}^{-1}.\text{cm}^{-1})$	$\nu^2_{\max}(\text{cm}^{-1})^2$	$\Delta\nu_{1/2} \text{cm}^{-1}$	$\tau_0$ ns
DMF	525	110000	$3.63 \times 10^8$	559.7	15.6
NMP	525	106000	$3.63 \times 10^8$	1317.7	6.9
CHL	525	97000	$3.63 \times 10^8$	951.1	10.5
Acetone	515	40000	$3.8 \times 10^8$	1516.3	15.18
Ethanol	520	30000	$3.7 \times 10^8$	1516.3	20.8

Table 4-10: Theoretical Radiative Lifetimes of Br-PDI Measured in Different Solvents

Solvent	$\lambda_{\max}$ (nm)	$E_{\max}(\text{M}^{-1}.\text{cm}^{-1})$	$\nu^2_{\max}(\text{cm}^{-1})^2$	$\Delta\nu_{1/2}(\text{cm}^{-1})$	$\tau_0$ (ns)
DMF	523	25200	$3.65 \times 10^8$	1258.73	30.2
NMP	523	20000	$3.65 \times 10^8$	1273.41	37.6
CHL	526	120000	$3.65 \times 10^8$	1087.91	7.54

Table 4-11: Theoretical Radiative Lifetimes of Br-PDA Measured in Different Solvents

Solvent	$\lambda_{\max}(\text{nm})$	$E_{\max}(\text{M}^{-1}.\text{cm}^{-1})$	$\nu^2_{\max}(\text{cm}^{-1})^2$	$\Delta\nu_{1/2}(\text{cm}^{-1})$	$\tau_0(\text{ns})$
DMF	515	40000	$3.77 \times 10^8$	1440.32	18.2
NMP	515	30000	$3.77 \times 10^8$	1104.96	28

#### 4.4 Calculations of Fluorescence Rate Constant ( $k_f$ )

The theoretical fluorescence rate constants for the synthesized perylene derivatives are calculated by the equation given below.

$$K_f = \frac{1}{\tau_0}$$

Where,  $K_f$ : Fluorescence rate constant in  $s^{-1}$

$\tau_0$ : theoretical radiative lifetime in s

### Fluorescence Rate constant of PDI-M-Cresol

$$K_f = \frac{1}{1.05 \times 10^{-8}} = 9.5 \times 10^7 \text{ s}^{-1}$$

Table 4-12: Fluorescence Rate Constants Data of PDI-M-Cresol in Different Solvents

Solvent	$\tau_0$ (ns)	$k_f$ ( $s^{-1}$ )
CHL	$1.05 \times 10^{-8}$	$9.5 \times 10^7$
DMF	$1.56 \times 10^{-8}$	$6.4 \times 10^7$
NMP	$6.9 \times 10^{-9}$	$1.4 \times 10^8$
Acetone	$1.5 \times 10^{-8}$	$6.6 \times 10^7$
ETOH	$2.08 \times 10^{-8}$	$4.8 \times 10^7$

Table 4-13: Fluorescence Rate Constants Data of Br-PDI in Different Solvents

Solvent	$\tau_0$ (ns)	$K_f$ ( $s^{-1}$ )
DMF	$3.02 \times 10^{-8}$	$3.3 \times 10^7$
NMP	$3.7 \times 10^{-8}$	$2.7 \times 10^7$
CHL	$7.45 \times 10^{-9}$	$1.3 \times 10^8$

Table 4-14: Fluorescence Rate Constants Data of Br-PDA in Different Solvents

Solvent	$\tau_0$ (ns)	$K_f$ ( $s^{-1}$ )
DMF	$1.82 \times 10^{-8}$	$5.5 \times 10^7$
NMP	$2.8 \times 10^{-8}$	$3.5 \times 10^7$

## 4.5 Calculations of oscillator strength (f)

The oscillator strength is a dimensionless quantity infers the strength of an electronic transition. It can be estimated by the equation below.

$$f = 4.32 \times 10^{-9} \Delta\nu_{1/2} \epsilon_{\max}$$

Where,  $f$ : Oscillator strength

$\Delta\nu_{1/2}$ : Half-width of the selected absorption in units of  $\text{cm}^{-1}$

$\epsilon_{\max}$ : The maximum extinction coefficient in  $\text{L. mol}^{-1} \cdot \text{cm}^{-1}$  at the maximum absorption wavelength,  $\lambda_{\max}$

### Oscillator strength of PDI-M-Cresol in DMF

$$f = 4.32 \times 10^{-9} \times 559.7 \times 110000 = 0.27$$

The following table presents the calculated rate constants of the radiationless deactivation for PDI-M-Cresol

Table 4-15: Oscillator Strength Data of PDI-M-Cresol Measured in Different Solvents

Solvent	$\Delta\nu_{1/2} (\text{cm}^{-1})$	$\epsilon_{\max} (\text{M}^{-1} \cdot \text{cm}^{-1})$	$f$
DMF	559.7	110000	0.27
NMP	1317.7	106000	0.6
CHL	951.1	97000	0.4
Acetone	1516.3	40000	0.26
EtOH	1516.3	30000	0.2

Table 4-16: Oscillator Strength Data of Br-PDI Measured in Different Solvents

Solvent	$\Delta\nu_{1/2}$ (cm <sup>-1</sup> )	$\epsilon_{\max}$ (M <sup>-1</sup> .cm <sup>-1</sup> )	<i>F</i>
DMF	1258.7	25200	0.14
NMP	1273.4	20000	0.11
CHL	1087.91	120000	0.56

Table 4-17: Oscillator Strength Data of Br-PDA Measured in Different Solvents

Solvent	$\Delta\nu_{1/2}$ (cm <sup>-1</sup> )	$\epsilon_{\max}$ (M <sup>-1</sup> .cm <sup>-1</sup> )	<i>F</i>
DMF	1440.32	40000	0.25
NMP	1104.96	30000	0.14

#### 4.6 Calculations of Singlet Energy

Singlet energy is the required amount of energy for the electronic transitions of a chromophore from ground state to an excited state.

$$E_s = \frac{2.86 \times 10^5}{\lambda_{\max}}$$

Where,  $E_s$ : singlet energy in kcal mol<sup>-1</sup>

$\lambda_{\max}$ : the maximum absorption wavelength in Å

Singlet energy of PDI-M-Cresol

$$E_s = \frac{2.86 \times 10^5}{5220} = 54.8 \text{ kcal.mol}^{-1}$$

Similarly, the singlet energies of PDI-M-Cresol were calculated and listed in the following table.

Table 4-18: Singlet Energies Data of PDI-m-Cresol in Different Solvents

Solvent	$\lambda_{\max}$ (Å)	$E_s$ (kcal mol <sup>-1</sup> )
CHL	5250	54.5
DMF	5250	54.5
NMP	5250	54.5
Acetone	5150	55.5
EtOH	5200	55

Table 4-19: Singlet Energies Data of Br-PDI in Different Solvents

Solvent	$\lambda_{\max}$ (Å)	$E_s$ (kcal mol <sup>-1</sup> )
DMF	5230	54.6
NMP	5230	54.6
CHL	5260	54.3

Table 4-20: Singlet Energies Data of Br-PDA in Different Solvents

Solvent	$\lambda_{\max}$ (Å)	$E_s$ (kcal mol <sup>-1</sup> )
DMF	5150	55.5
NMP	5150	55.5

#### 4.7 Calculations of Optical Band Gap Energies ( $E_g$ )

The optical band gap energy gives important information relating to its HOMO and LUMO energy states to be applicable in solar cells and can be calculated from the following equation

$$E_g = \frac{1240 \text{ eV nm}}{\lambda}$$

Where,  $E_g$ : Band gap energy in eV

$\lambda$ : cut-off wavelength of the absorption band can be estimated from the maximum absorption band in nm

## Band gap energy of PDI-M-Cresol

The cut-off wavelength of the absorption band can be estimated from the maximum absorption band (0→0 absorption band) by extrapolating it to zero absorbance as shown below (Figure 4.3

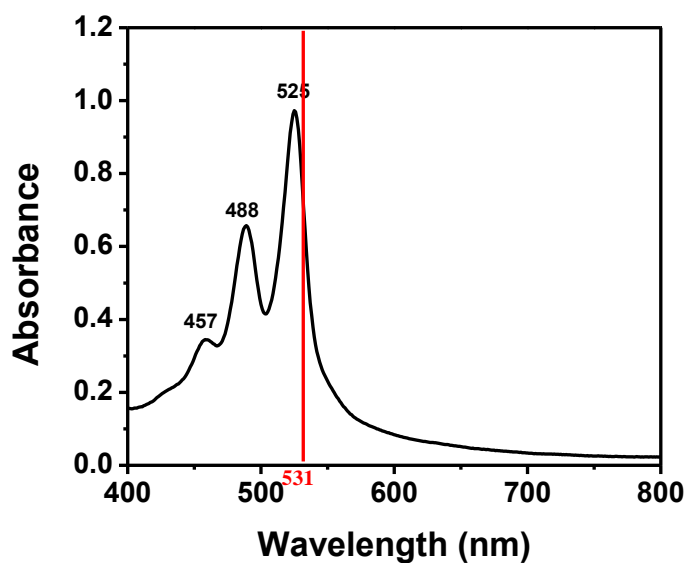


Figure 4-3: Absorption spectrum of PDI-M-Cresol and the cut-off wavelength

$$E_g = \frac{1240 \text{ eVnm}}{531 \text{ nm}} = 2.33 \text{ eV}$$

Similarly, the band gap energies of PDI-M-Cresol were calculated in different solvents and listed in the following table

Table 4-21: Band Gap Energies of PDI-M-Cresol Were Calculated in Different Solvents

Solvents	$\lambda$ (nm)	$E_g$ (eV)
DMF	540	2.3
NMP	542	2.28
Acetone	537	2.31
EtOH	576	2.15
CHL	531	2.33

Table 4-22: Band Gap Energies of Br-PDI Were Calculated in Different Solvents

Solvent	Cut-off $\lambda$ (nm)	$E_g$ (eV)
DMF	552	2.24
NMP	550	2.25
CHL	542	2.28

Table 4-23: Band Gap Energies of Br-PDA Were Calculated in Different Solvents

Solvent	Cut-off $\lambda$ (nm)	$E_g$ (eV)
DMF	579	2.14
NMP	553.8	2.24

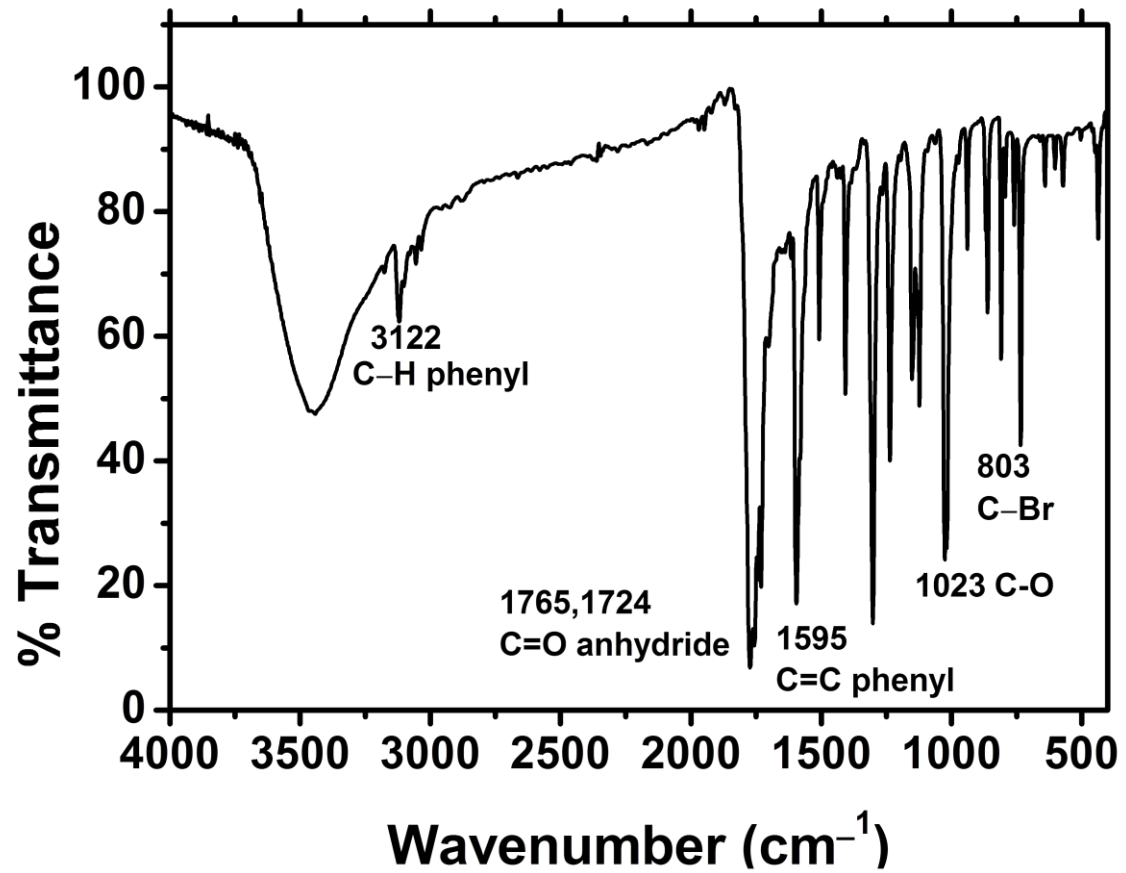


Figure 4.4 FTIR spectrum of Br-PDA

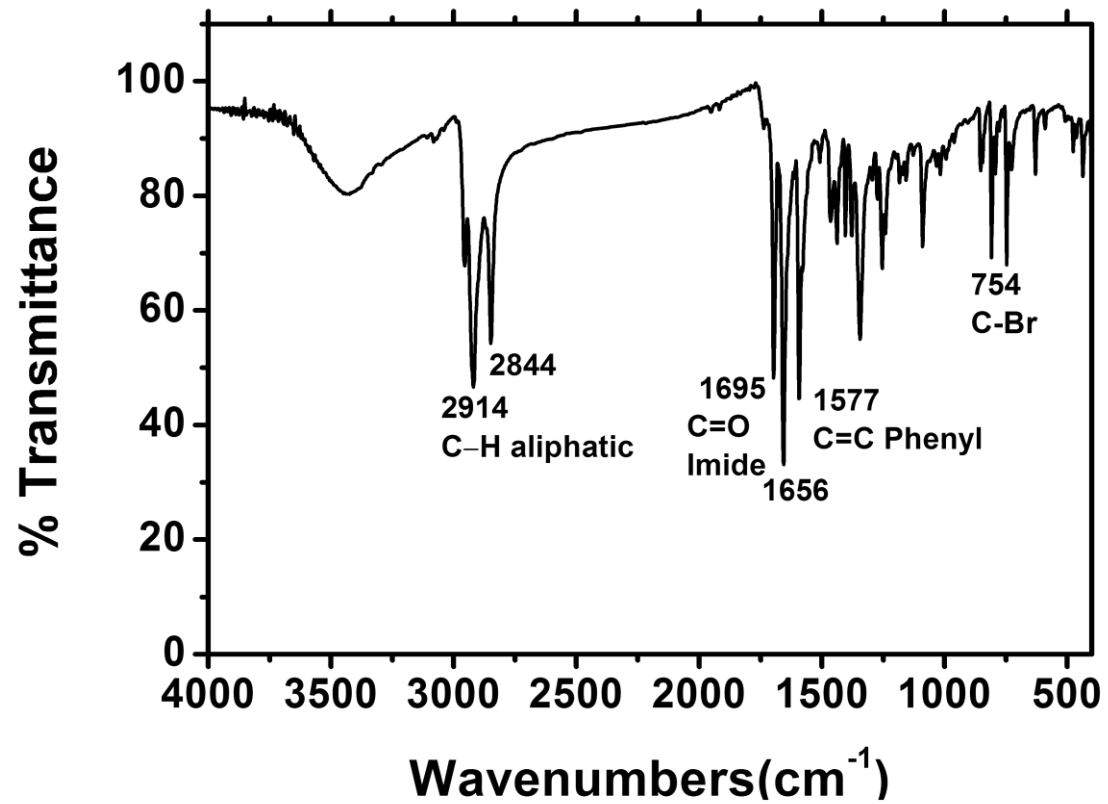


Figure 4.5 FTIR spectrum of Br-PDI

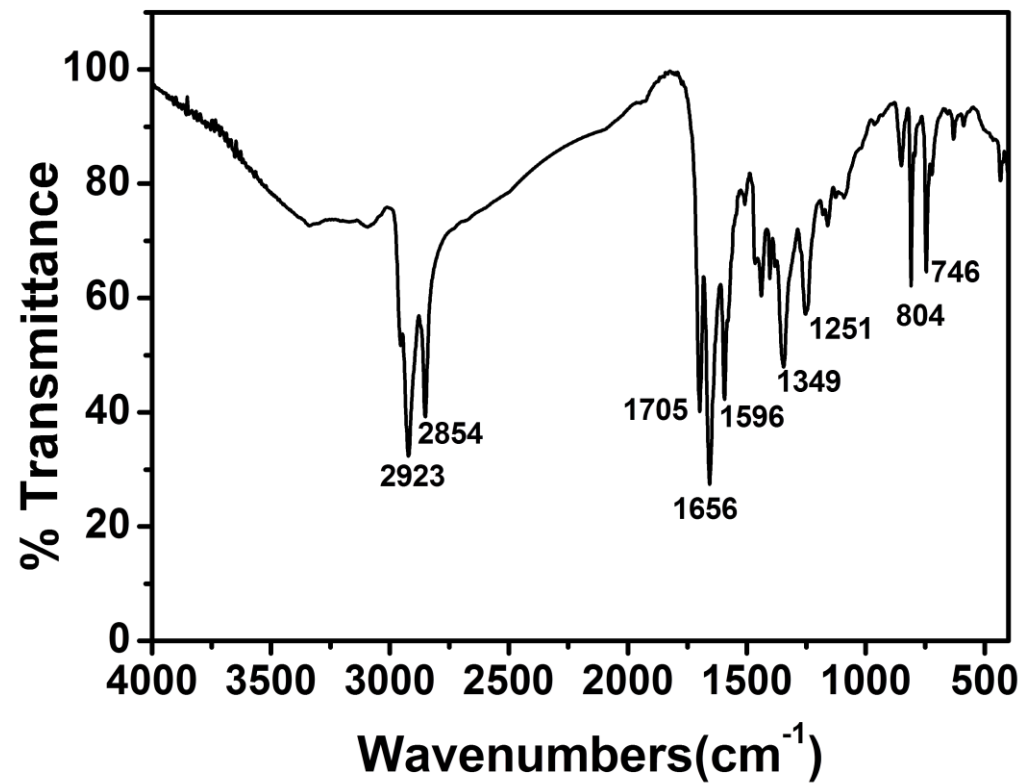


Figure 4.6 FTIR spectrum of PDI-m-Creso

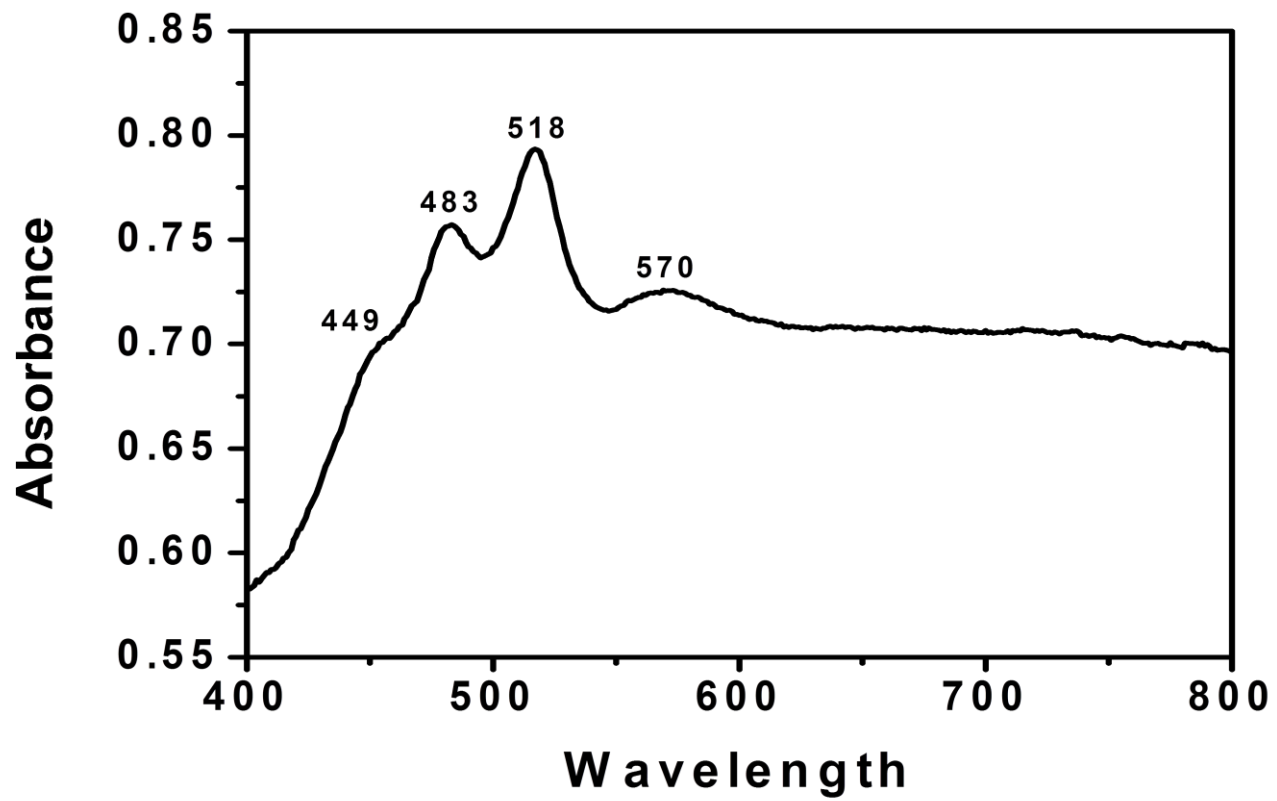


Figure 4.7 UV-vis absorption spectrum of Br-PDA in DMF

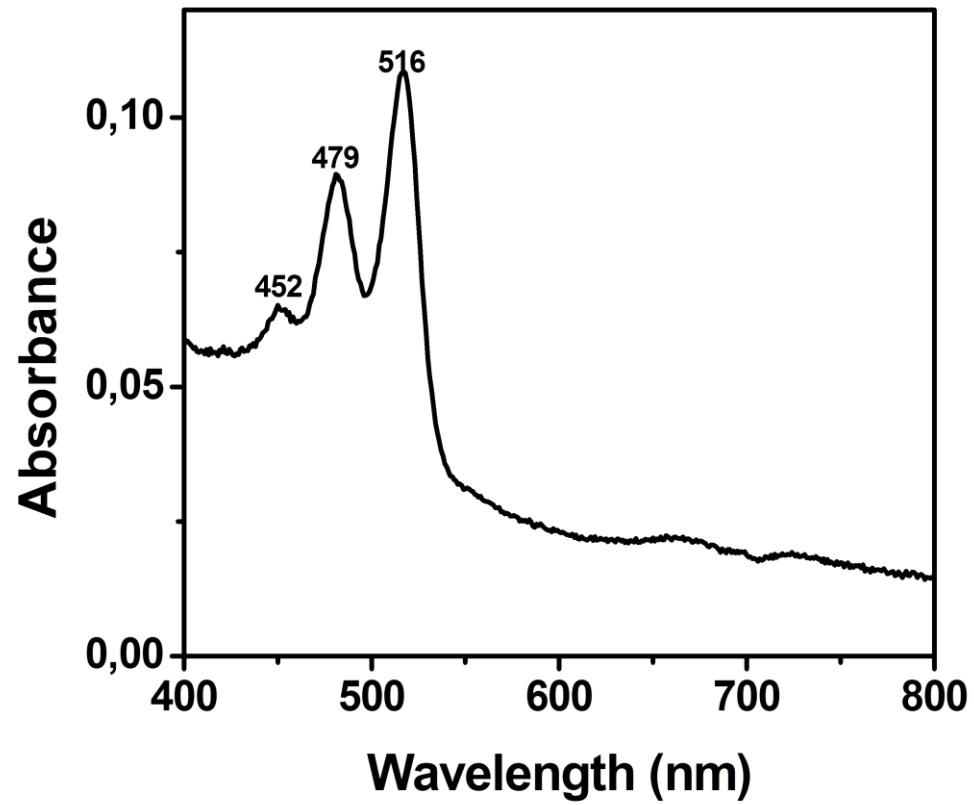


Figure 4.8 UV-vis absorption spectrum of Br-PDA in DMF after micro filtration

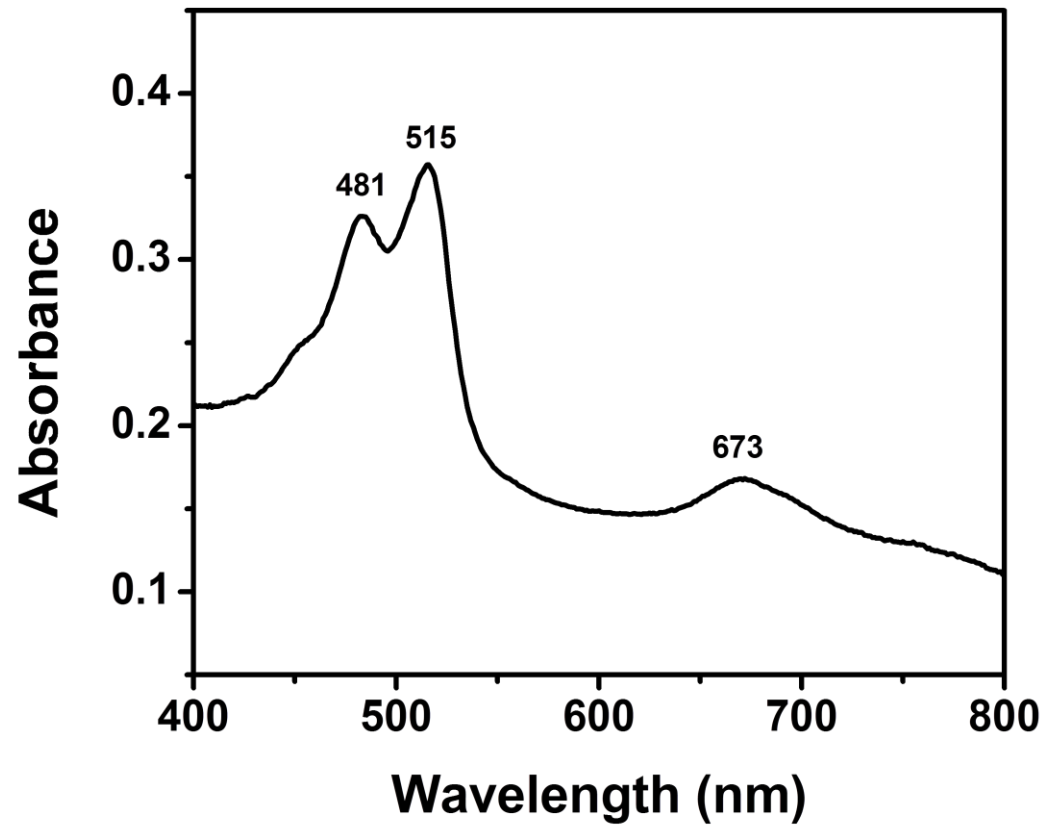


Figure 4.9 UV-vis absorption spectrum of Br-PDA in NMP

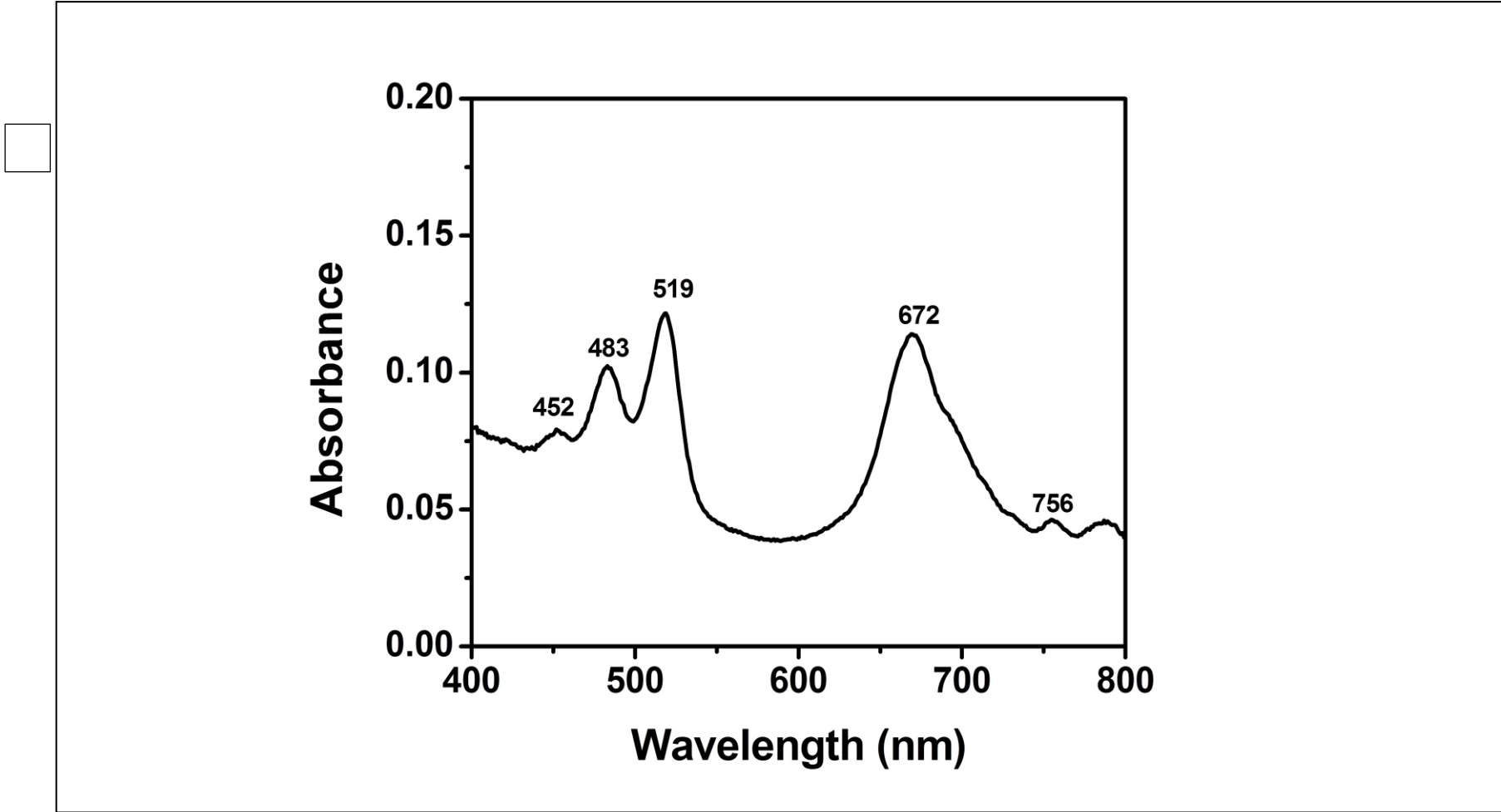


Figure 4.10 UV-vis absorption spectrum of Br-PDA in NMP after micro filtration

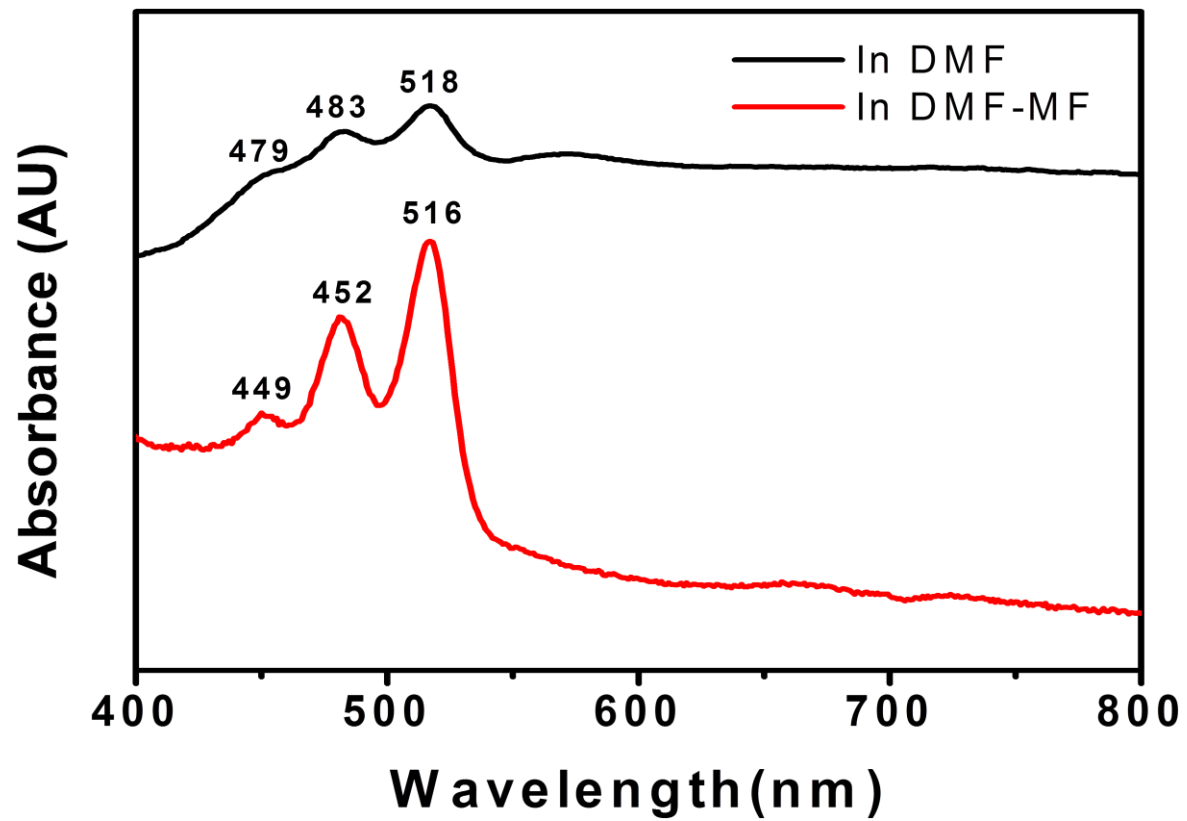


Figure 4.11 overlap UV-vis absorption of Br-PDA in DMF, in DMF after Micro filtration

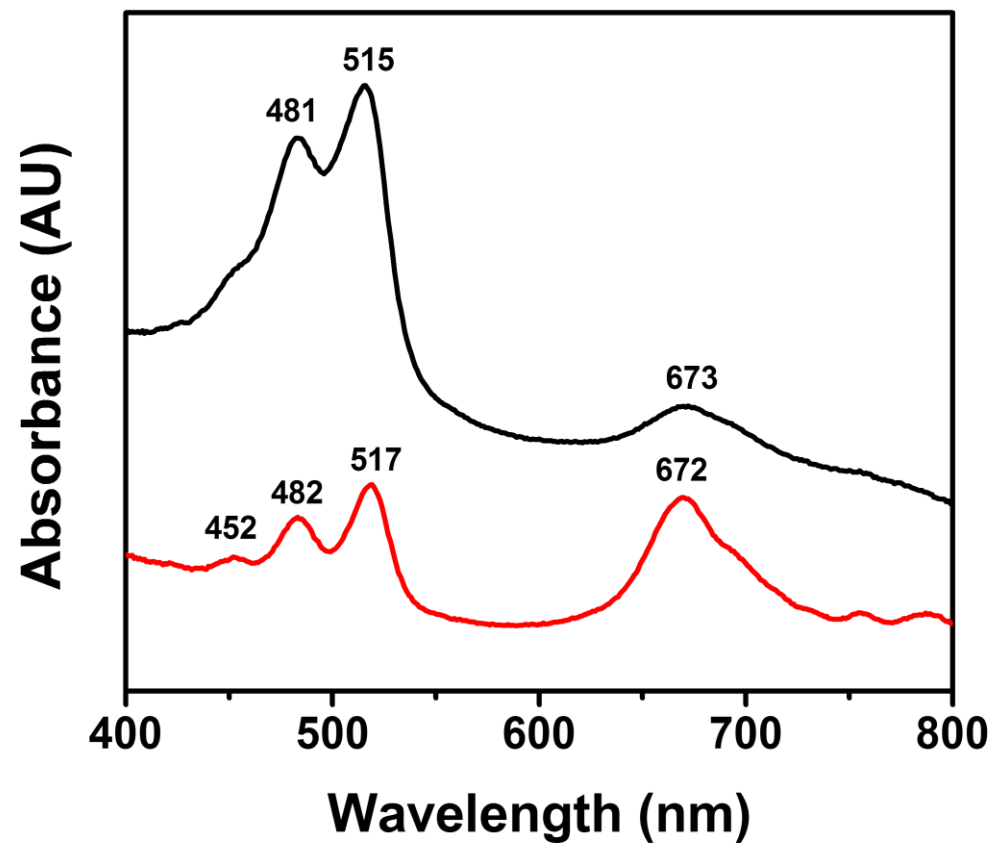


Figure 4.12 overlap of UV-vis absorption of Br-PDA in NMP, NMP after M.F

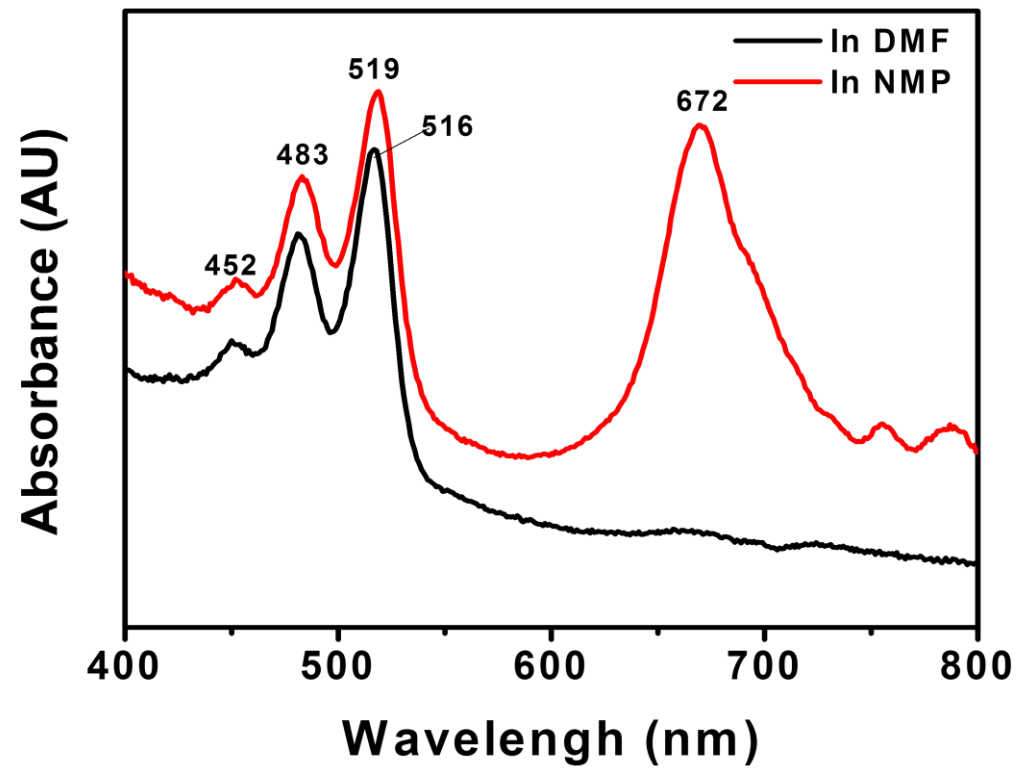


Figure 4.13 overlap of UV-vis absorption of Br-PDA in DMF, NMP

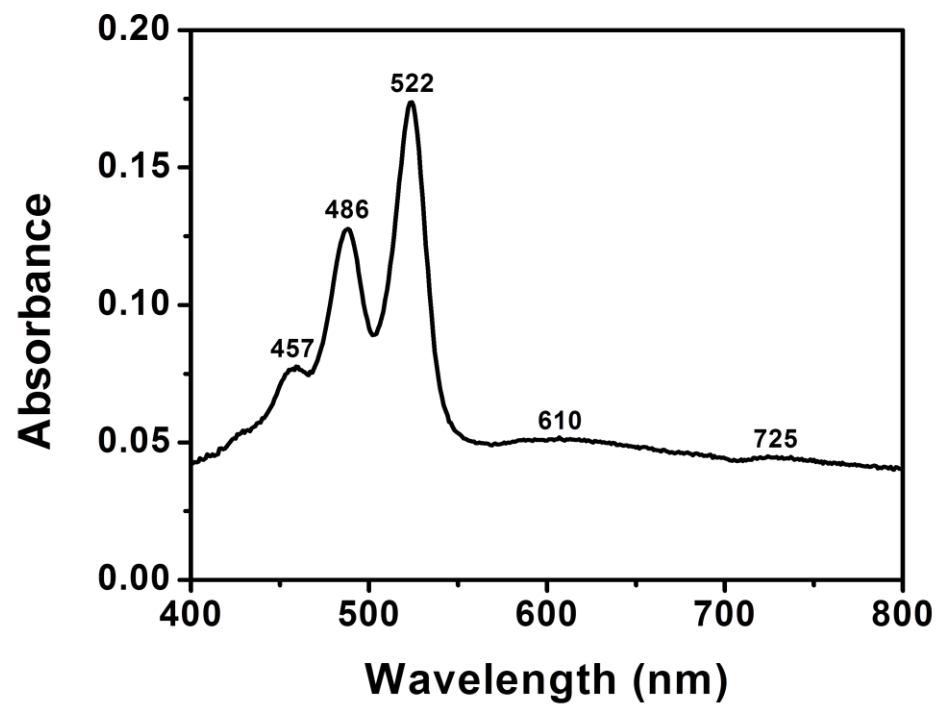


Figure 4.14 UV-vis absorption spectrum of Br-PDI in DMF

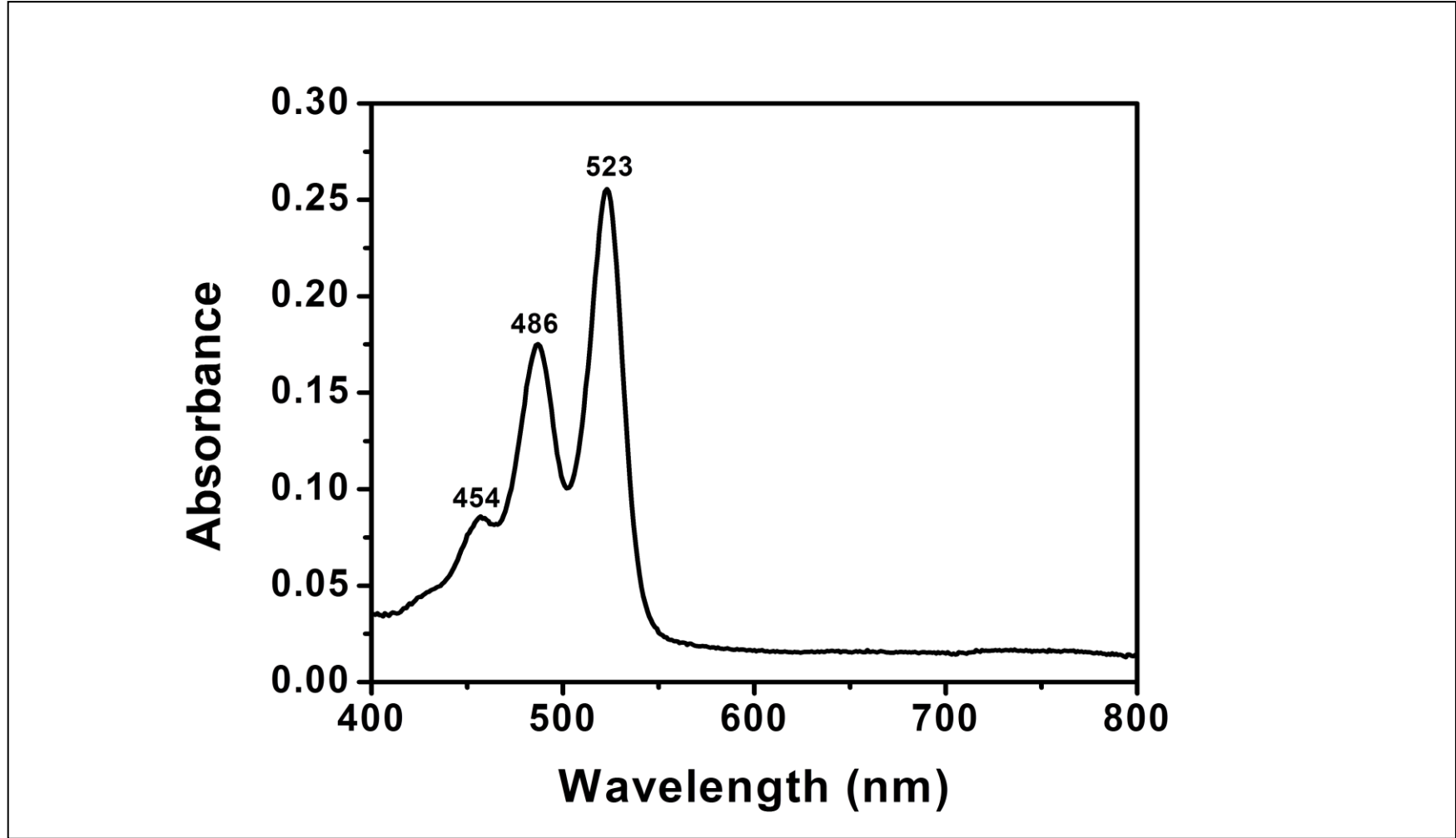


Figure 4.15 UV-vis absorption spectrum of Br-PDI in DMF after M.F

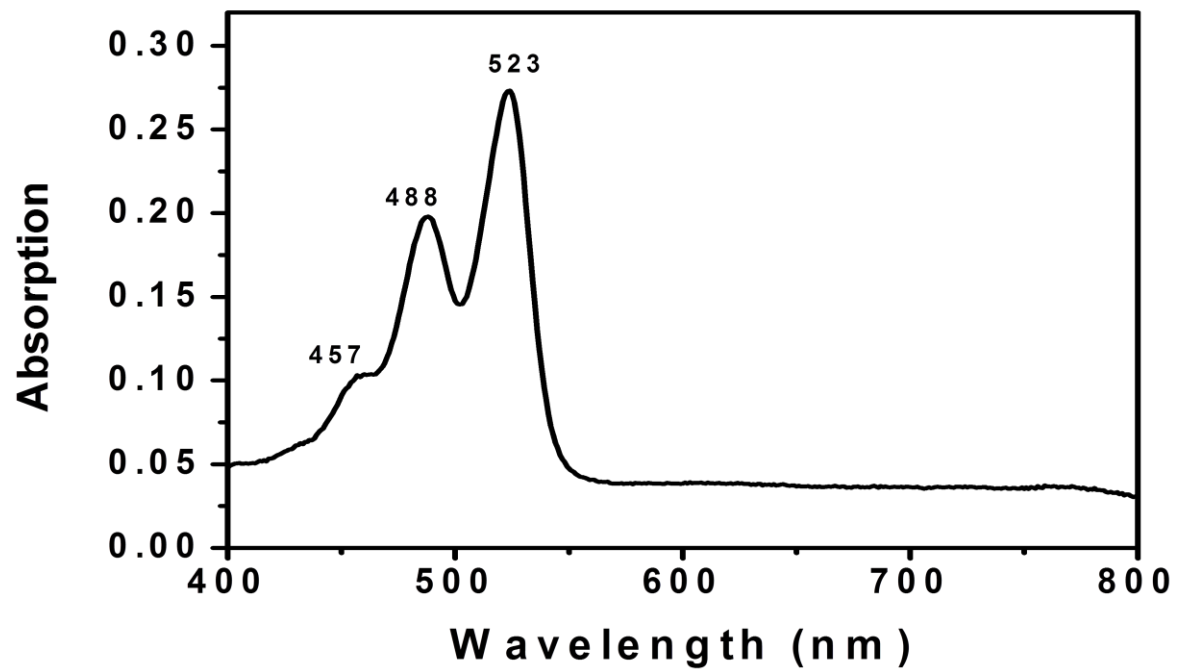


Figure 4.16 UV-vis absorption spectrum of Br-PDI in NMP

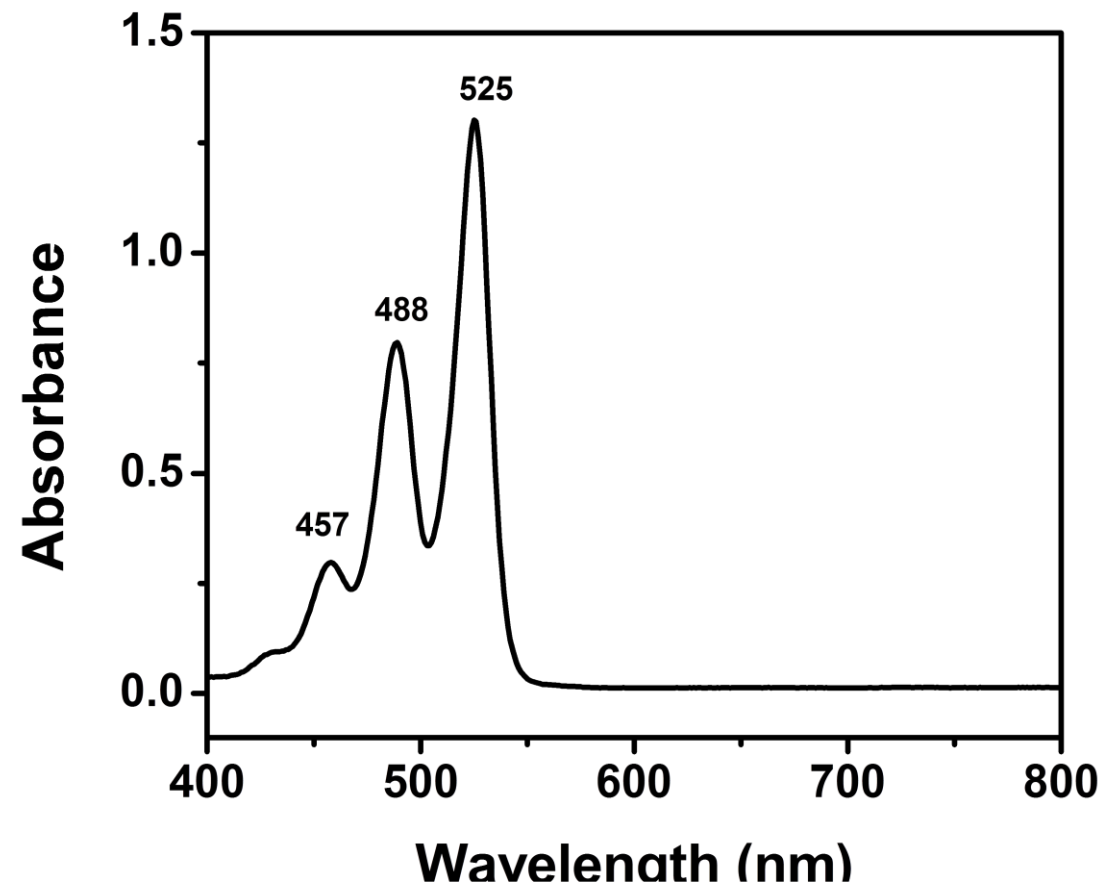


Figure 4.17 UV-vis absorption spectrum of Br-PDI in CHL

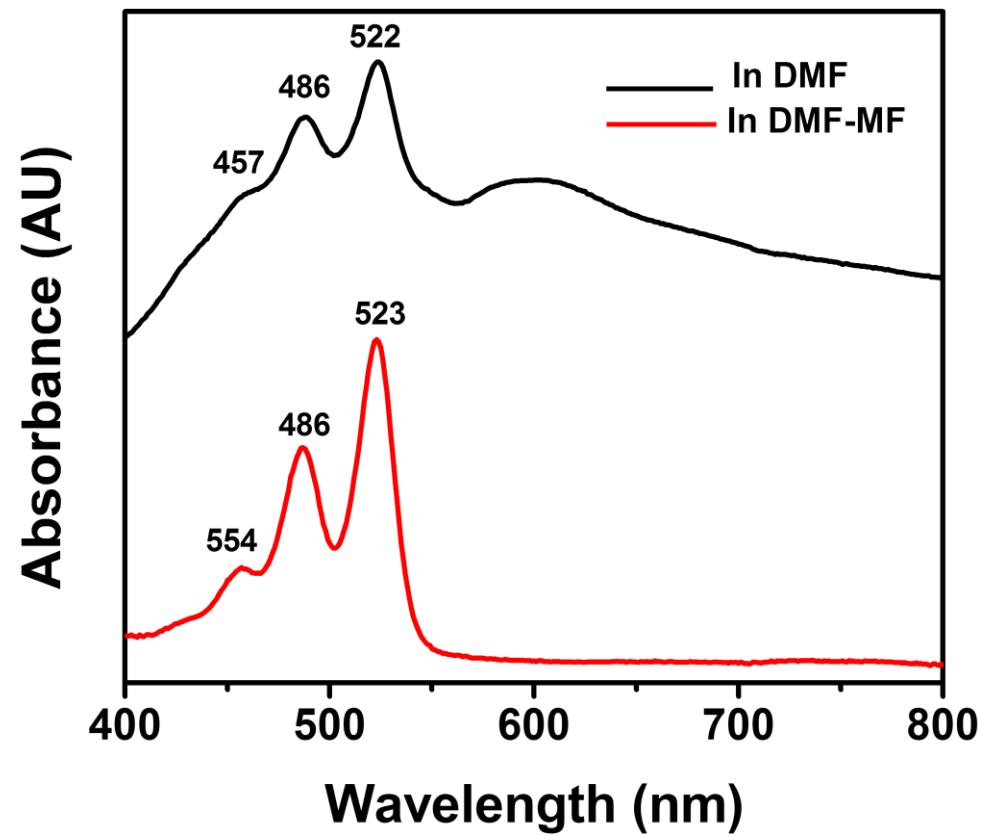


Figure 4.18 UV-vis absorption spectrum of Br-PDI in DMF and DMF after micro filtration

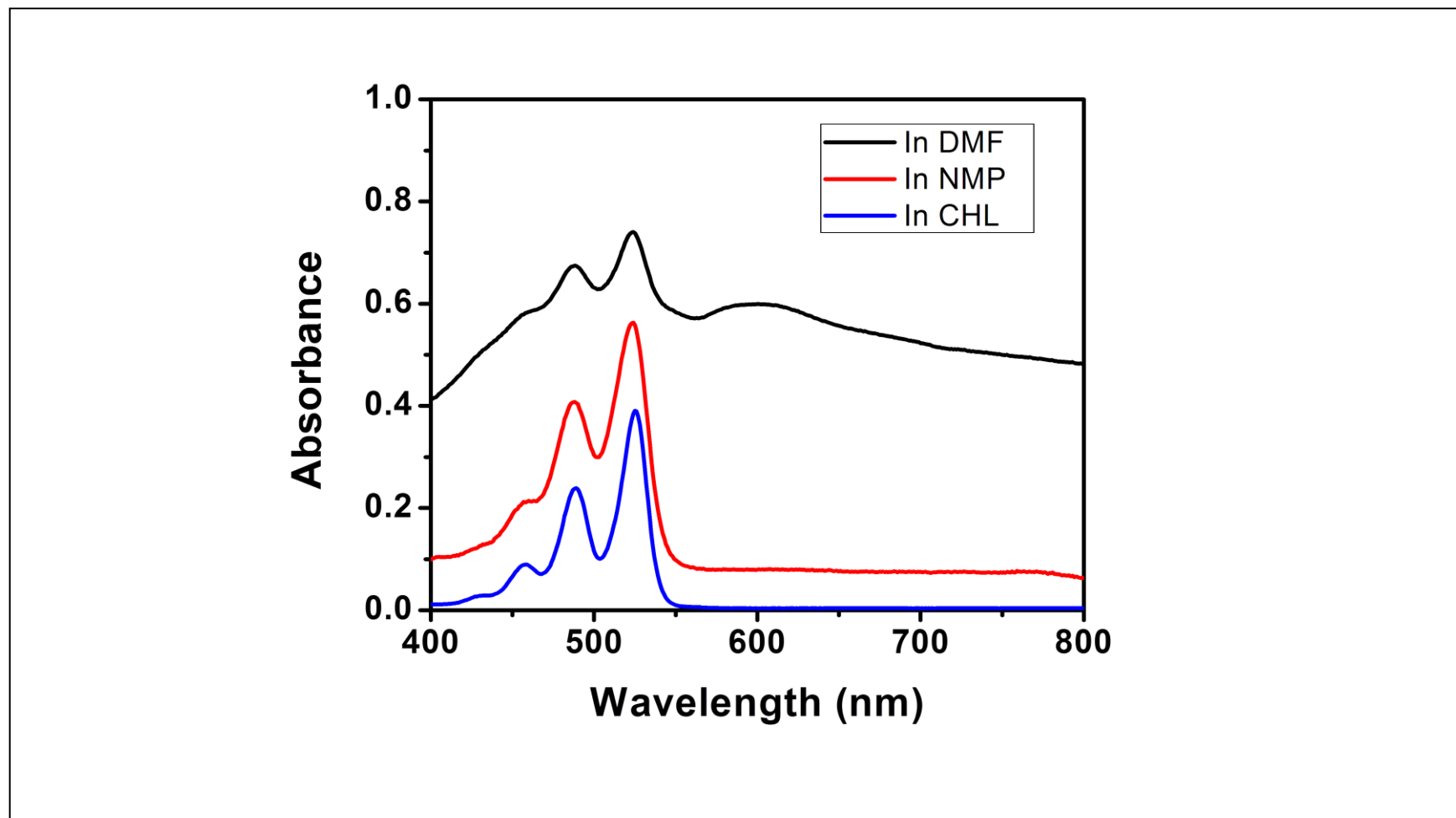


Figure 4.19 UV-vis absorption spectrum of Br-PDI in DMF, NMP and CHL

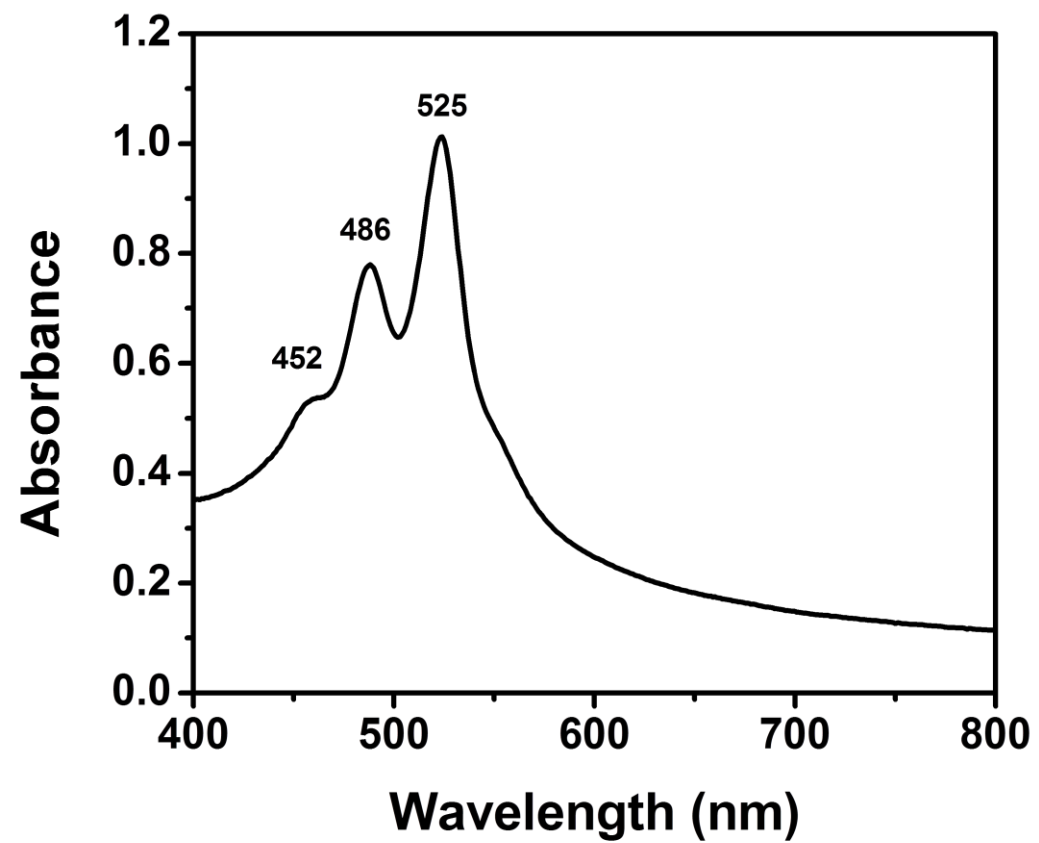


Figure 4.20 UV-vis absorption spectrum of PDI-M-CRESOL IN DMF

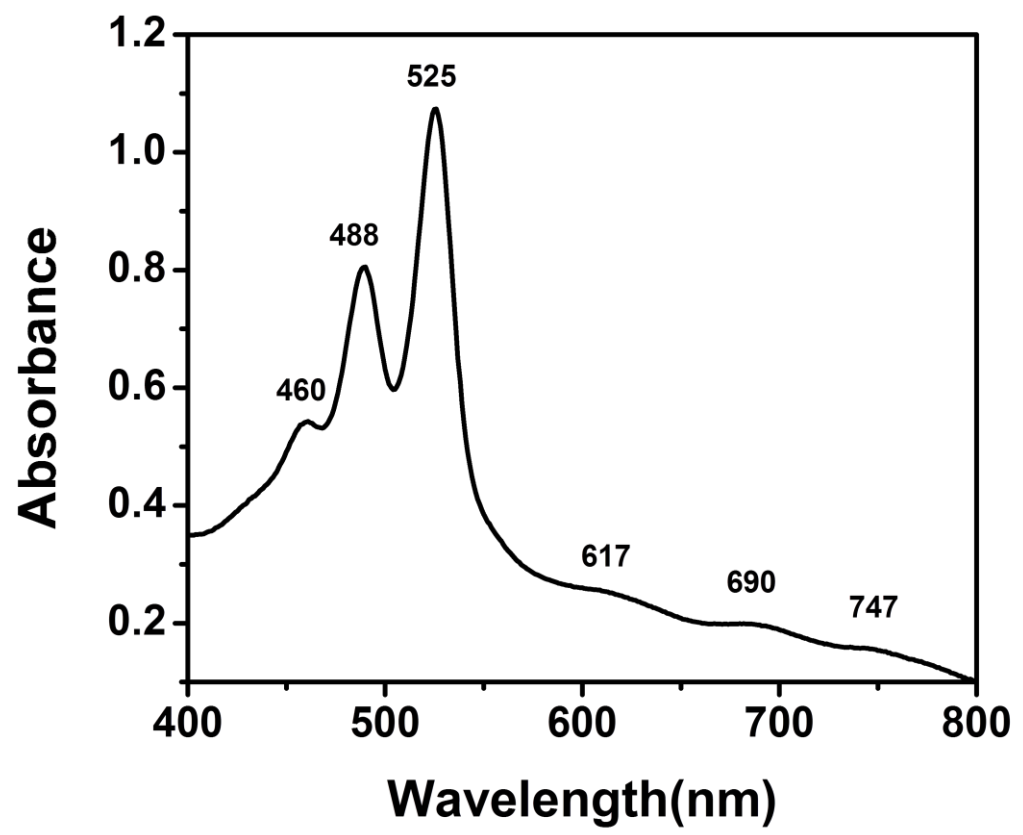


Figure 4.21 UV-vis absorption spectrum of PDI-M-Cresol in NMP

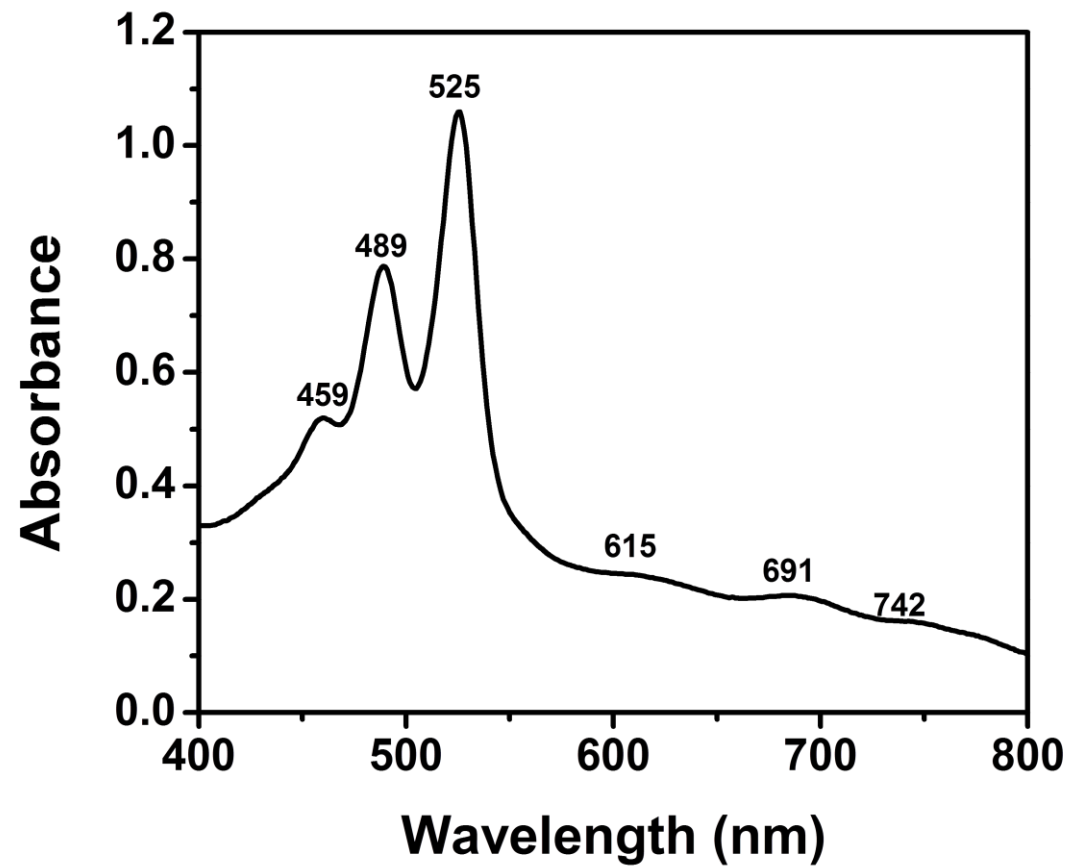


Figure 4.22 UV-vis absorption spectrum of PDI-M-CRESOL IN NMP after micro filtration

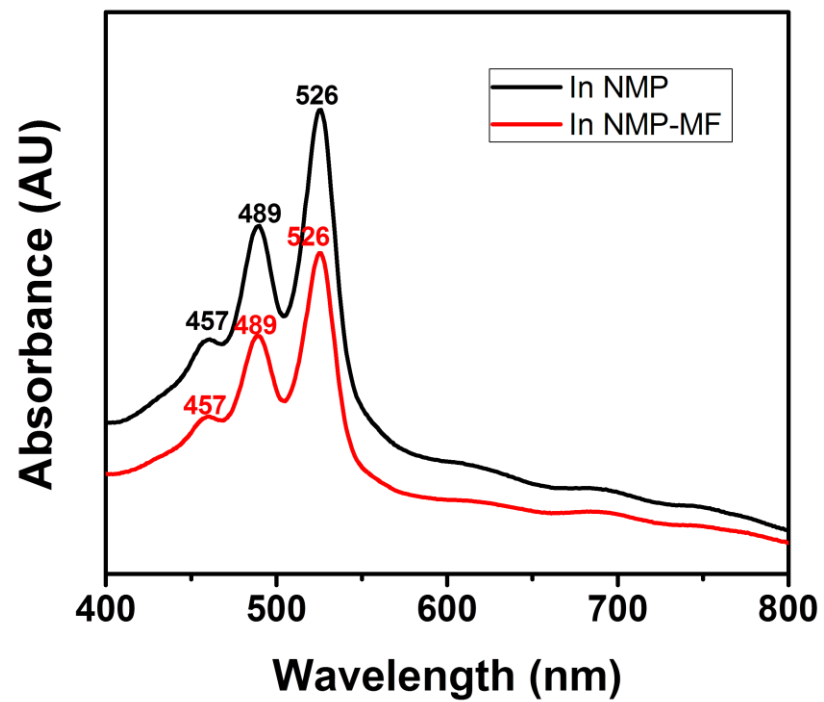


Figure 4.23 UV-vis absorption spectrum of PDI-m-Cresol in NMP and NMP after micro filtration

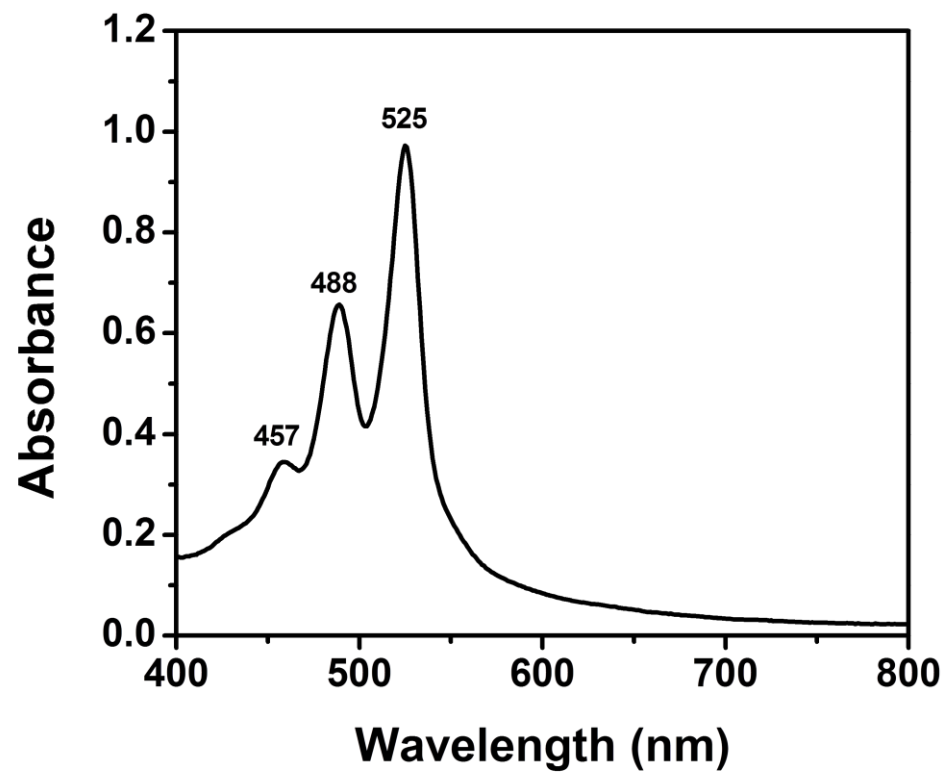


Figure 4.24 UV-vis absorption spectrum of PDI-M-CRESOL in CHL

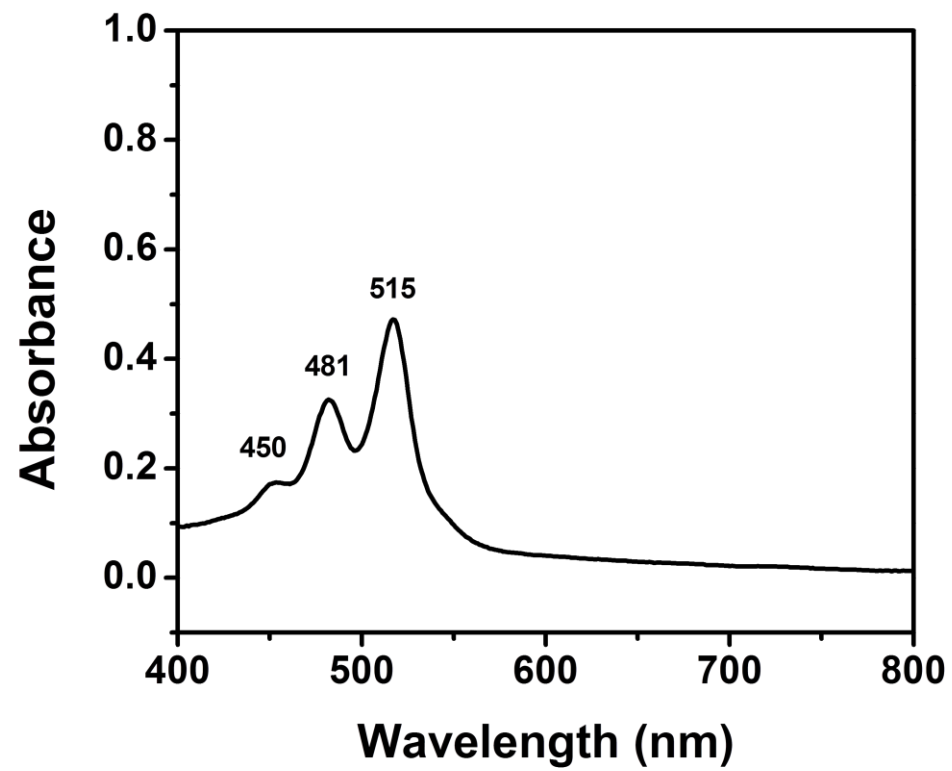


Figure 4.25 UV-vis absorption spectrum of PDI-M-CRESOL in Acetone

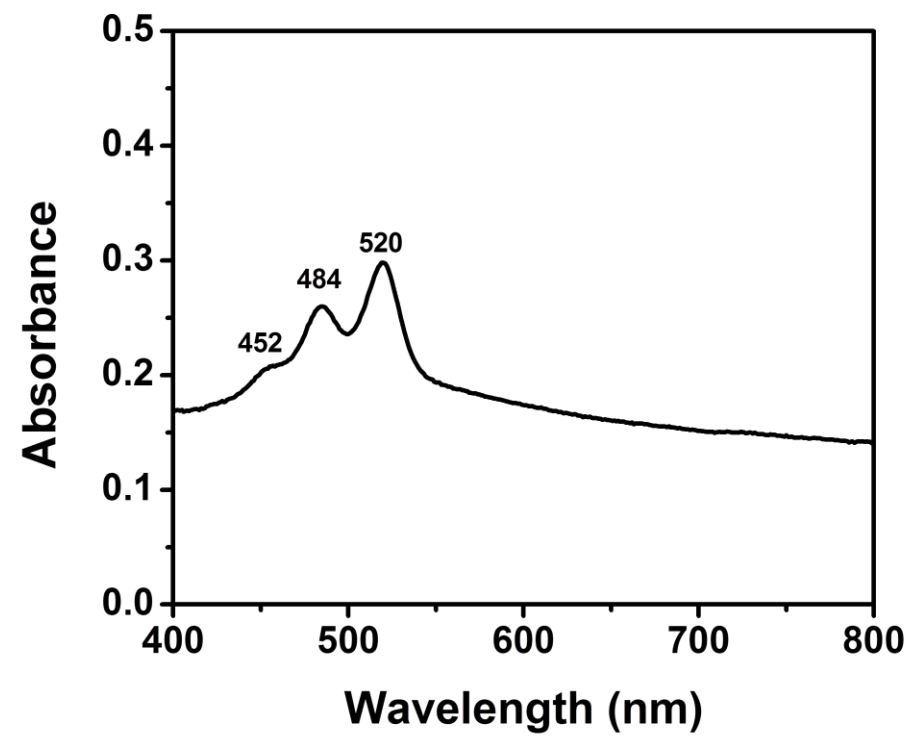


Figure 4.26 UV-vis absorption spectrum of PDI-M-Cresol in Ethanol

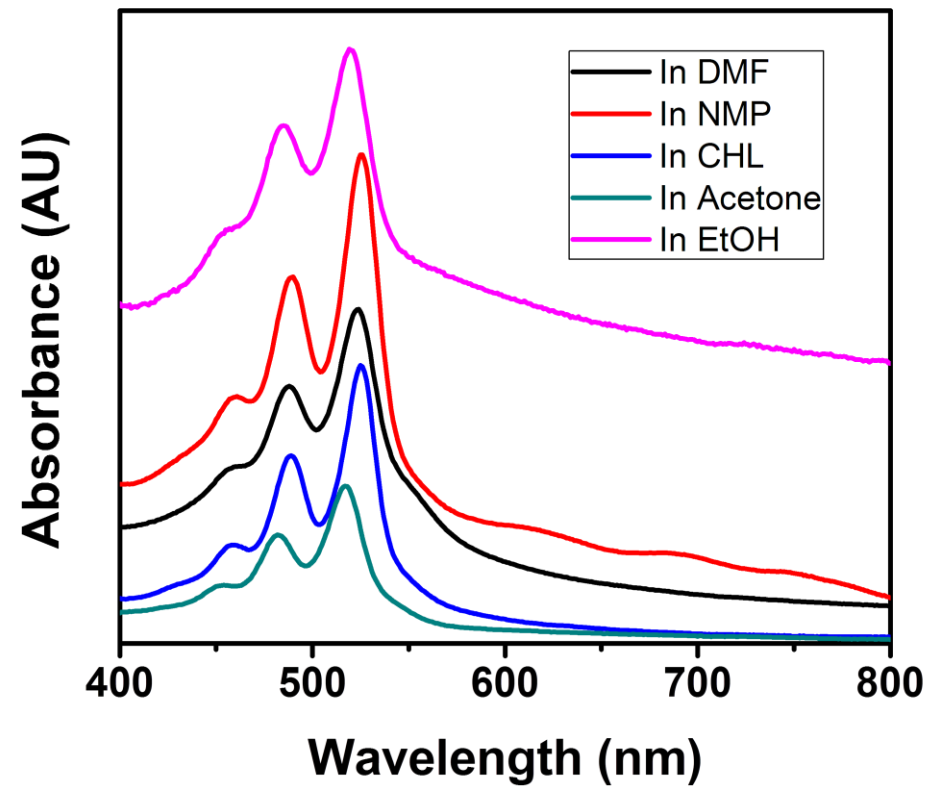


Figure 4.27 UV-vis absorption spectrum of PDI-M-Cresol in DMF,NMP,CHL,Acetone and EtOH

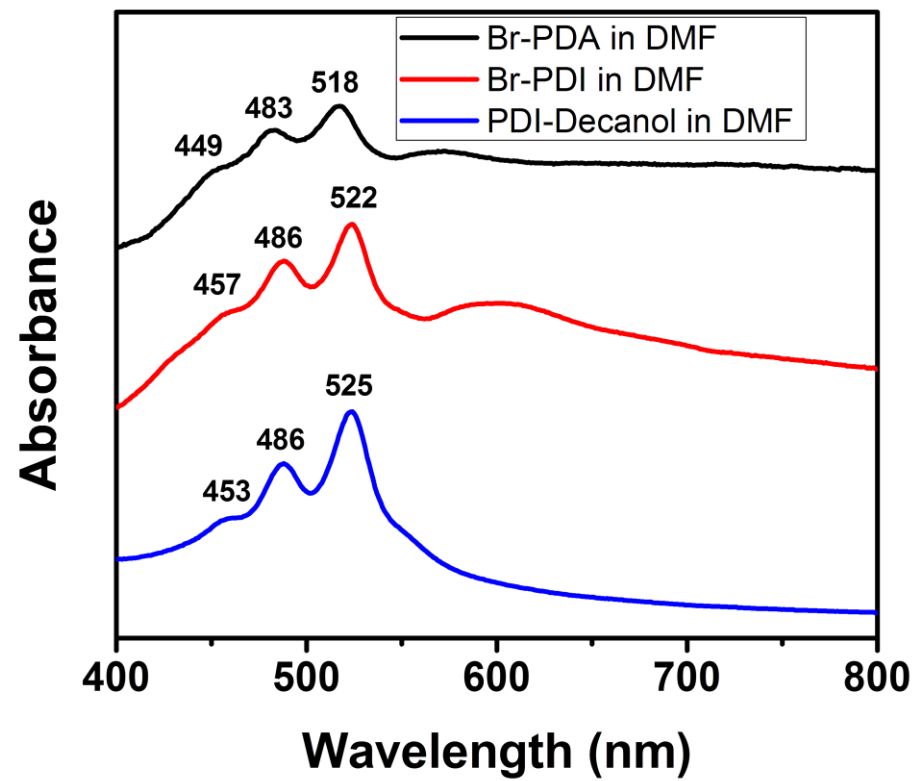


Figure 4.28 UV-Vis absorption spectrum of PDI-m-Cresol, Br-PDI and Br-PDA in DMF

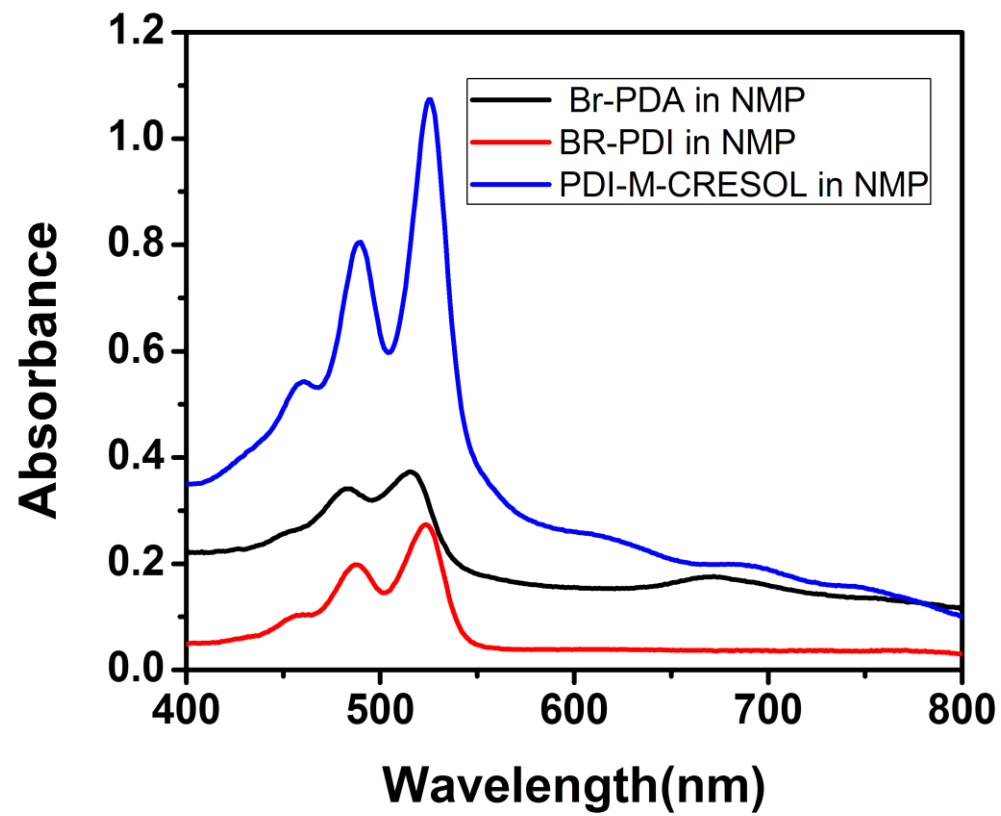


Figure 4.29 UV-Vis absorption spectrum of PDI-m-Cresol, Br-PDI and Br-PDA in NMP

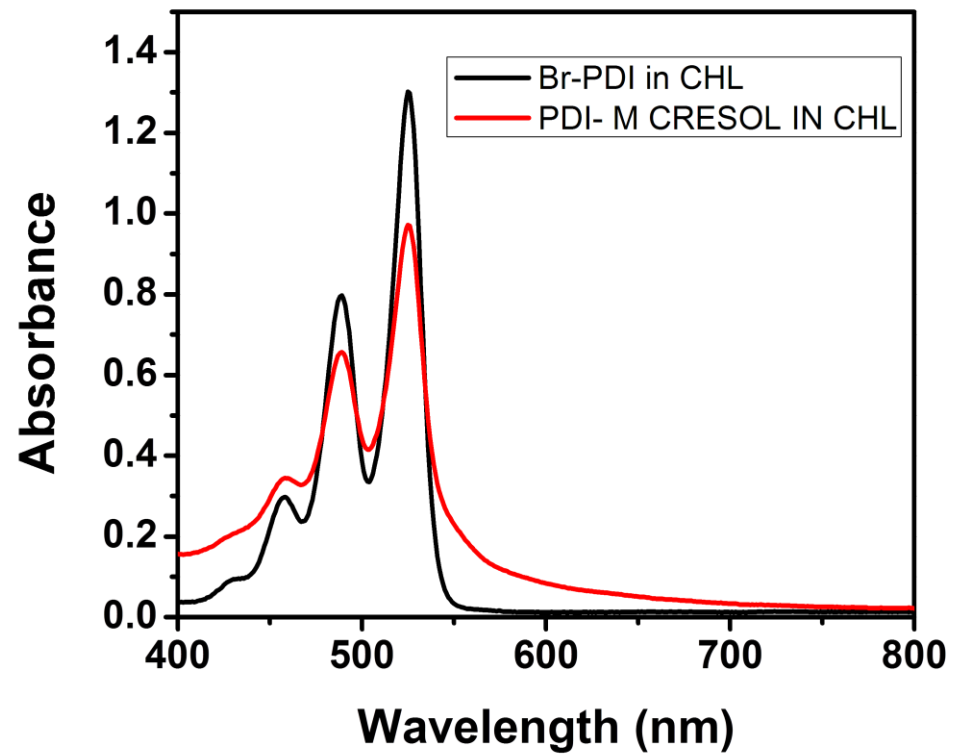


Figure 4.30 UV-V is absorption spectrum of PDI-m-Cresol Br-PDI in CHL

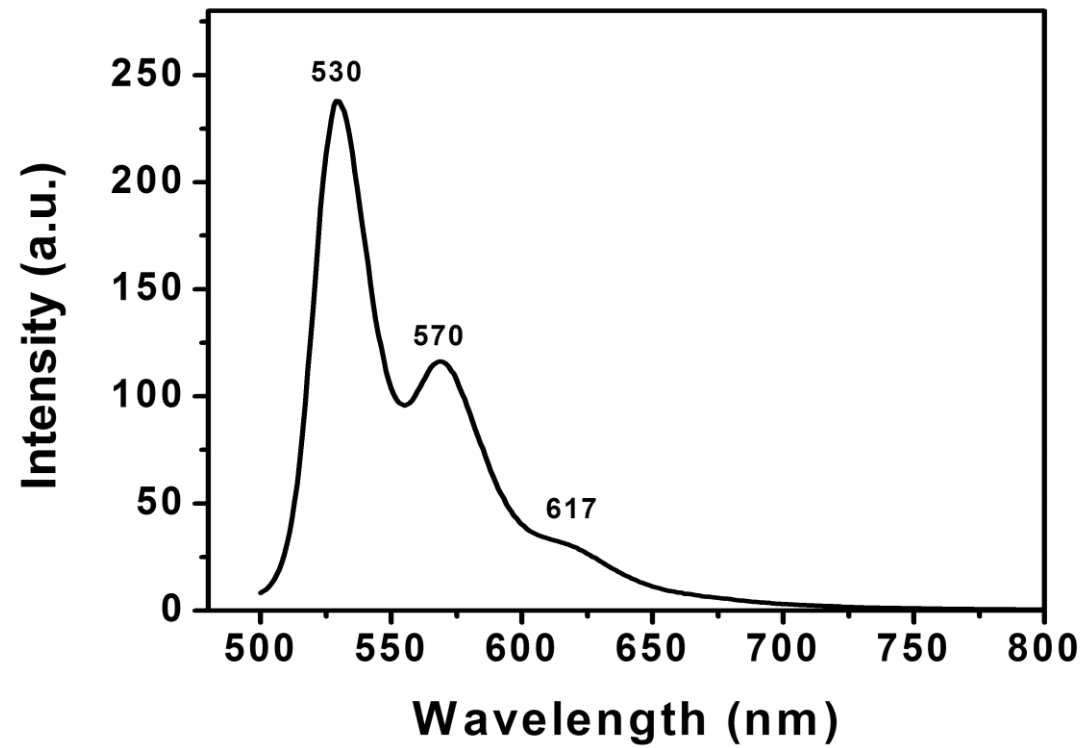


Figure 4.31 Emission spectrum ( $\lambda_{exc}=485\text{nm}$ ) of Br-PDA in DMF

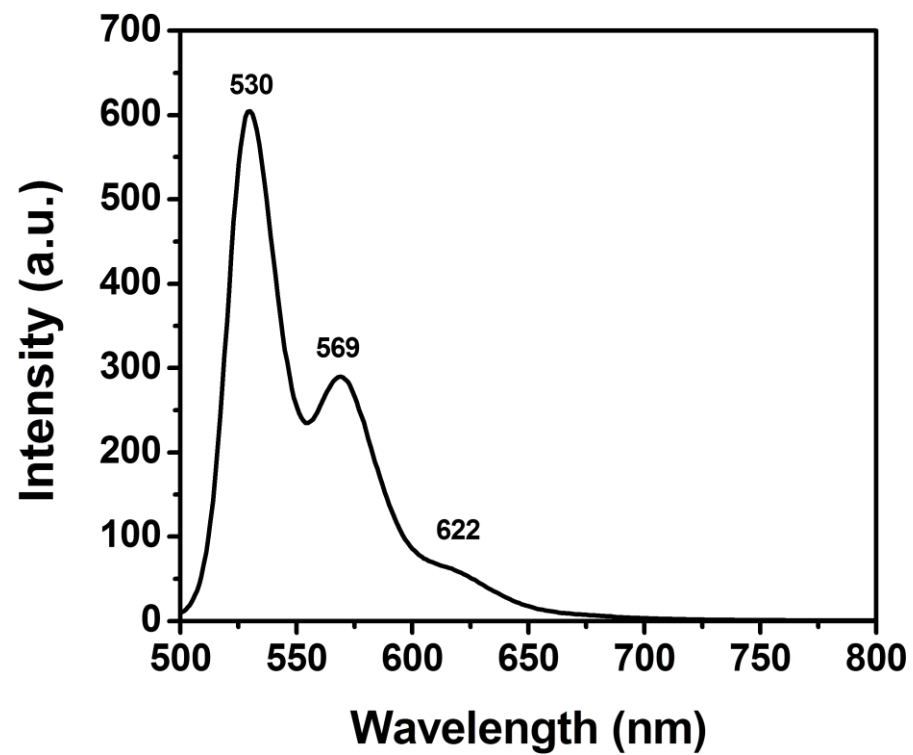


Figure 4.32 Emission spectrum ( $\lambda_{exc}=485\text{nm}$ ) of Br-PDA in DMF after micro filtration

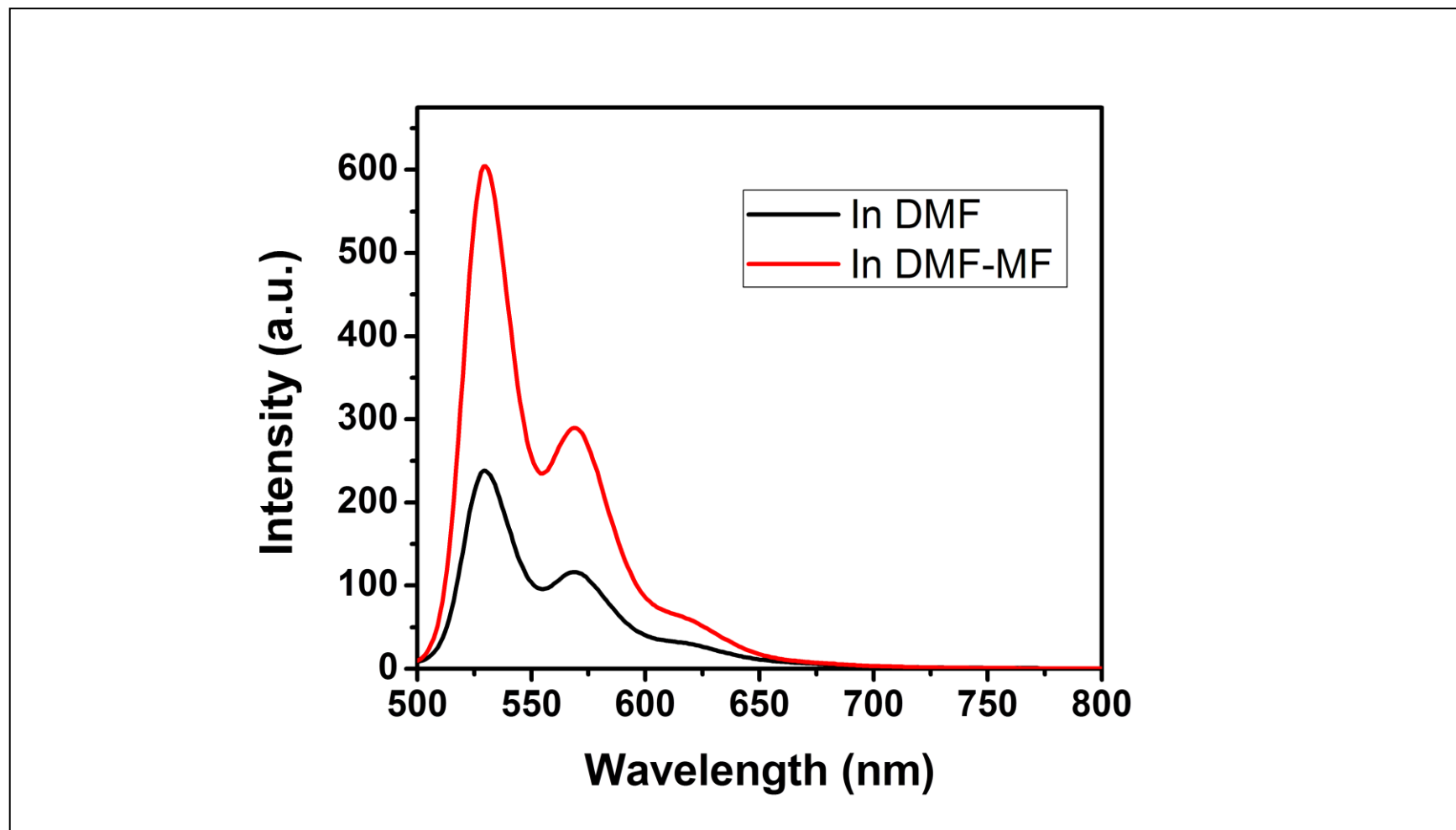


Figure 4.33 Emission spectrum ( $\lambda_{exc}=485\text{nm}$ ) of Br-PDA in DMF and in DMF after micro filtration

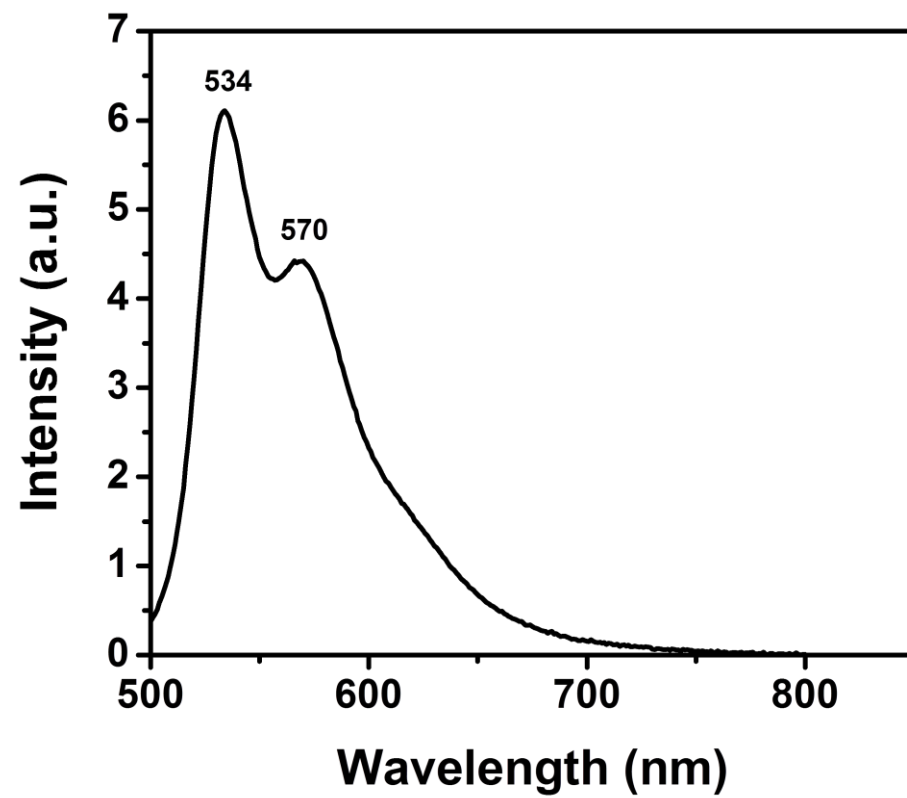


Figure 4.34 Emission spectrum ( $\lambda_{exc}=485\text{nm}$ ) of Br-PDA in NMP

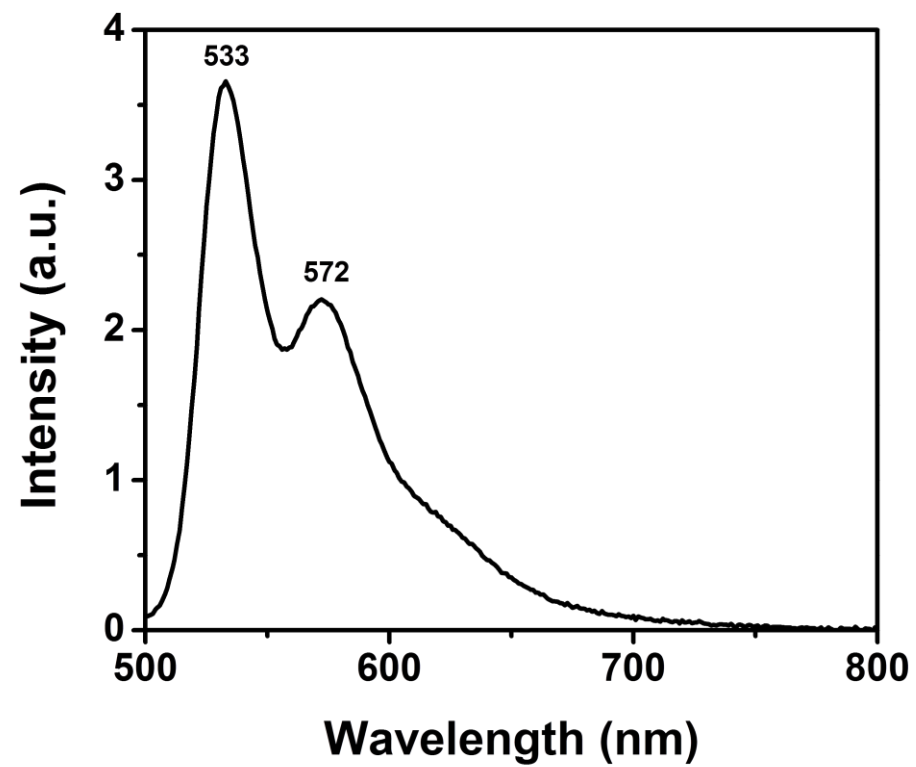


Figure 4.35 Emission spectrum ( $\lambda_{exc}=485\text{nm}$ ) of Br-PDA in NMP after micro filtration

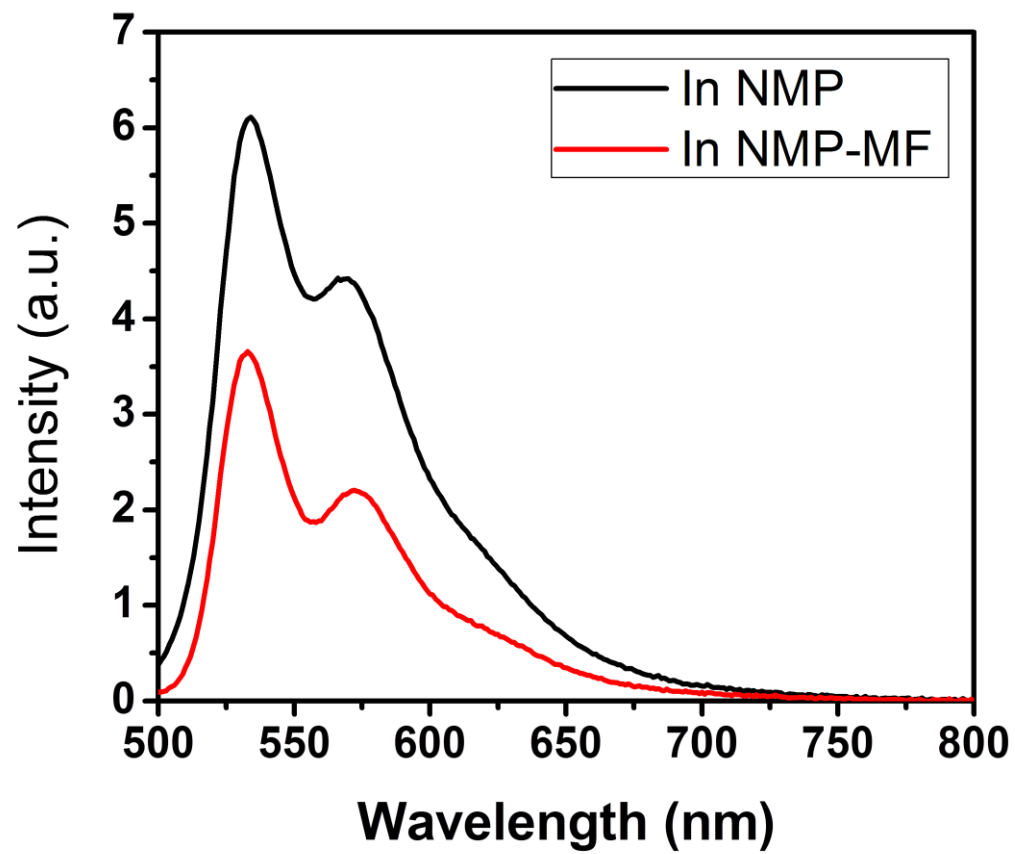


Figure 4.36 Emission spectrum ( $\lambda_{exc}=485\text{nm}$ ) of Br-PDA in NMP and in NMP after micro filtration

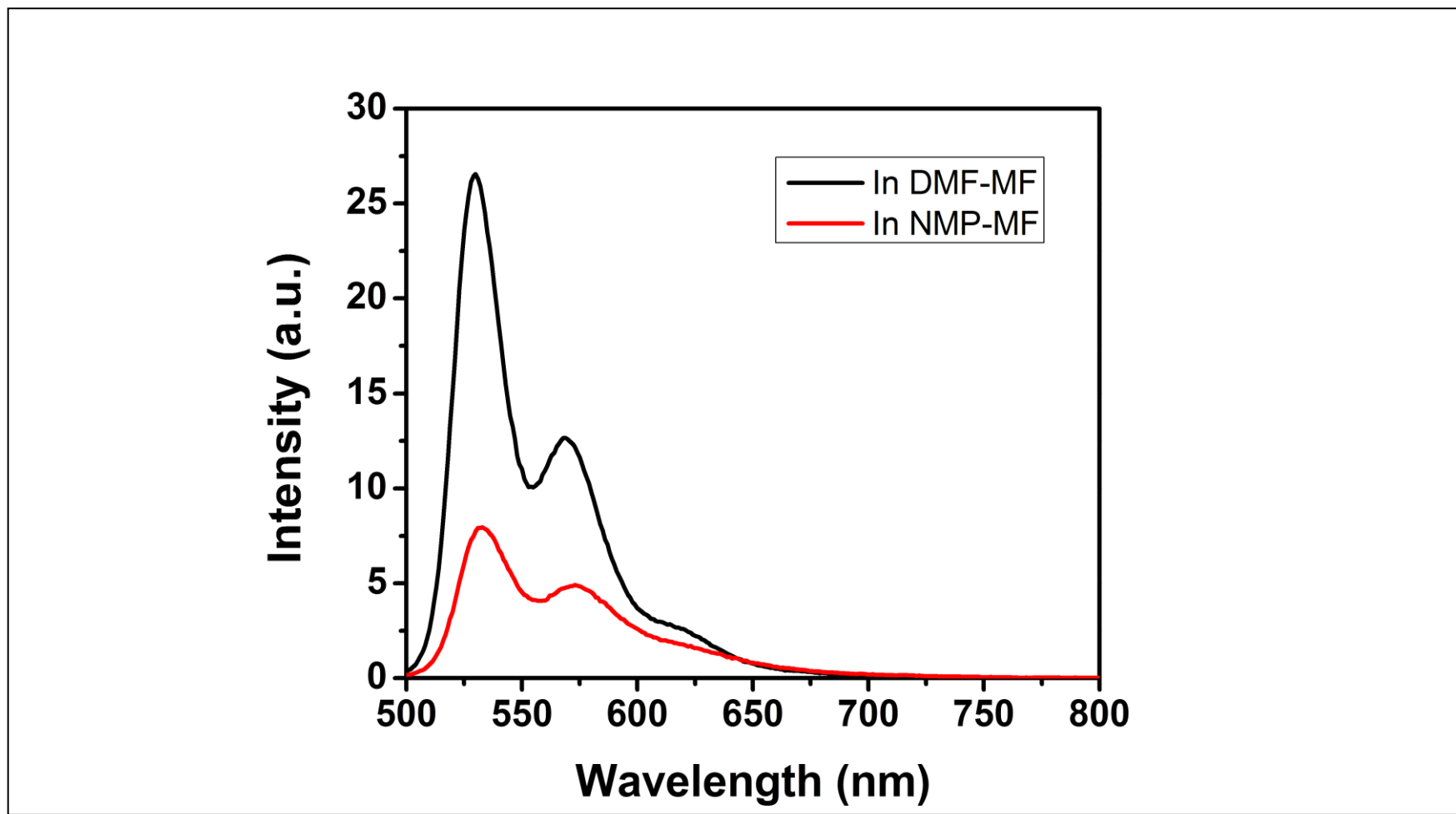


Figure 4.37 Emission spectrum ( $\lambda_{exc}=485\text{nm}$ ) of Br-PDA in NMP and in DMF

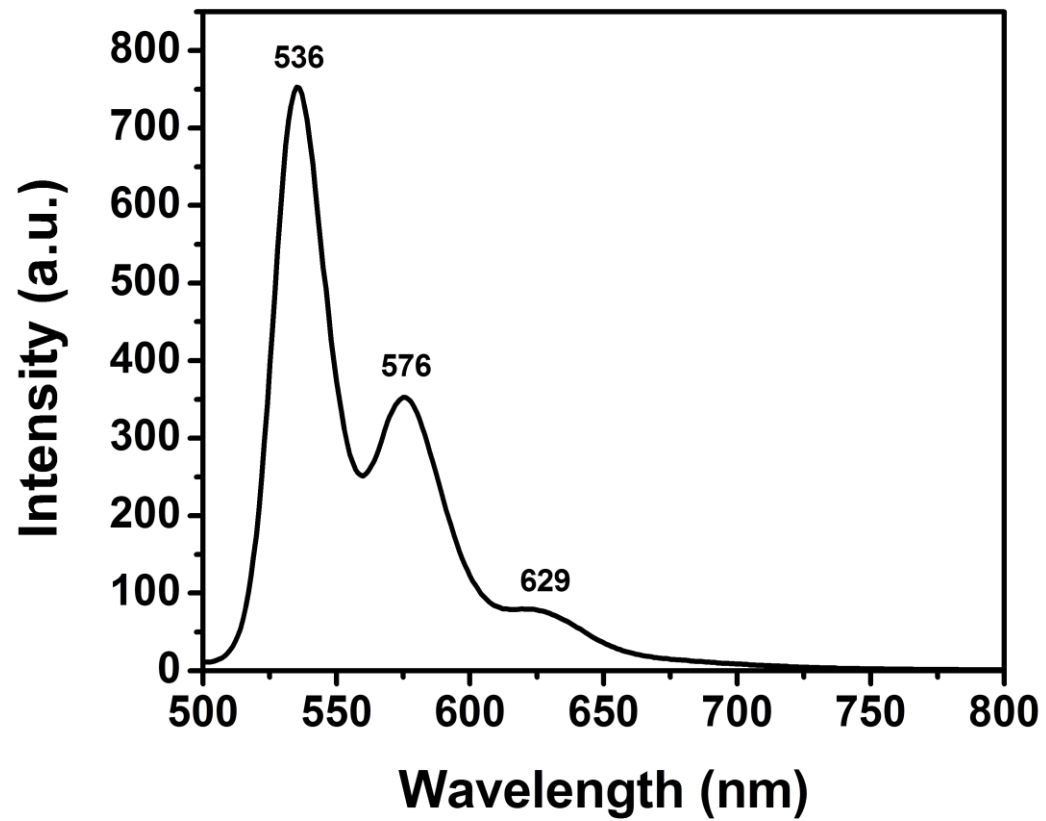


Figure 4.38 Emission spectrum ( $\lambda_{exc}=485\text{nm}$ ) of Br-PDI in DMF

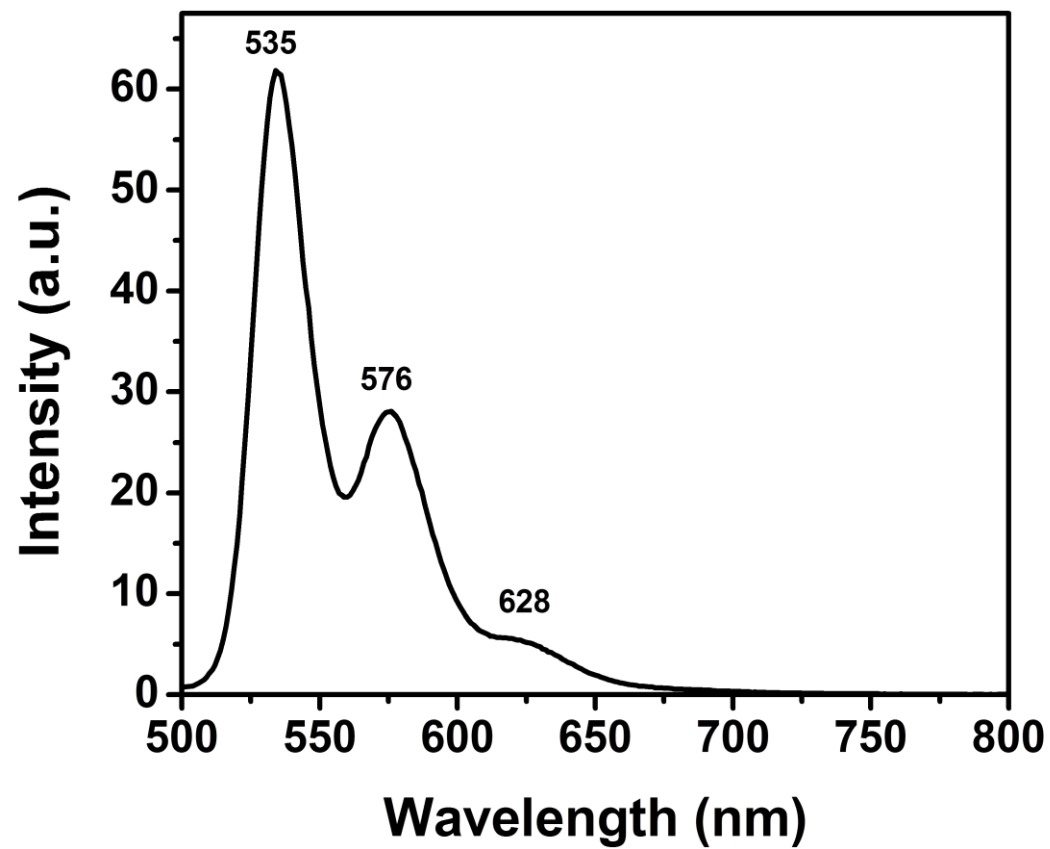


Figure 4.39 Emission spectrum ( $\lambda_{exc}=485\text{nm}$ ) of Br-PDI in DMF after micro filtration

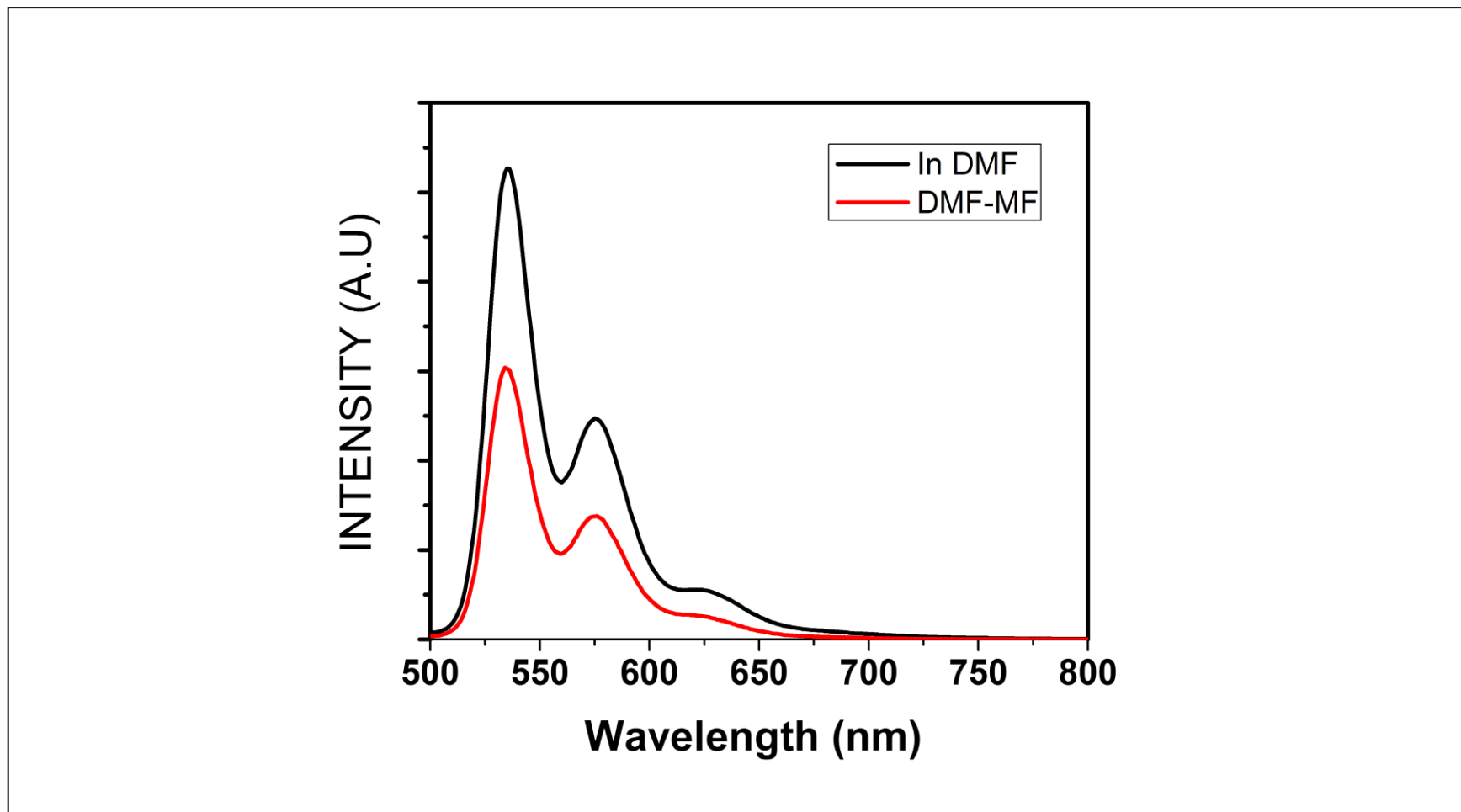


Figure 4.40 Emission spectrum ( $\lambda_{exc}=485\text{nm}$ ) of Br-PDI in DMF and in DMF after micro filtration

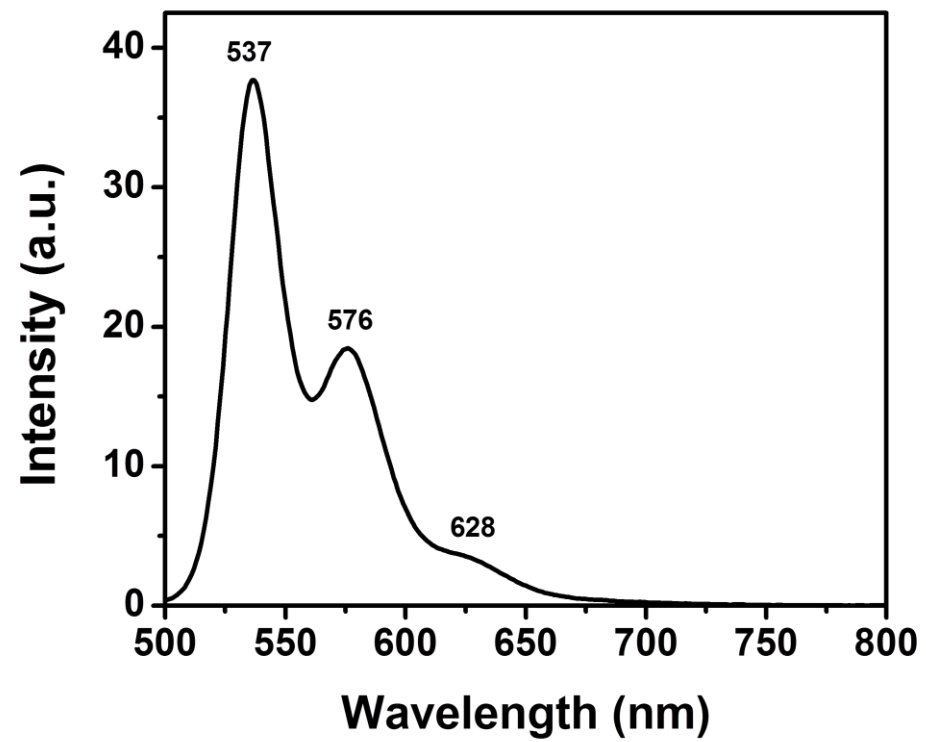


Figure 4.41 Emission spectrum ( $\lambda_{exc}=485\text{nm}$ ) of Br-PDI in NMP

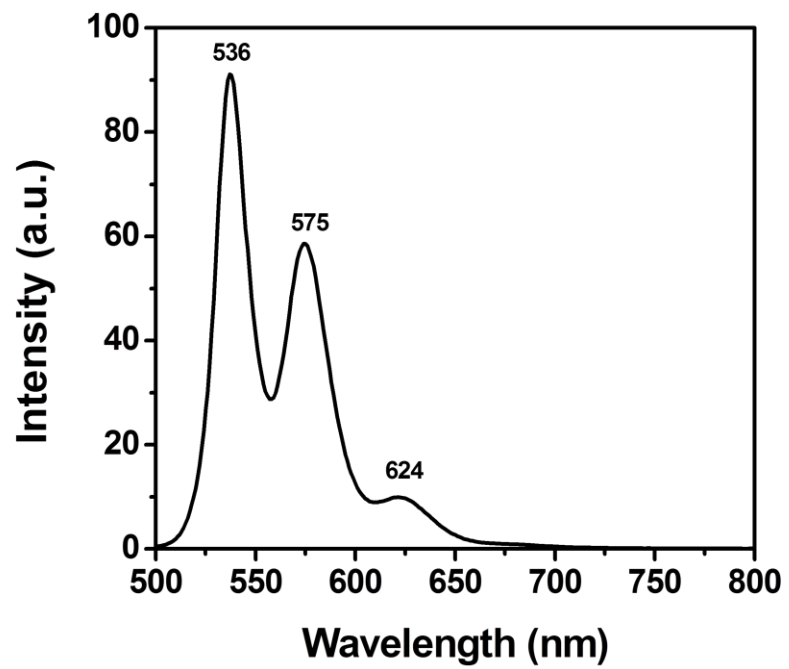


Figure 4.42 Emission spectrum ( $\lambda_{exc}=485\text{nm}$ ) of Br-PDI in CHL

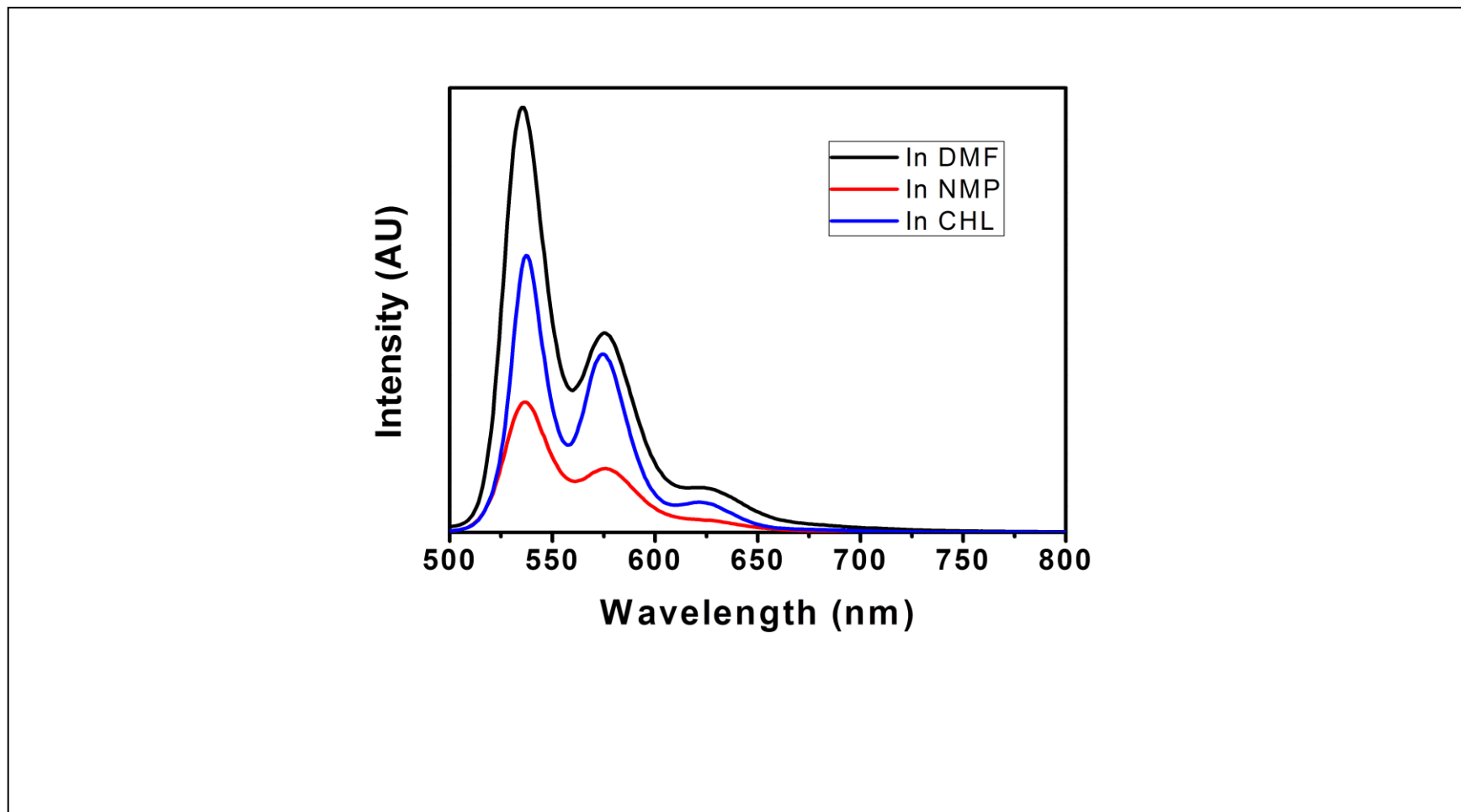


Figure 4.43 Emission spectrum ( $\lambda_{exc}=485\text{nm}$ ) of Br-PDI in DMF, NMP and CHL

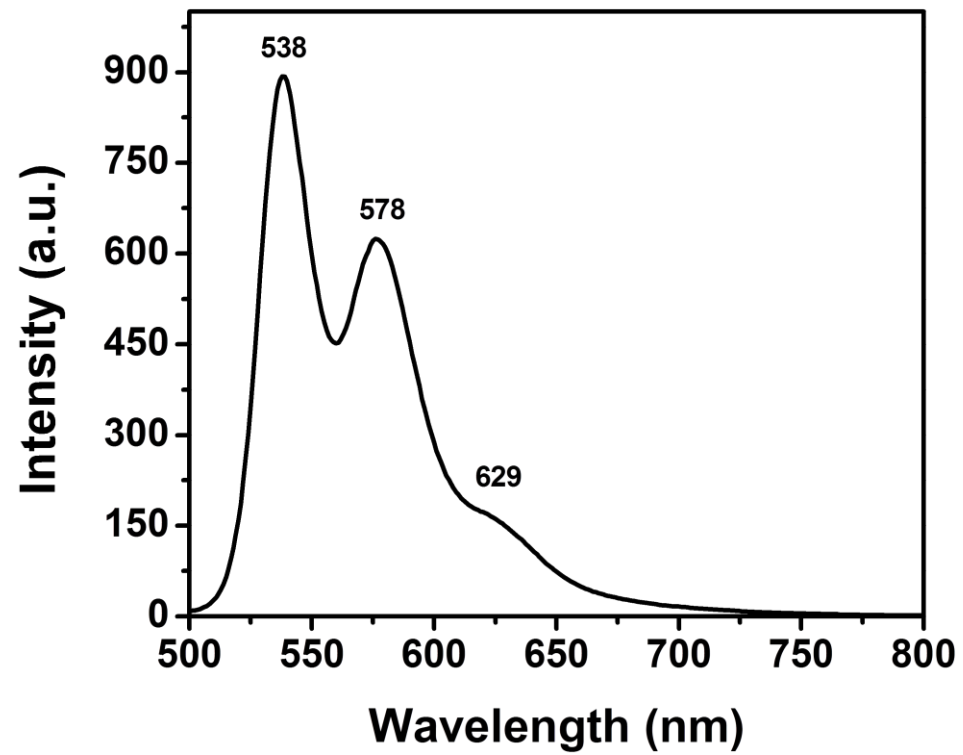


Figure 4.44 Emission spectrum ( $\lambda_{exc}=485\text{nm}$ ) of PDI-m-Cresol in DMF

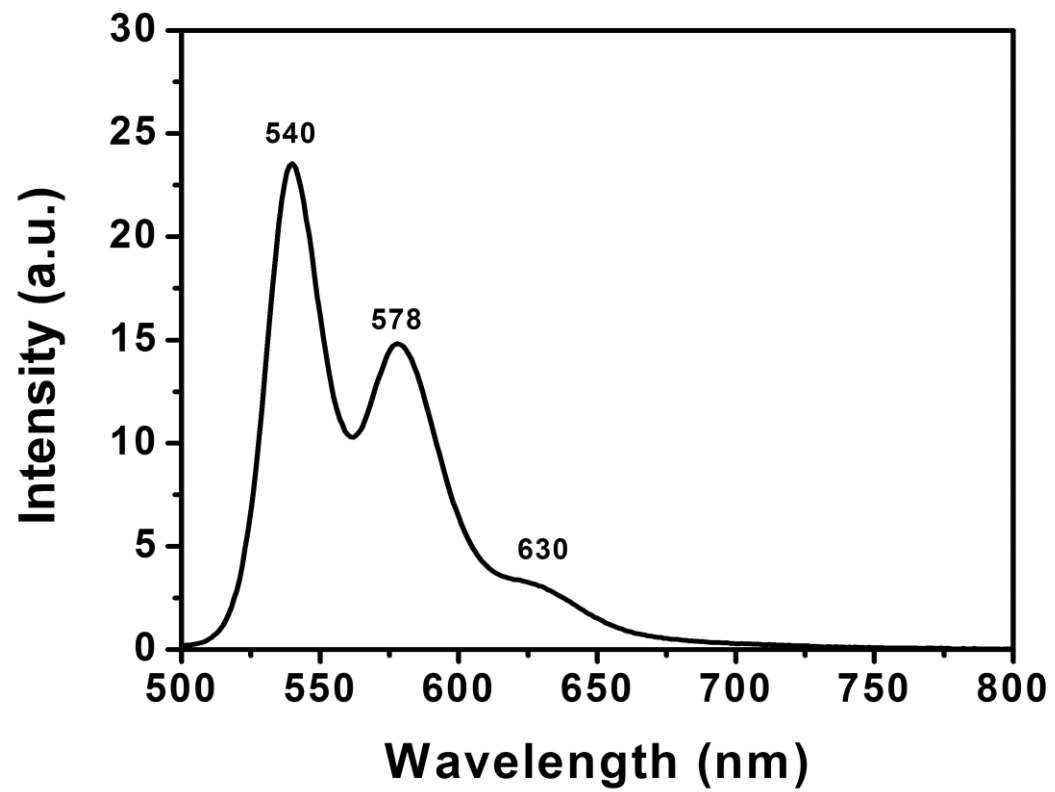


Figure 4.45 Emission spectrum ( $\lambda_{exc}=485\text{nm}$ ) of PDI-m-Cresol in NMP

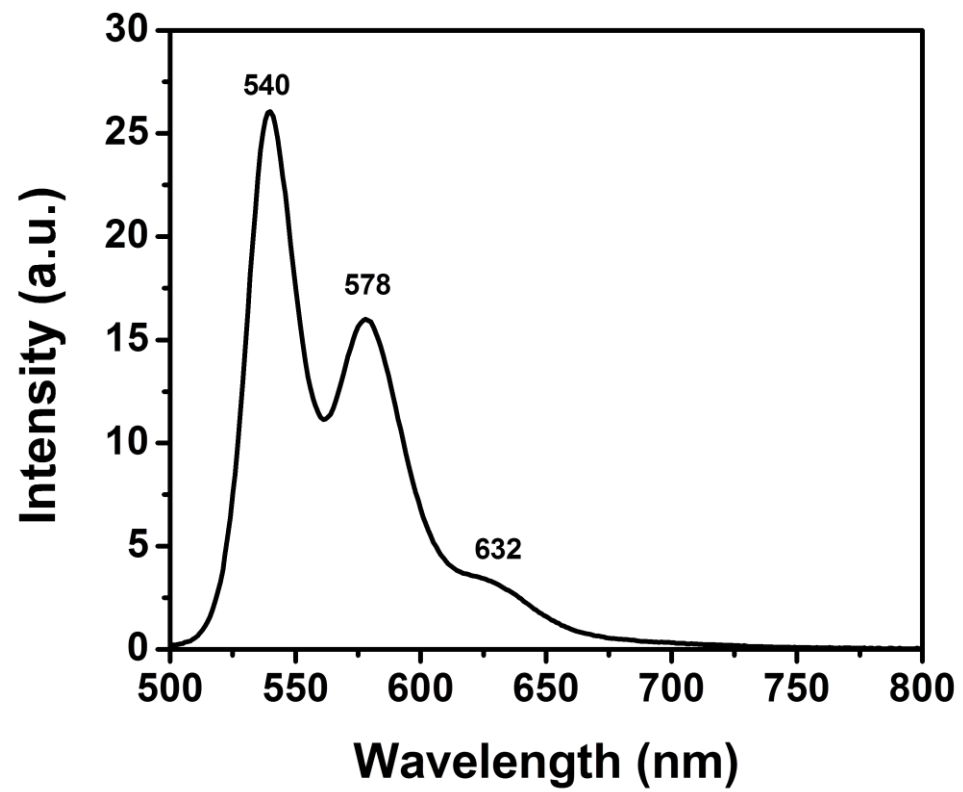


Figure 4.46 Emission spectrum ( $\lambda_{exc}=485\text{nm}$ ) of PDI-m-Cresol in NMP after micro filtration

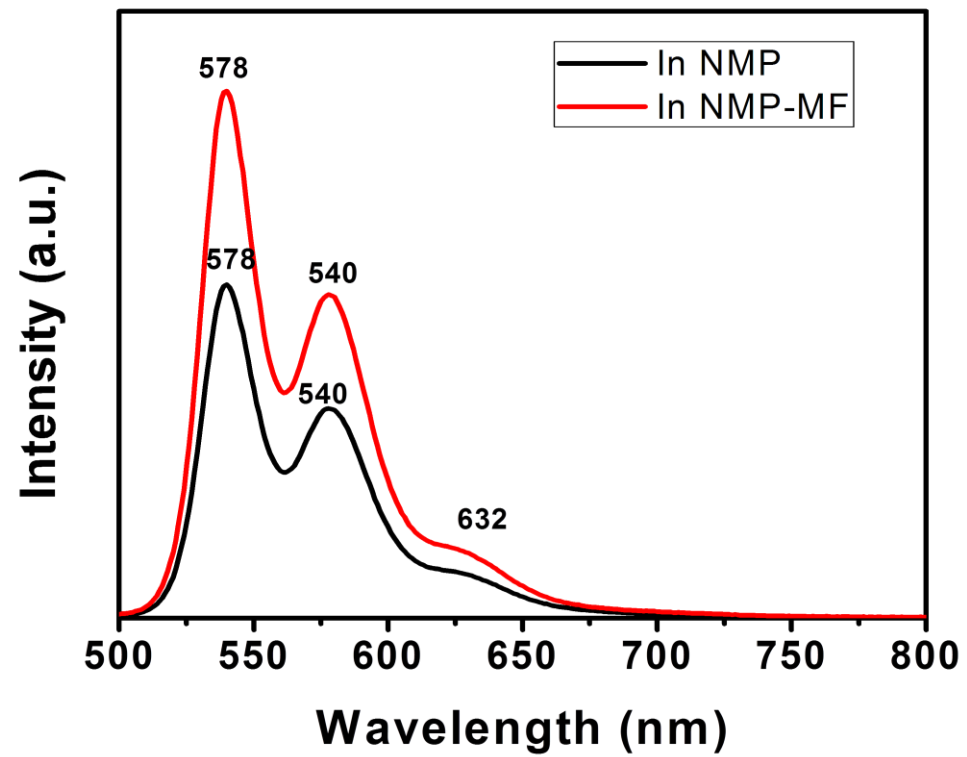


Figure 4.47 Emission spectrum ( $\lambda_{exc}=485\text{nm}$ ) of PDI-m-Cresol in NMP and in NMP after micro filtration

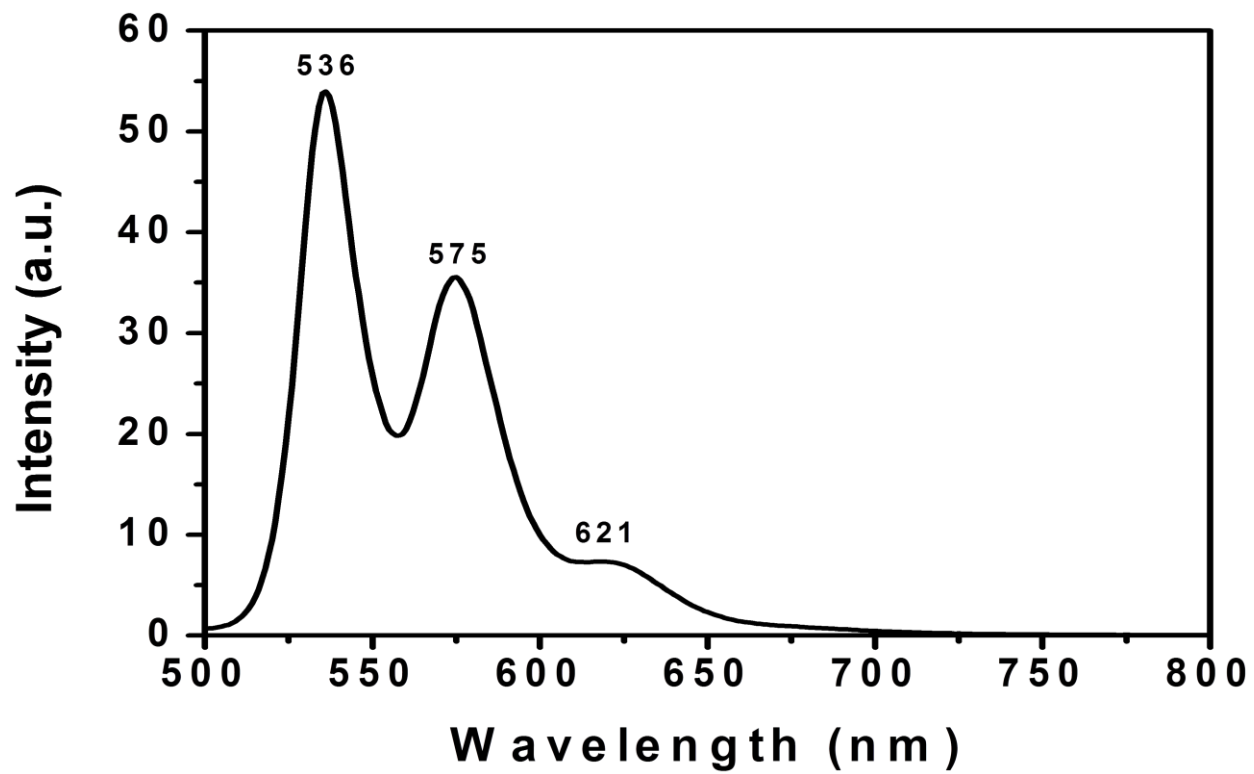


Figure 4.48 Emission spectrum ( $\lambda_{exc}=485\text{nm}$ ) of PDI-m-Cresol in CHL

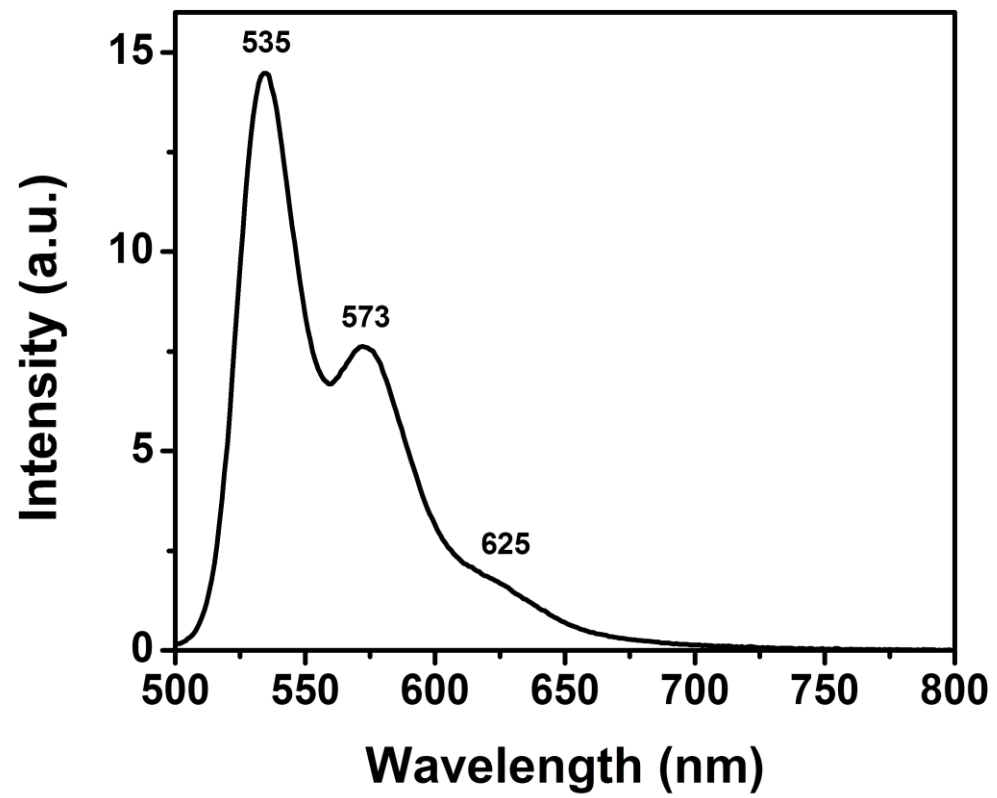


Figure 4.49 Emission spectrum ( $\lambda_{exc}=485\text{nm}$ ) of PDI-m-Cresol in EtOH

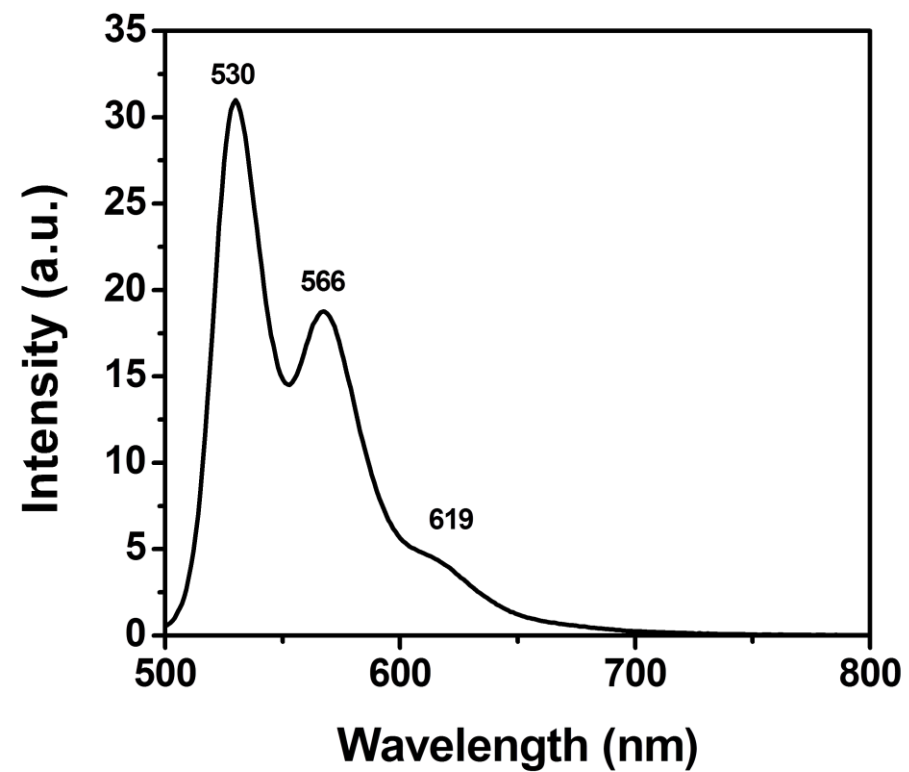


Figure 4.50 Emission spectrum ( $\lambda_{exc}=485\text{nm}$ ) of PDI-m-Cresol in Acetone

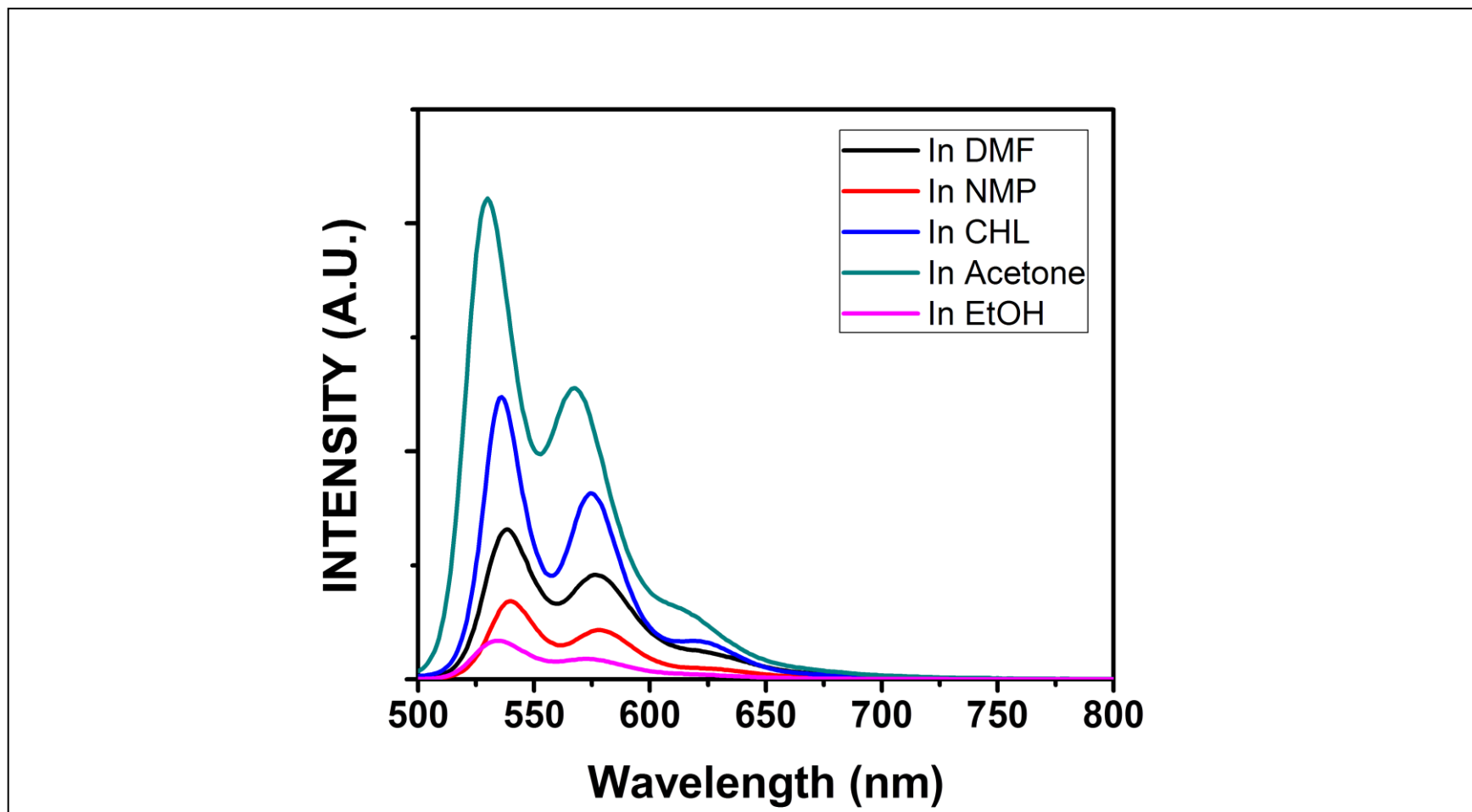


Figure 4.51 Emission spectrum ( $\lambda_{exc}=485\text{nm}$ ) of PDI-m-Cresol in DMF, NMP, CHL, Acetone and EtOH

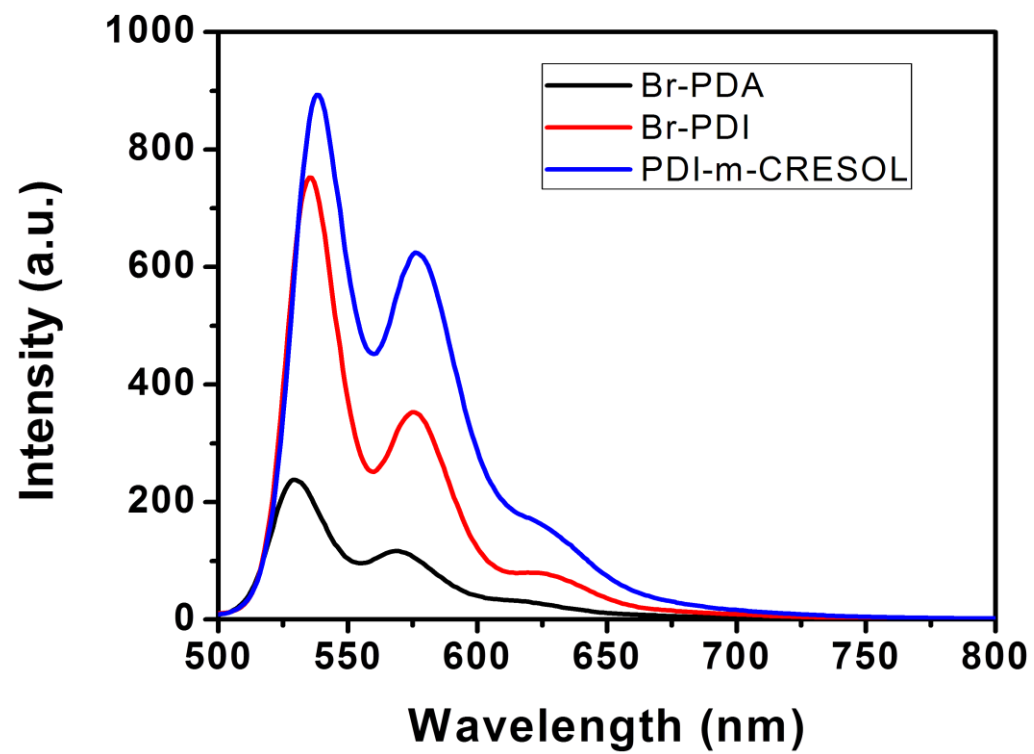


Figure 4.52 Emission spectrum ( $\lambda_{exc}=485\text{nm}$ ) of Br-PDA, Br-PDI and PDI-m-Cresol in DMF

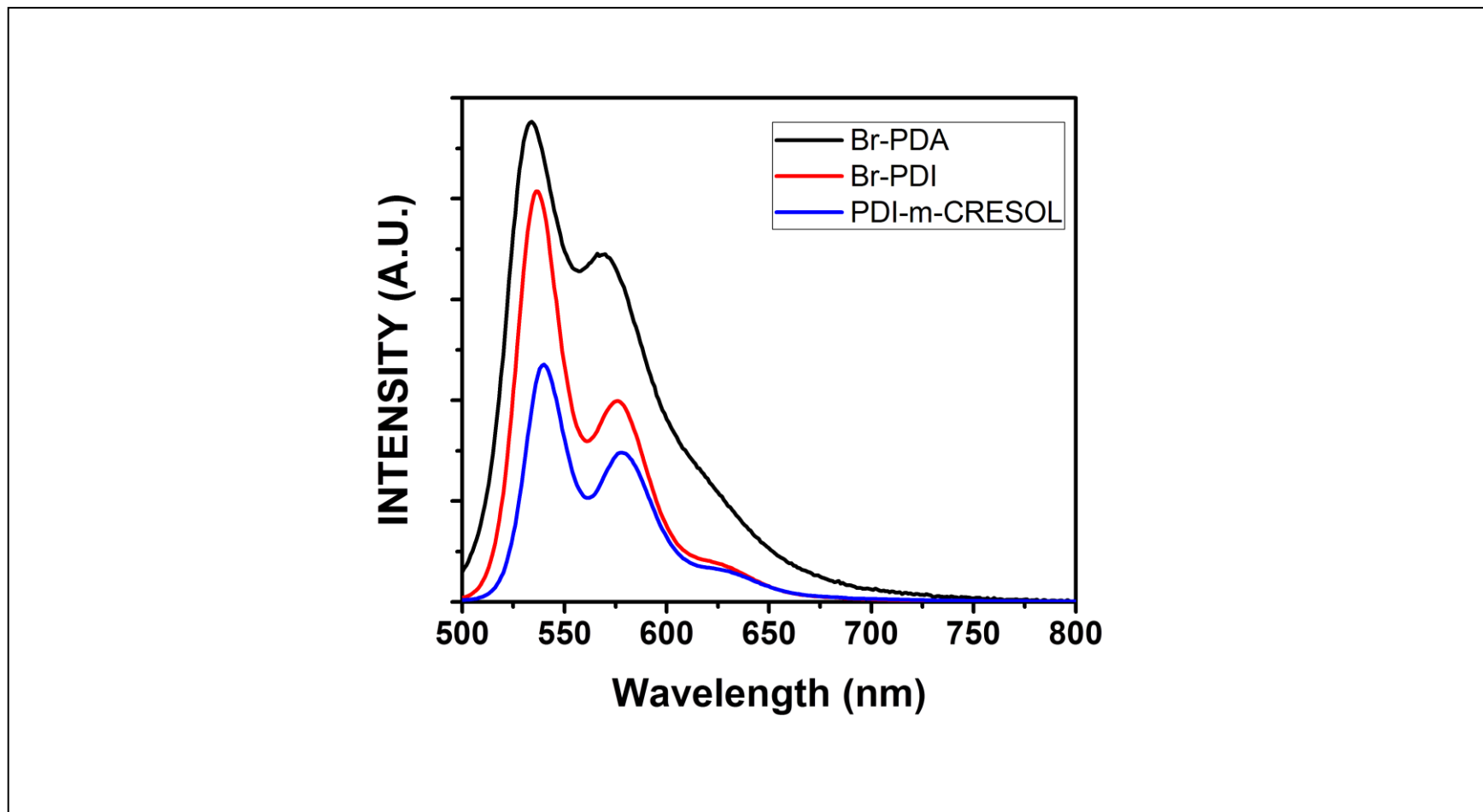


Figure4.53 Emission spectrum ( $\lambda_{exc}=485\text{nm}$ ) of Br-PDA, Br-PDI and PDI-m-Cresol in NMP

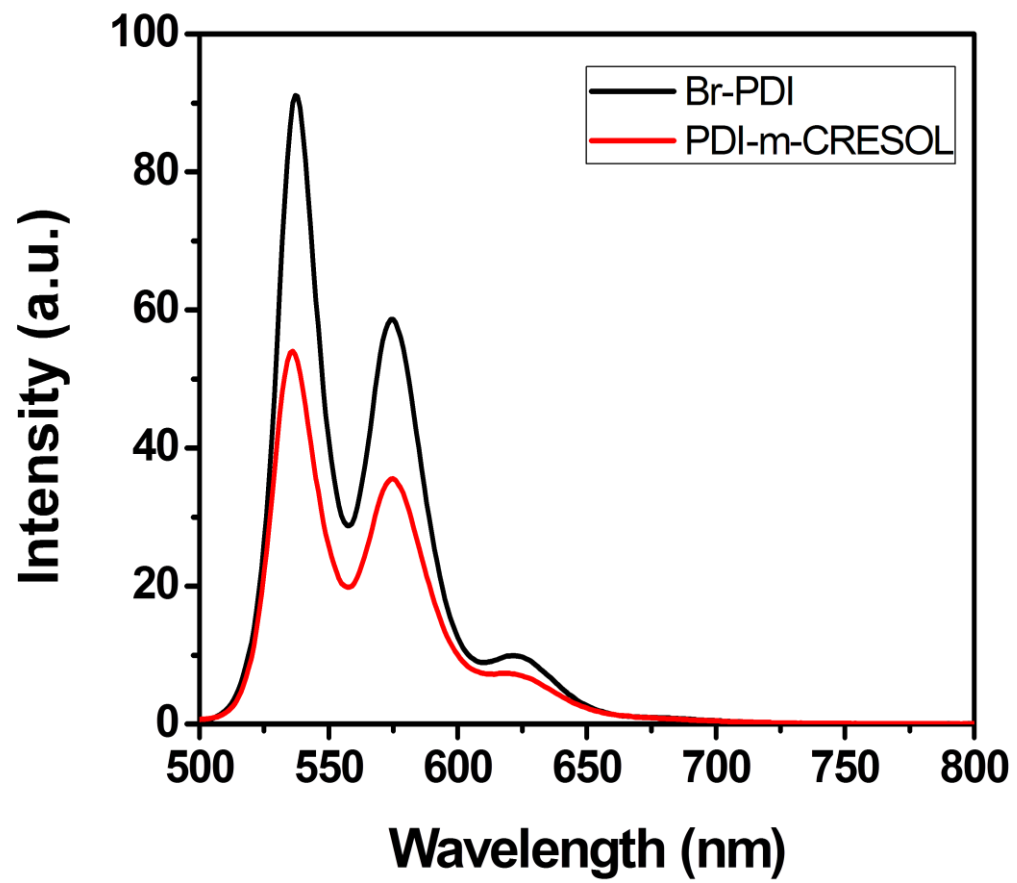
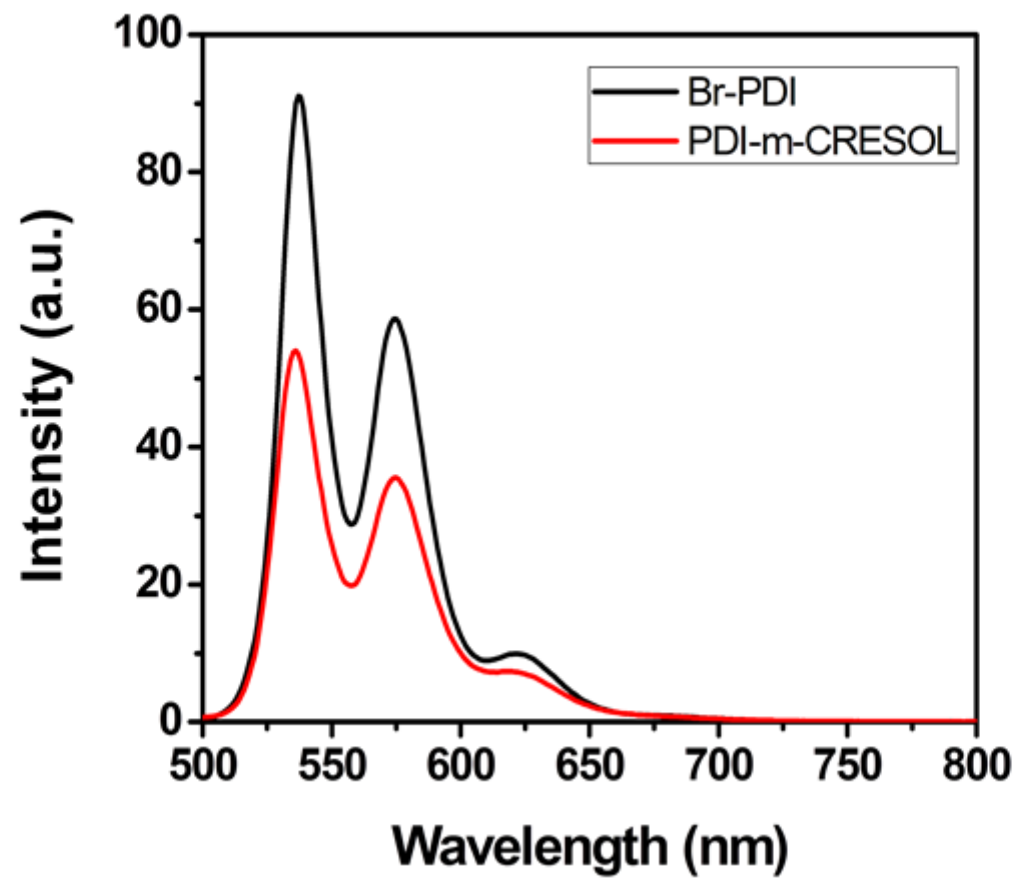


Figure 4.54 Emission spectrum ( $\lambda_{exc}=485\text{nm}$ ) of Br-PDI and PDI in CHL



## Chapter 5

### RESULTS AND DISCUSSION

#### 5.1 Synthesis of the Compounds

The core substituted perylene diimide (PDI-M-CRESOL) was successfully synthesized in three consecutive steps.

a) The first step includes bromination of the perylene core with the reaction between perylene dianhydride (PDA) and sulphuric acid in presence of iodine. Although many research papers discuss the bromination of PDA, careful observation is required to avoid the substitution at unwanted 1, 6-positions.

b) The second step carries the reaction between the product of the first step, brominated perylene dianhydride (Br-PDA) and the amine to yield the traditional perylene diimide. The reaction is carried out with the carefully calculated mole ratios to yield the targeted brominated perylene diimide (Br-PDI) in high yield.

c) In the final third step, the product of the second step, the brominated perylene diimide (Br-PDI) is reacted with the m-cresol to replace the bromines at the bay positions. Consequently, the finally targeted m-cresol core substituted perylene diimide (PDI-M-CRESOL) was produced.

The synthesis of core substituted perylene diimides can be widely found in literature [1, 34]. The crucial point that determines the successful synthesis of core substituted perylene chromophores is the purity of the targeted compound from various other possible core substituted perylene dyes. There is a plenty of possibility to remain with 1,6-substituted perylene dyes in major instead of targeted 1,7-substituted perylene dyes. This needs a careful experimentation with the materials and their mole ratios. Furthermore, the purification plays a great role in ending up with the targeted material.

Our targeted m-cresol core substituted (1, 7-substituted) perylene diimide (PDI-m-Cresol) was synthesized and purified accordingly.

## 5.2 Solubility of the synthesized perylene derivatives

Table 5.1 solubility test (++) soluble at room temperature; (- +) soluble on heating at 60°C; the solubility increases upon heating

Solvents	Br-PDA	Br-PDI	PDI-m-Cresol
DMF	(- +)Light red	(- +)Red	(- +)Red
NMP	(- +)Light red	(+ +)Red	(+ +)Dark red
CHL	(- -)	(+ +)Orange	(+ +)Red
ACETONE	(- -)	(- -)	(+ +)Red
EtOH	(- -)	(- -)	(- +)Red
DMSO	(- +)Red	(- -)	(+ +)Red
Dichloromethane	(- -)	(+ +)Red	(+ +) Red

Solubility details of compounds in various solvents were presented in table 5.1. Obviously, Br-PDA, Br-PDI, and PDI-m-Cresol exhibited differences in solubility based on their structures. The solubility of Br-PDA was limited due to their rigidity of the planar structure of anhydride. Br-PDI has shown better solubility than Br-PDA which could be attributed to the perylene imide with long-chain aliphatic substituent. Bay substituted target product has shown perfect solubility in most organic solvent as can be seen in the Table 5.1.

### **5.3 Analysis of FTIR spectra**

Figures (4.4, 4.5, and 4.6) show FTIR spectra of Br-PDA, Br-PDI and PDI-m-Cresol, the spectrum of Br-PDA Figure 4.4 present the following characteristic bands: aromatic C-H stretch at  $3122\text{ cm}^{-1}$ , anhydride C=O stretches at  $1765$  and  $1724\text{ cm}^{-1}$ , aromatic C=C stretch at  $1595\text{ cm}^{-1}$  and C-Br stretch at  $803\text{ cm}^{-1}$ . The spectrum of Br-PDI figure 4.5 presents the following characteristic bands: aromatic C-H stretches at  $3060\text{ cm}^{-1}$  and aliphatic C-H stretches at  $2914$  and  $2844\text{ cm}^{-1}$ , Imide C=O stretches at  $1695$  and  $1656\text{ cm}^{-1}$  and C-Br stretch at  $803\text{ cm}^{-1}$ .

The spectrum of PDI-m-Cresol Figure 4.6 presents the following characteristic bands: aromatic C-H stretch at  $3060\text{ cm}^{-1}$ , aliphatic C-H stretches at  $2923\text{ cm}^{-1}$  and  $2854\text{ cm}^{-1}$ , imide C=O stretches at  $1705\text{ cm}^{-1}$  and  $1656\text{ cm}^{-1}$ , aromatic C=C stretches at  $1596\text{ cm}^{-1}$ , ether C-O at  $1251\text{ cm}^{-1}$  and aromatic C-C bend at  $804\text{ cm}^{-1}$

### **5.4 Analysis of the UV-vis Absorption Spectra**

The method of core/bay substitution of perylene dyes is proved to be one of the great opportunities to alter the electronic structure and hence the electronic properties of the perylene derivatives. In addition, the imide- substitution with various linear and bulky groups provides a chance to functionalize the optical properties of perylene

derivatives. Concerning the application of the perylene derivatives toward photovoltaic cells, both electronic and optical properties are very important. The optical properties are studied via absorption and emission spectra of the synthesized compounds. For comparison, the intermediate products are also analyzed.

The absorption spectrum of brominated perylene dianhydride (Figure 4.7) shows major three characteristic absorption peaks at 452, 479, and 516 nm respectively in dipolar aprotic solvent, DMF. The three characteristic  $0 \rightarrow 2$ ,  $0 \rightarrow 1$ , and  $0 \rightarrow 0$  peaks represent the strong  $\pi-\pi^*$  electronic transitions of aromatic perylene chromophore.

The absorption spectra of brominated perylene dianhydride in NMP before and after microfiltration were shown in Figures 4.9 and 4.10. As can be seen from Figure 4.9, before microfiltration there are two dominant absorption peaks noticed in addition to the weak and broad absorption peak at 673 nm. This is due to strong solvent and solute interactions. The possibility of aggregation is discarded due to the increase in absorption intensity of the additional band at 672 nm after microfiltration. Moreover, the traditional perylene chromophoric absorption bands are better resolved after microfiltration.

The absorption spectra of brominated perylene dodecyl diimide (Br-PDI) in DMF are shown in Figures 4.14 – 4.15. As can be seen from Figure 4.14, the absorption spectrum is broad including three traditional perylene aromatic electronic transition peaks at 454, 488 and 522 nm followed by a broad absorption shoulder band at 610 nm, when the solution is micro filtered with a micro filter, the additional shoulder band at longer wavelengths is disappeared which indicates the aggregation (Figure

4.15). The aggregation at higher concentration is probably due to the presence of long aliphatic chains at imide positions.

For comparison, the absorption of the brominated perylene dodecyl diimide was studied in another high polar dipolar aprotic solvent, NMP (Figure 4.16). In contrary, the absorption spectrum in NMP has no indications of aggregation. The spectrum shows three perylene core absorption peaks at 457, 488, and 523 nm, respectively.

Similar to the absorption spectra noticed for brominated PDI in NMP, the spectra in nonpolar solvent chloroform have no signs of any aggregation concentrations (FIGURES 4.17) The spectra show characteristic  $\pi-\pi^*$  absorption peaks of perylene chromophore at 457, 488 and 525 nm, respectively.

The absorption spectrum of core/bay substituted perylene dodecyl diimide (PDI-M-CRESOL) from Figure 4.21 shows three traditional perylene chromophoric absorption peaks at 452, 482, and 525 nm, respectively with a very weak shoulder at around 550 nm in high polar dipolar aprotic solvent, DMF.

The absorption spectrum of PDI-m-Cresol from Figures 4.22 in NMP shows three traditional perylene chromophoric absorption peaks at 460, 488, and 525 nm, respectively with multiple very weak shoulder absorption bands. These absorption bands indicate the extended conjugation due to core substitution and resulting bathochromic shift. These absorption bands were not disappeared upon microfiltration as can be seen from Figure 4.23.

The absorption spectra in nonpolar solvents (Figure 4.25 in chloroform and Figure 4.26 in acetone) indicate the three characteristic aromatic electronic transition absorption peaks at around 450, 481, and 515 nm, respectively

The absorption spectrum in polar protic solvent methanol (Figure 4.27) indicate the three characteristic aromatic electronic transition absorption peaks at around 452, 484, and 520 nm, respectively. The peaks are similar to the peaks observed in non-polar solvents.

### **5.5 Analysis of the Emission Spectra**

The emission spectra of brominated perylene dianhydride (Figures 4.28 and 4.29) show major three characteristic emission peaks at 530, 569, and 622 nm respectively in dipolar aprotic solvent, DMF. The three characteristic peaks represent the 0→0, 0→1, and 0→2 transitions of perylene chromophore which were unchanged before and after microfiltration. The emission spectra are mirror images of their absorption spectra.

The emission spectra of brominated perylene dianhydride (Figures 4.31 and 4.32) show major three characteristic emission peaks (which were mostly mirror images of their absorption spectra) at around 530, 570 nm in dipolar aprotic solvent, NMP. The three characteristic peaks were slightly changed after microfiltering the solution. Before microfiltration, the peaks were broader. Interestingly, the additional peaks found in absorption spectra of the dye in the same solvent have no significance on the emission of the perylene derivative.

The emission spectra of brominated perylene diimide (Figures 4.35 and 4.36) show major three characteristic emission peaks (which were mostly mirror images of their

absorption spectra) at around 535, 576, and 628 nm, respectively in dipolar aprotic solvent, DMF. The three characteristic peaks were unchanged after microfiltering the solution. Interestingly, the additional peaks found in absorption spectra of the dye in the same solvent have no significance on their corresponding emission of the perylene derivative.

The emission spectra of brominated perylene diimide (Figures 4.38 and 4.ccc) show major three characteristic emission peaks (which were mirror images of their absorption spectra) at around 536, 575, and 632 nm, respectively in dipolar aprotic solvent, NMP.

The emission spectrum of brominated perylene diimide (Figures 4.39) show major three characteristic emission peaks (which were mirror images of their absorption spectra) at around 536, 575, and 624 nm, respectively in nonpolar aprotic solvent, chloroform.

The spectrum figure (4.41) show major three traditional emission peaks of  $0 \rightarrow 0$ ,  $0 \rightarrow 1$ , and  $0 \rightarrow 2$  transitions of perylene chromophore which were mirror images of their respective absorption spectra.

The emission spectra of core substituted perylene diimide in NMP before and after microfiltration were reported in Figures 4.42 and 4.43. The figures clearly show no differences in their emission spectra in terms of spectral shape and peak positions. Moreover, there was no effect of additional absorption bands on the corresponding emission spectra. The spectra show major three traditional emission peaks of  $0 \rightarrow 0$ ,

0→1, and 0→2 transitions of perylene chromophore which were mirror images of their respective absorption spectra.

The emission spectrum of core/bay substituted perylene diimide (Figure 4.45) shows major three characteristic emission peaks (which were mirror images of their absorption spectra) at around 536, 575, and 621 nm, respectively in nonpolar aprotic solvent, chloroform.

The emission spectrum of core/bay substituted PDI-M-CRESOL (Figure 4.46) shows major three characteristic emission peaks (which were mirror images of their absorption spectra) at around 535, 573, and 625 nm, respectively in polar protic solvent, ethanol.

The emission spectrum of core/bay substituted perylene diimide (Figure 4.47) shows major three characteristic emission peaks (which were mirror images of their absorption spectra) at around 530, 566, and 619 nm, respectively in nonpolar aprotic solvent, acetone.

## Chapter 6

### CONCLUSION

The preparation of a Bay- Functionalized Perylene Dye N,N'-Didodecyl-1,7-di(3-methylphenoxy)- perylene-3,4:9,10-tetracarboxylic Acid Bisimide has been successfully achieved under special conditions in a high yield , and its structure has been characterized by FT/IR spectroscopy ,and the photophysical properties have been investigated by UV absorption and emission spectroscopy .

The solubility of Br-PDA was limited due to their rigidity of the planar structure of anhydride. Br-PDI has shown better solubility than Br-PDA which could be attributed to the perylene imide with long-chain aliphatic substituent. Bay substituted target product has shown perfect solubility in most organic solvent as can be seen in the table 5.1.

The method of core/bay substitution of perylene dyes is proved to be one of the great opportunities to alter the electronic structure and hence the electronic properties of the perylene derivatives. In addition, the imide- substitution with various linear and bulky groups provides a chance to functionalize the optical properties of perylene derivatives. Concerning the application of the perylene derivatives toward photovoltaic cells, both electronic and optical properties are very important.

## REFERENCES

- [1] Shockley, W., & Queisser, H. J. (1961). Detailed Balance Limit of Efficiency of PN Junction Solar Cells. *Journal of Applied Physics*. 32: 510.
- [2] Wöhrle, D., & Meissner, D. (1991). Organic Solar Cells. *Advance Materials*. 3:129
- [3] Kim, J. Y., Lee, K., Coates, N. E., Moses, D., Nguyen, T. -Q., Dante, M., & Heeger, A. J. (2007). Efficient tandem polymer solar cells fabricated by all-solution processing. *Science*. 317: 222.
- [4] Weil, T., Vosch, T., Hofkens, J., Peneva, K., & Müllen, K. (2010). The Rylene Colorant Family—Tailored Nanoemitters for Photonics Research and Applications. *Angewandnte.Chem. Int. Ed.* 49: 9068-9093.
- [5] Wöhrle, D., Kreienhoop, L., Schnurpfeil, G., Elbe, J., Tennigkeit, B., Hiller, S., & Schlettwein, D. (1995). Investigations of n/p-Junction Photovoltaic Cells of Perylenetetracarboxylic Acid Diimides and Phthalocyanines. *J. Mater. Chem.* 5 : 1819-1829.
- [6] Quante, H., Geerts, Y., & Müllen, K. (1997). Synthesis of Soluble Perylenebisamidine derivatives. Novel Long-Wavelength Absorbing and Fluorescent Dyes. *Chemistry of Materials*. 9: 495-500.202
- [7] Shibano, Y., Umeyama, T., Matano, Y., & Imahori, H. (2007). Electron-Donating

Perylene Tetracarboxylic Acids for Dye-Sensitized Solar Cells. *Organic Letters*.

9: 1971-1974.

[8] Wang, W., Han, J. J., Wang, L. -Q., Li, L. -S., Shaw, W. J. & Li, A. D. Q. (2003).

Dynamic  $\pi$ - $\pi$  Stacked Molecular Assemblies Emit from Green to Red Colors.

*Nano Letters*. 3: 455-458.

[9] Bodapati, J. B., & Icil, H. (2008). Highly Soluble Perylene Diimide and Oligomeric

Diimide Dyes Combining Perylene and Hexa(ethylene glycol) Units: Synthesis,

Characterization, Optical and Electrochemical Properties. *Dyes and Pigments*. 79: 224-

235.

[10] Bodapati, J. B., & Icil, H. (2006). A New Tunable Light-Emitting and  $\pi$ -Stacked

Naphthalene Oligomer: Synthesis, Photophysics and Electrochemical Properties.

*Photochemical and Photobiological Sciences*.

[11] Pasaogullari, N., Icil, H., & Demuth, M. (2006). Symmetrical and Unsymmetrical

Perylene Diimides: Their Synthesis, Photophysical and Electrochemical

Properties. *Dyes and Pigments*. 69: 118-127.

[12] Yuney, K., & Icil, H. (2007). Symmetrical and Unsymmetrical Perylene Diimides:

Their

Synthesis, Photochemical, and Electrochemical Properties of Naphthalene-

1,4,5,8-tetracarboxylic acid-bis-(N,N'-bis-(2,2,4(2,4,4)-trimethylhexylpolyimide)) and

Poly(N,N'-bis-(2,2,4(2,4,4)-trimethyl-

6203aminohexyl)3,4,9,10perylene-tetracarboxydiimide. *European Polymer Journal*.43: 2308-2320.

[13] Amiralaei, S., Uzun, D., & Icil, H. (2008). Chiral Substituent Containing Perylene Monoanhydride Monoimide and its Highly Soluble Symmetrical Diimide: Synthesis, Photophysics and Electrochemistry from Dilute Solution to Solid State. *Photochemical and Photobiological Sciences*. 7: 936-947.

[14] Asir, S., Demir, A. S., & Icil, H. (2009). The Synthesis of Novel, Unsymmetrically Substituted, Chiral Naphthalene and Perylene Diimides: Photophysical, Electrochemical, Chiroptical and Intramolecular Charge Transfer Properties. *Dyes and Pigments*. 84: 1-14.

[15] Ozdal, D., Asir, S., Bodapati, J. B., & Icil, H. (2011, *in press*).

[16] Yamashita, Y. (2009). Organic Semiconductors for Organic Field-Effect Transistors. *Science and Technology of Advanced Materials*. 10: 024313.

[17] Ahrens, M. J., Fuller, M. J., Wasielewski, M. R. (2003). Cyanated Perylene-3,4-dicarboximides and Perylene-3,4,9,10-bis(dicarboximide): facile Chromophoric Oxidants for Organic Photonics and Electronics. *Chemistry of Materials*. 15: 2684-2686.

[18] Würthner, F. (2004). Perylene Bisimide Dyes as Versatile Building Blocks for Functional Supramolecular Architectures. *Chemical Communications*.:1564-1579.204

[19] Qu, J., Zhang, J., Grimsdale, A. C., Mllen, K., Jaiser, F., Yang, X., & Neher, D. (2004).

Dendronized Perylene Diimide Emitters: Synthesis, Luminescence, and Electron and Energy Transfer Studies. *Macromolecules*.37: 8297-8306.

[20] Lee, S., Miller, A. M., Al-Kaysi, R., & Bardeen, C. J. (2006).Using Perylene-Doped Polymer Nanotubes as Fluorescence Sensors. *Nano Letters*. 6: 1420-1424.

[21] Bevers, S., Schuttle, S., & McLaughlin, L. W. (2000). Naphthalene- and Perylene-Based Linkers for the Stabilization of Hairpin Triplexes. *J. Am. Chem. Soc.* 122:5905-5915.

[22] Ofir, Y., Zelichenok, A., & Yitzchaik, S. (2006). 1,4;5.8-Naphthalene-tetracarboxylic Diimide Derivatives as Model Compounds for Molecular Layer Epitaxy. *J. Mater. Chem.* 16: 2142-2149.

[23] Jones, B. A., Facchetti, A., Wasielewski, M. R., & Marks, T. J. (2007).Tuning Orbital Energetics in Arylene Diimide Semiconductors. Materials Design for Ambient Stability of *n*-type Charge Transport. *J. Am. Chem. Soc.* 129: 15259-15278.

[24] Fukaminato, T., Tanaka, M., Doi, T., Tamaoki, N., Katayama, T., Mallick, A., Ishibashi, Y., Miyasaka, H., & Irie, M. (2010).Fluorescence Photoswitching of a Diarylethene-Perylenebisimide Dyad Based on Intramolecular Electron Transfer. *Photochemical and Photobiological Sciences*. 9: 181-187.205

- [25] Thelakkat, M., Schmitz, C., & Schmidt, H. -W. (2002). Fully Vapor-Deposited Thin-Layer Titanium Dioxide Solar Cells. *Adv. Mater.* 14: 577.
- [26] Pandey, A. K., Unni, K. N. N., & Nunzi, J. -M. (2006). Pentacene/Perylene Co-Deposited Solar Cells. *Thin Solid Films.* 511-512: 529-532.
- [27] Breeze, A. J., Salomon, A., Ginley, D. S., Gregg, B. A., Tillmann, H., & Hörhold, H. -H. (2002). Polymer-Perylene Diimide Heterojunction Solar Cells. *Applied Physics Letters.* 81: 3085-3087.
- [28] Nakamura, J. -I., Yokoe, C., Murata, K., & Takahashi, K. (2004). Efficient Organic Solar Cells by Penetration of Conjugated Polymers into Perylene Pigments. *J. App. Phys.* 96: 6878-6883.
- [29] Foster, S., Finlayson, C. E., Keivani, P. E., Huang, Y. -S., Hwang, I., Friend, R. H., Otten, M. B. J., Lu, L. -P., Schwartz, E., Nolte, R. J. M., & Rowan, A. E. (2009). Improved Performance of Perylene-Based Photovoltaic Cells Using Polyisocyanopeptide Arrays. *Macromolecules.* 42: 2023-2030.
- [30] Tomizaki, K. -Y., Loewe, R. S., Kirmaier, C., Schwartz, J. K., Retsek, J. L., Bocian, D. F., Holten, D., & Lindsey, J. S. (2002). Synthesis and Photophysical Properties of Light-Harvesting Arrays Comprised of a Porphyrin Bearing Multiple Perylene-Monoimide Accessory Pigments. *J. Org. Chem.* 67:6519-6534.206
- [31] Ishi-i, T., Murakami, K. -I., Imai, Y., & Mataka, S. (2005). Light-Harvesting and Energy Transfer System Based on Self-Assembling Perylene Diimide-Appended

Hexaazatriphenylene. *Org. Lett.* 7: 3175-3178.

[32] Sautter, A., Kaleta, B. K., Schmid, D. G., Dobraza, R., Zimine, M., Jung, G., Stokkum, I. H. M. V., Cola, L. D., Williams, R. M., & Würthner, F. (2005). Ultrafast Energy-Electron Transfer Cascade in a Multichromophoric Light-Harvesting Molecular Square. *J. Am. Chem. Soc.* 127: 6719-6729.

[33] Edvinsson, T., Li, C., Pschirer, N., Schneboom, J., Eickemeyer, F., Sens, R., Boschloo, G., Herrmann, A., Mllen, K., & Hagfeldt, A. (2007). Intramolecular Charge-Transfer Tuning of Perylenes: Spectroscopic Features and Performance in Dye-Sensitized Solar Cells. *The Journal of Physical Chemistry C.* 111: 15137-15140.

[34] Bauer, P., Wietasch, H., Lindner, S. M., & Thelakkat, M. (2007). Synthesis and Characterization of Donor-Bridge-Acceptor Molecule Containing Tetraphenylbenzidine and Perylene Bisimide. *Chemistry of Materials.* 19:88-94.

[35] Beckers, E. H. A., Meskers, S. C. J., Schenning, A. P. H. J., Chen, Z., Würthner, F., Marsal, P., Beljonne, D., Cornil, J., & Janssen, R. A. J. (2006). Influence of Intermolecular Orientation on the Photoinduced Charge Transfer Kinetics in Self-Assembled Aggregates of Donor-Acceptor Arrays. *J. Am. Chem. Soc.* 128: 649-657.207

[36] Balakrishnan, K., Datar, A., Naddo, T., Huang, J., Oitker, R., Yen, M., Zhao, J., & Zang, L. (2006). Effect of Side-Chain Substituents on Self-Assembly of Perylene Diimide Molecules: Morphology Control. *J. Am. Chem. Soc.* 128: 7390-7398.

- [37] Ghosh, S., & Ramakrishnan, S. (2005) .Structural Fine-Tuning of (-Donor-Spacer-Acceptor-Spacer-)<sub>n</sub> Type Foldamers. Effect of Spacer Segment Length, Temperature, and Metal-Ion Complexation on the Folding Process *Macromolecules*. 38: 676-686.
- [38] Hoppe, H., & Sariciftci, N. S. (2004). Organic Solar Cells: An Overview. *J. Mater. Res.* 19: 1924-1945.
- [39] Brunetti, F. G., Kumar, R., & Wudl, F. (2010). Organic Electronics from Perylene to Organic Photovoltaics: Painting a Brief History with a Broad Brush. *J. Mater. Chem.* 20: 2934-2948.
- [40] Günes, S., Neugebauer, H., & Sariciftci, N. S. (2007). Conjugated Polymer-Based Organic Solar Cells. *Chem. Rev.* 107: 1324-1338.
- [41] Benanti, T. L, & Venkataraman, D.(2006). Organic Solar Cells: An Overview Focusing on Active Layer Morphology. *Photosynthesis Research*. 87: 73-81.
- [42] Pron, A., & Rannou, P. (2002).Processible Conjugated Polymers: from Organic Semiconductors to Organic Metals and Super Conductors. *Prog. Polym. Sci.* 27: 135-190.208
- [43] Anthony, J. E., Facchetti, A., Heeney, M., Marder, S. R., & Zhan, X. (2010).*n*-Type Organic Semiconductors in Organic Electronics. *Adv. Mater.* 22: 3876-3892.

[44] Bredas, J. -L., Beljonne, D., Coropceanu, V., & Cornil, J. (2004). Charge-Transfer and Energy-Transfer Processes in  $\pi$ -Conjugated Oligomers and Polymers: A Molecular Picture. *Chem. Rev.* 104: 4971-5003.

[45] Deibel, C., Strobel, T., & Dyakonov, V. (2010). Role of the Charge Transfer State in Organic Donor-Acceptor Solar Cells. *Adv. Mater.* 22 : 4097-4111.

[46] Albinsson, B., & Martensson, J. (2010). Excitation Energy Transfer in Donor-Bridge-Acceptor Systems. *Phys. Chem. Chem. Phys.* 12: 7338-7351.

[47] Würthner, F., & Meerholz, K. (2010). Systems Chemistry Approach in Organic Photovoltaics. *Chem. Eur. J.* 16: 9366-9373.

[48] Balzani, V., Credi, A., & Venturi, M. (2003). *Molecular Devices and Machines – A Journey into the Nano World*, Wiley-VCH Verlag GmbH & Co. KGaH, Weinheim.

[49] Sermet K.,Mahmut K.,& Seraftin D.(2007).electrochemical and optical properties of novel donor-acceptor thiophene-perylene-thiophene polymers,wiley interscience ,department of chemistry faculty of art and science,mugla university ,48000,mugla,turkey